Probing the first order electroweak phase transition by measuring gravitational waves in scalar extension models

Toshinori Matsui (松井 俊憲)
KIAS

KOREA INSTITUTE FOR ADVANCED STUDY

Collaborators: Katsuya Hashino[1], Mitsuru Kakizaki[1], Shinya Kanemura[1], Pyungwon Ko[2]
[1]University of TOYAMA, [2]KIAS

M.Kakizaki, S.Kanemura, T.Matsui, Phys. Rev. D **92**, no. 11, 115007 (2015),
K.Hashino, M.Kakizaki, S.Kanemura, T.Matsui, Phys. Rev. D **94**, no. 1, 015005 (2016),
K.Hashino, M.Kakizaki, S.Kanemura, T.Matsui, P.Ko, **Phys. Lett. B to appear** (arXiv:1609.00297)

Probing the first order electroweak phase transition by measuring gravitational waves in scalar extension models

Contents

- Motivation: EWBG is detectable at future colliders and GW observations
- Review: GWs from 1st order phase transition
- Models: "O(*N*) models & "Higgs singlet model"

Probing the first order electroweak phase transition by measuring gravitational waves in scalar extension models

Contents

- Motivation: EWBG is detectable at future colliders and GW observations
- Review: GWs from 1st order phase transition
- Models: "O(*N*) models & "Higgs singlet model"

Motivation

- Discovery of the Higgs boson
  - Mass generation mechanism is confirmed
  - The Standard Model (SM) as an effective theory is established
- What is the nature of EW symmetry breaking?
  - SM have minimal Higgs potential…**no principle**
  - Higgs self-couplings **have not been measured**

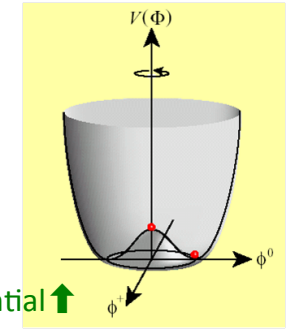

Higgs potential ⬆

- New physics is required to solve BSM phenomena

  Baryon asymmetry of the Universe, Existence of Dark Matter, inflation,…
  - BSM might be rerated to the extended Higgs sector
- Exploring the structure of the Higgs sector is important to understand physics behind EWSB.

Electroweak Baryogenesis (EWBG)

~ Importance to understand the Higgs potential ~

- Observed Baryon number: $n_B/s \simeq \mathcal{O}(10^{-10})$
- Sakharov's 3 conditions

  1. #B violation, 2. CP violation, 3. Departure from equilibrium

→Strongly 1st order phase transition

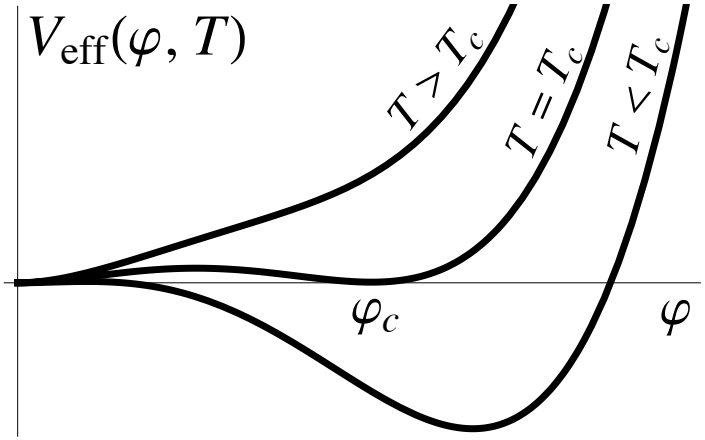

$$\varphi_c/T_c \gtrsim 1$$

- SM cannot satisfy these conditions (m_h=125GeV).
- EWBG is realized by models with extended Higgs sector.

(i) Triple Higgs boson (*hhh*) coupling

~ Probing the Higgs potential by future colliders ~

- e.g. Two Higgs doublet model (2HDM)

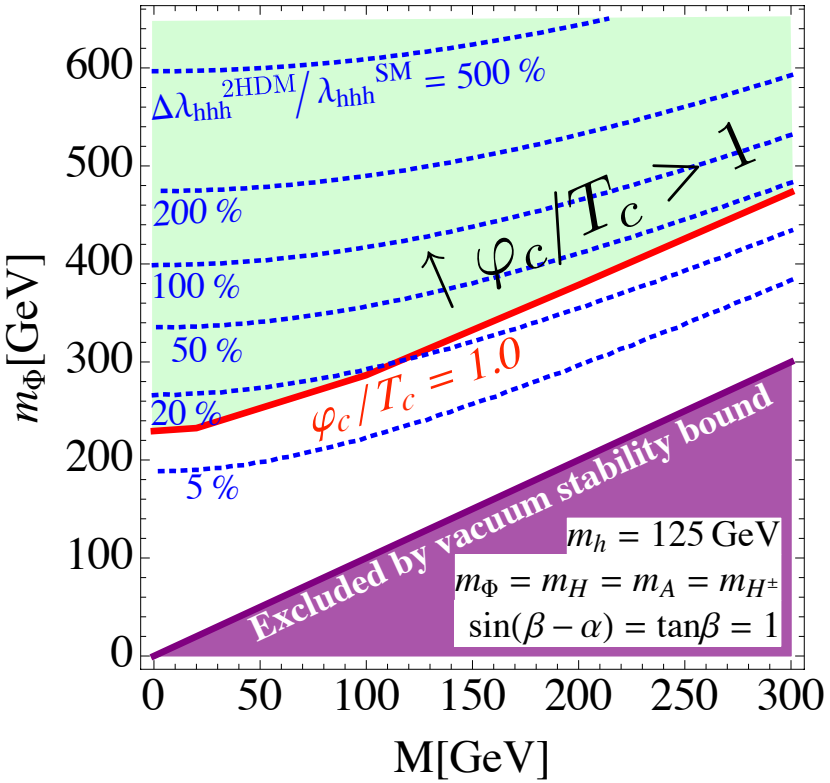

$$\Delta\lambda_{hhh}^{2\mathrm{HDM}}/\lambda_{hhh}^{\mathrm{SM}} \equiv (\lambda_{hhh}^{2\mathrm{HDM}} - \lambda_{hhh}^{\mathrm{SM}})/\lambda_{hhh}^{\mathrm{SM}}$$

$$m_\Phi^2 \simeq M^2 + \lambda_i v^2$$
$$\Phi = H, A, H^\pm$$

Kanemura, Okada, Senaha, PLB**606** (2005) 361

The scenario of EWBG require $\Delta\lambda_{hhh}/\lambda_{hhh} > O(10)\%$.

(i) Triple Higgs boson (*hhh*) coupling

~ Probing the Higgs potential by future colliders ~

- e.g. Two Higgs doublet model (2HDM)

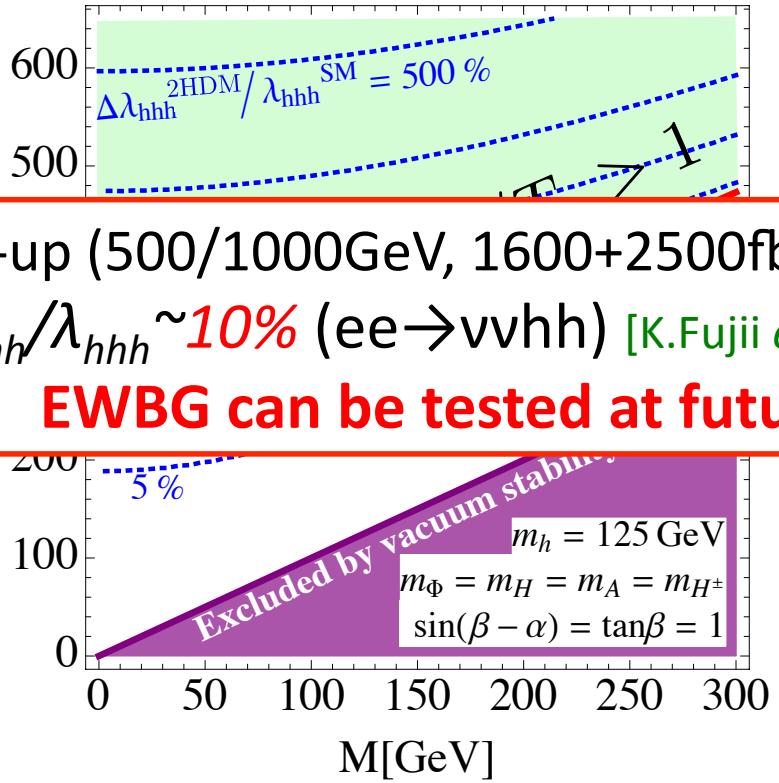

$$\Delta\lambda_{hhh}^{\rm 2HDM}/\lambda_{hhh}^{\rm SM} \equiv (\lambda_{hhh}^{\rm 2HDM} - \lambda_{hhh}^{\rm SM})/\lambda_{hhh}^{\rm SM}$$

ILC1000-up (500/1000GeV, 1600+2500fb^{-1})

$\Delta\lambda_{hhh}/\lambda_{hhh}$~*10%* (ee→vvhh) [K.Fujii *et al.*, arXiv:1506.05992]

EWBG can be tested at future colliders!

$$m_\Phi^2 \simeq M^2 + \lambda_i v^2$$
$$\Phi = H, A, H^\pm$$

Kanemura, Okada, Senaha, PLB**606** (2005) 361

The scenario of EWBG require $\Delta\lambda_{hhh}/\lambda_{hhh} > O(10)\%$.

(ii) Gravitational waves

～ Probing the Higgs potential by GW observations ～

LIGO have detected GWs directly. "GW150914", PRL. **116**, 061102 (2016), "GW151226", PRL. **116**, 241103 (2016)

- Ground exp.: aLIGO [USA], KAGRA [JPN], aVIRGO [ITA・FRA],…

  → Just now observing GWs directly from astronomical phenomena such as the binary of black holes, neutron stars, etc.

  The era of GW astronomy will come true!

- Future space exp.: eLISA [EU], DECIGO [JPN], BBO [USA]…

  → Will be exploring phenomena at the early stage of the Universe such as EW phase transition, cosmic inflation, topological defects, etc.

We expect GWs as a new technique to explore the BSM, in addition to the collider experiments!

Experimental status (eLISA)

- LISA pathfinder: launched on Dec., 2015, reported results PRL**116**, 231101 (2016)
- **eLISA design with 3 arms was decided**. http://www.physik.uzh.ch/events/lisa2016
- ESA approval : 2017, eLISA launch : **2028**

(ii) Gravitational waves

~ Probing the Higgs potential by GW observations ~

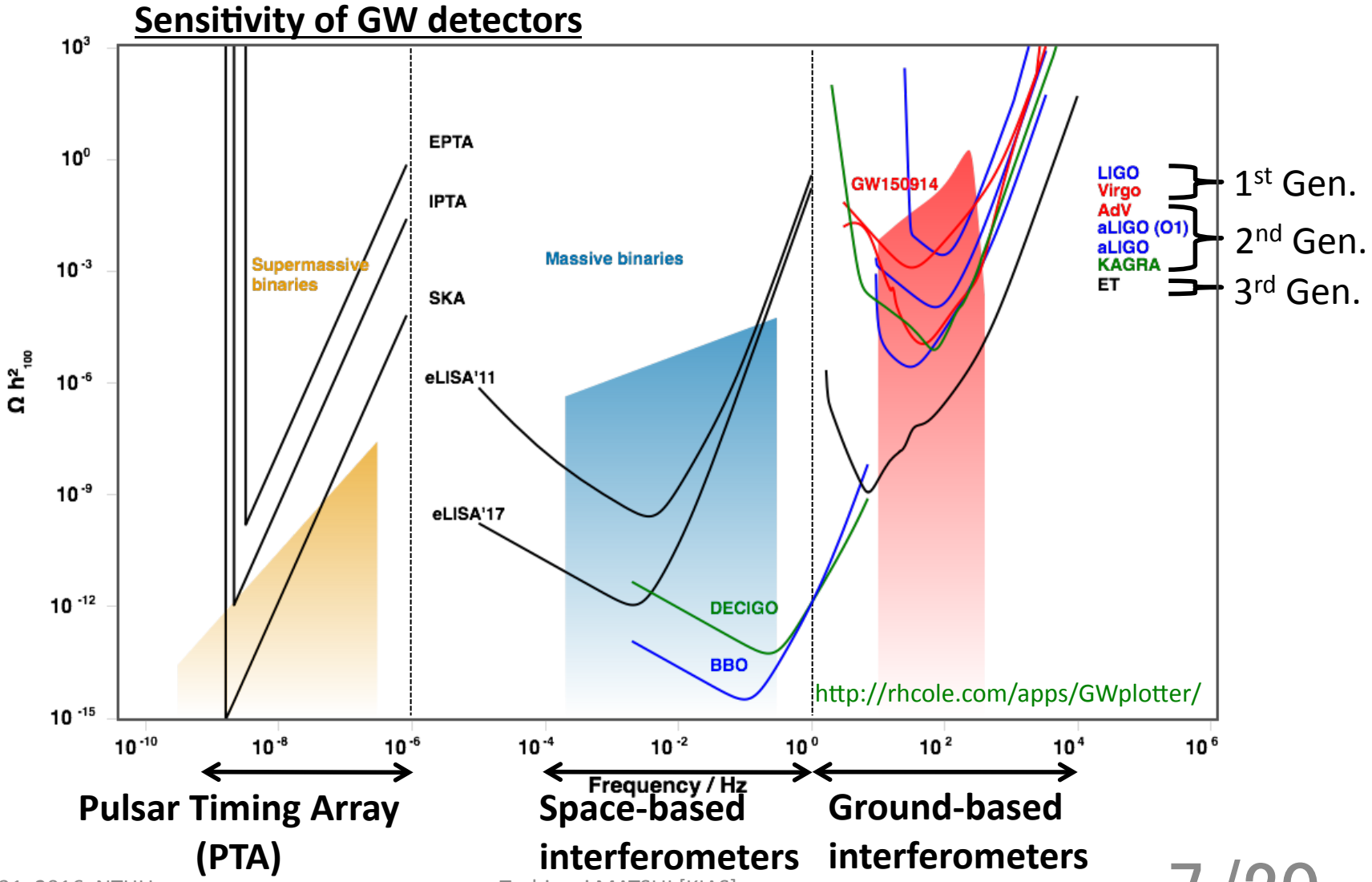

(ii) Gravitational waves

~ Probing the Higgs potential by GW observations ~

Sensitivity of GW detectors

Red shifted frequency:

$$f_0 = \frac{a_t}{a_0} f_t$$

↓

EWPT (~100GeV)

$$f_0 \simeq 10^{-5}\mathrm{Hz}\frac{T_t}{100\mathrm{GeV}}\frac{f_t}{H_t}$$

$$(f_t \simeq 10^{9}\mathrm{Hz})$$

EWPT can be explored by eLISA!

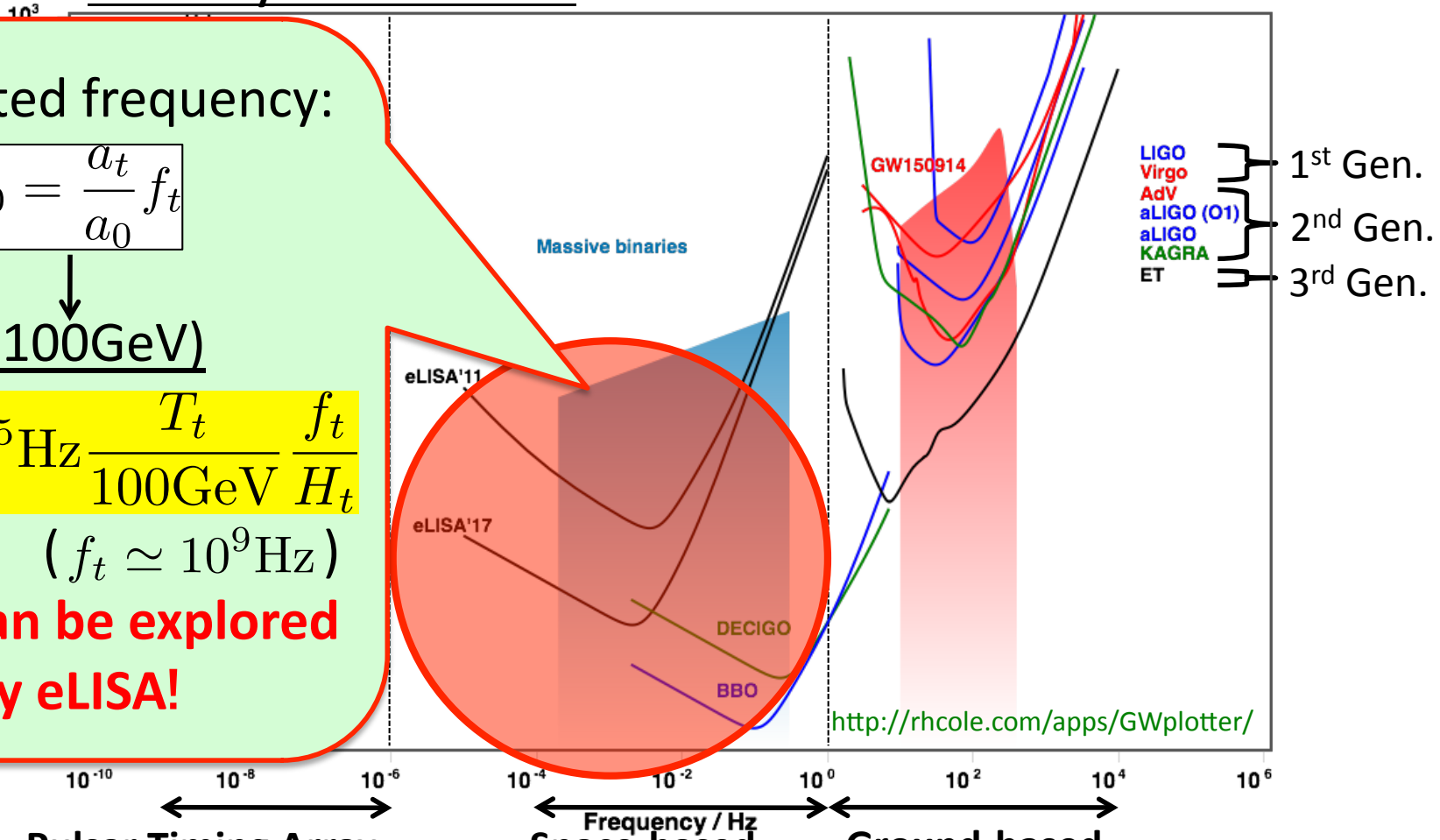

Probing the first order electroweak phase transition by measuring gravitational waves in scalar extension models

Contents

- Motivation: EWBG is detectable at future colliders and GW observations
- Review: GWs from 1st order phase transition
- Models: "O(*N*) models & "Higgs singlet model"

Phase transition - Bubble configuration

Model parameters

Input

$$V_{\rm eff}(\varphi, T)$$

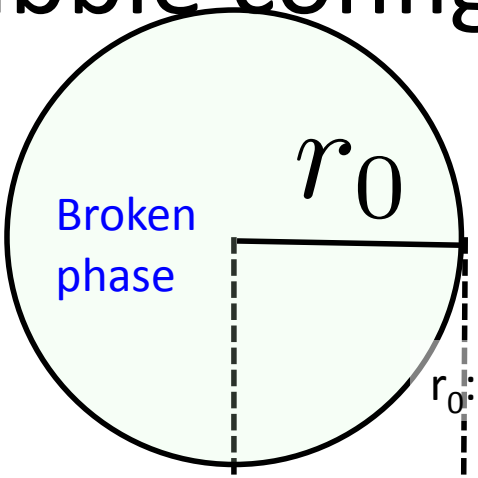

r_0: size of critical bubble

Potential:

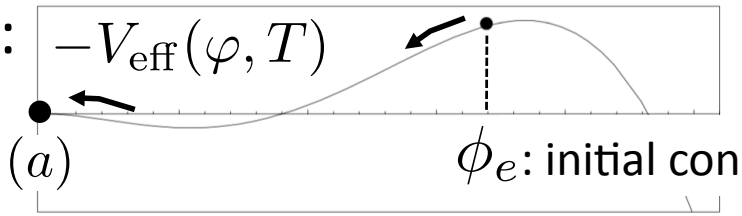

Eq. of motion: $\frac{d^2\varphi}{dr^2} + \frac{2}{r}\frac{d\varphi}{dr} - \frac{dV_{\rm eff}}{d\varphi} = 0$ → $\varphi(r)$

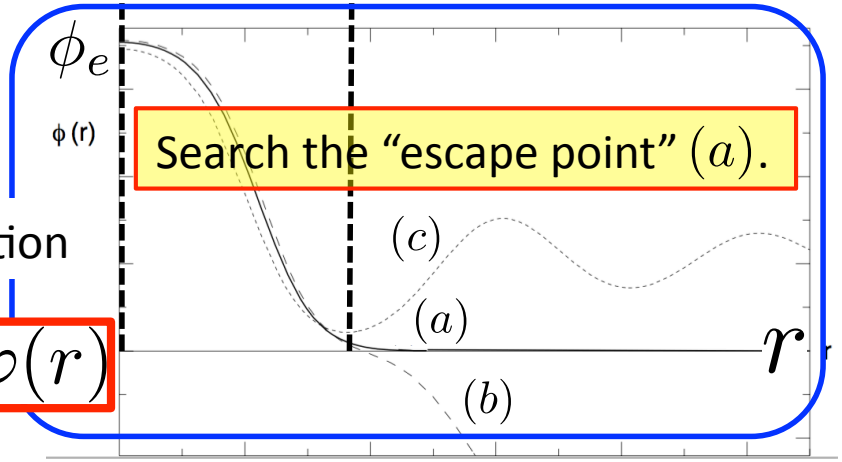

Phase transition - Bubble configuration

Model parameters

Input

$V_{\rm eff}(\varphi, T)$ → $\Gamma(T)$

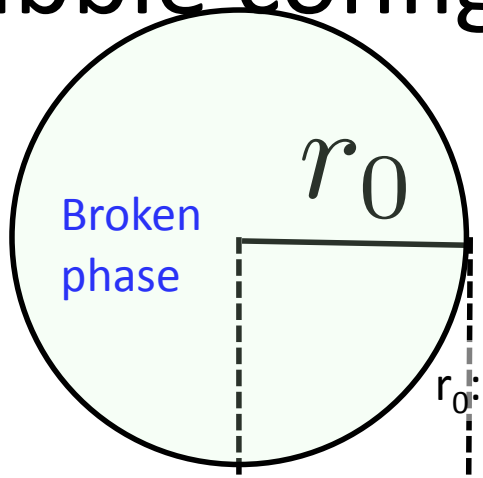

r_0: size of critical bubble

Potential:

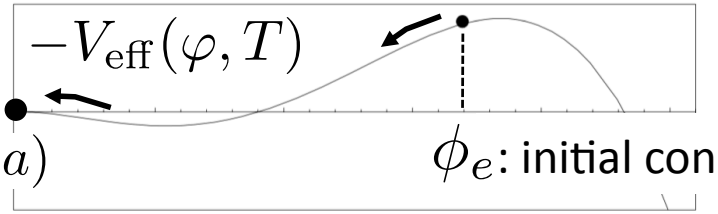

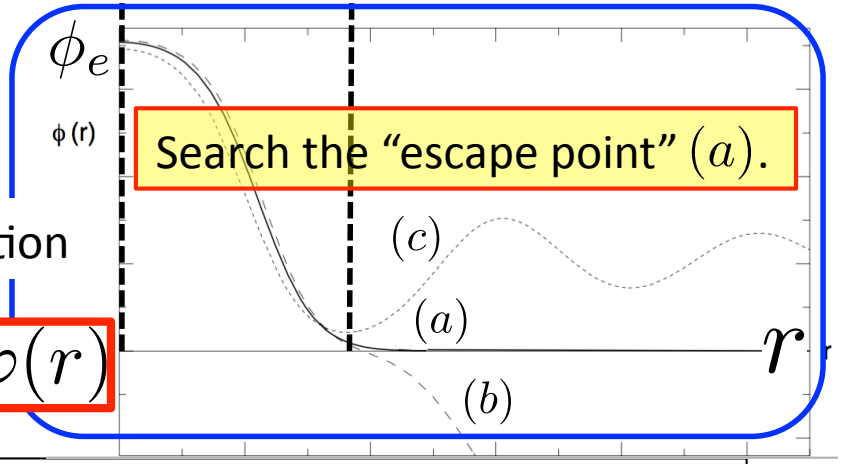

Eq. of motion: $\frac{d^2\varphi}{dr^2} + \frac{2}{r}\frac{d\varphi}{dr} - \frac{dV_{\rm eff}}{d\varphi} = 0$ → $\varphi(r)$

$\varphi(r)$ → each T

Bubble nucleation rate: $\Gamma(T) \simeq T^4 e^{-\frac{S_3(T)}{T}}$

3-dim. Euclidean action: $S_3(T) = \int dr^3 \left\{ \frac{1}{2} \left(\vec{\nabla}\varphi \right)^2 + V_{\rm eff}(\varphi, T) \right\}$

Phase transition - Transition temperature

Model parameters

Input

$V_{\rm eff}(\varphi, T)$ → $\Gamma(T)$

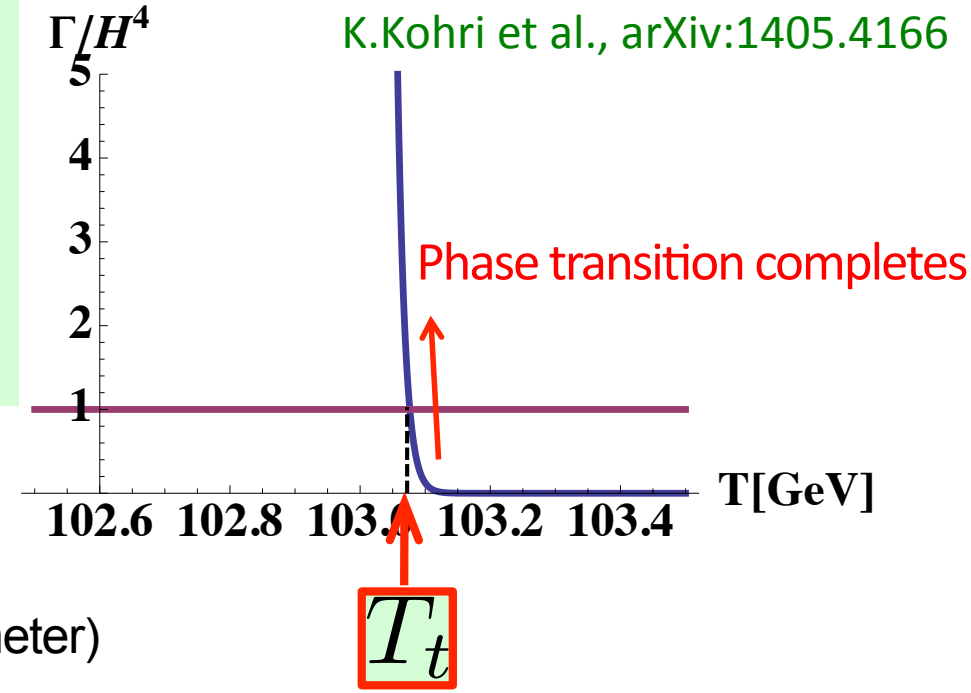

K.Kohri et al., arXiv:1405.4166

$$\left.\frac{\Gamma}{H^4}\right|_{T=T_t} \simeq 1$$ (*H*: Hubble parameter)

→Definition of phase transition temperature T_t

Bubble nucleation rate: $\Gamma(T) \simeq T^4 e^{-\frac{S_3(T)}{T}}$

3-dim. Euclidean action: $S_3(T) = \int dr^3 \left\{ \frac{1}{2} \left(\vec{\nabla}\varphi \right)^2 + V_{\rm eff}(\varphi, T) \right\}$

Phase transition - Characteristic parameters

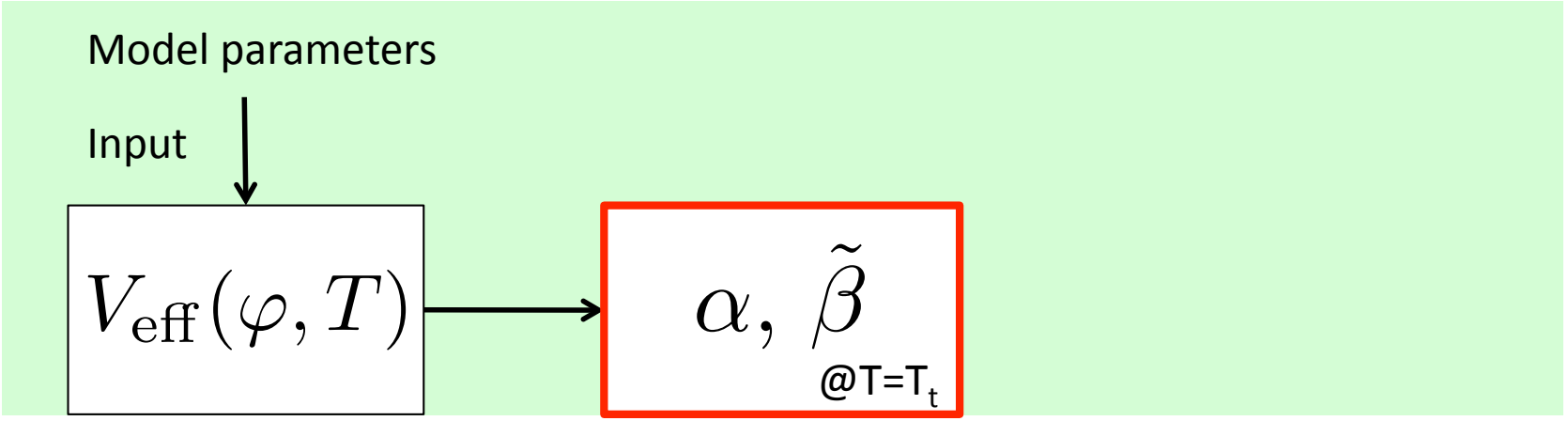

- α is defined as $\alpha \equiv \left.\dfrac{\epsilon}{\rho_{\rm rad}}\right|_{T=T_t}$ ($\rho_{\rm rad}$ is energy density of rad.)
  - Latent heat: $\epsilon(T) \equiv -\Delta V_{\rm eff}(\varphi_B(T), T) + T\dfrac{\partial \Delta V_{\rm eff}(\varphi_B(T))}{\partial T}$ cf. U=-F+T(dF/dT)

"Normalized difference of the potential minima"

- β is defined as $\beta \equiv \left.\dfrac{1}{\Gamma}\dfrac{d\Gamma}{dt}\right|_{t=t_t}$. $\rightarrow$ $\tilde{\beta}\left(\equiv \dfrac{\beta}{H_t}\right) = T_t \left.\dfrac{d(S_3(T)/T)}{dT}\right|_{T=T_t}$

"~How fast the minimum goes down"

GWs from 1stOPT

C.Caprini *et al.*, JCAP**1604**, 001 (2016)

Expanding
bubbles of the broken phase

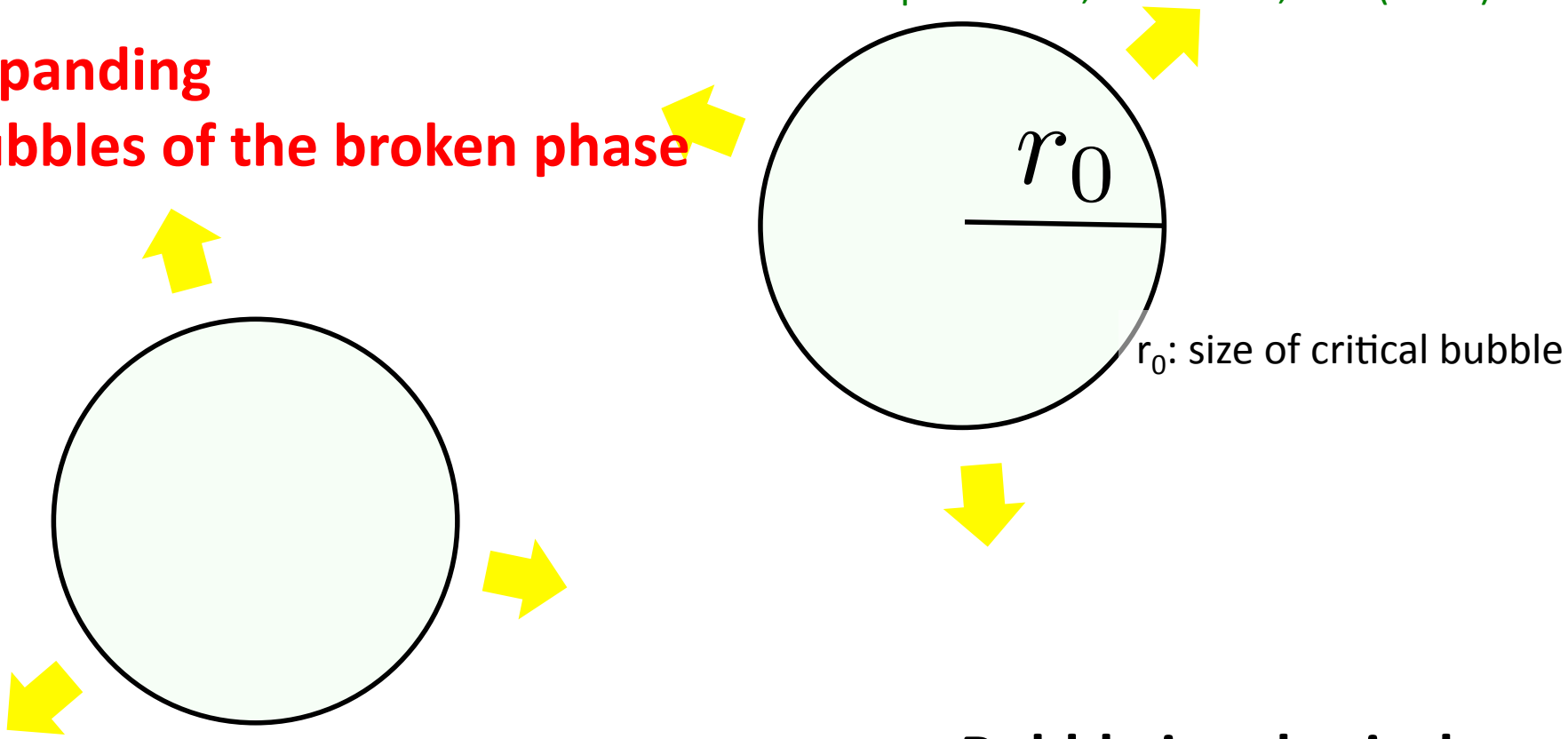

r_0: size of critical bubble

Bubble is spherical
No GW occurs

GWs from 1stOPT

C.Caprini *et al.*, JCAP**1604**, 001 (2016)

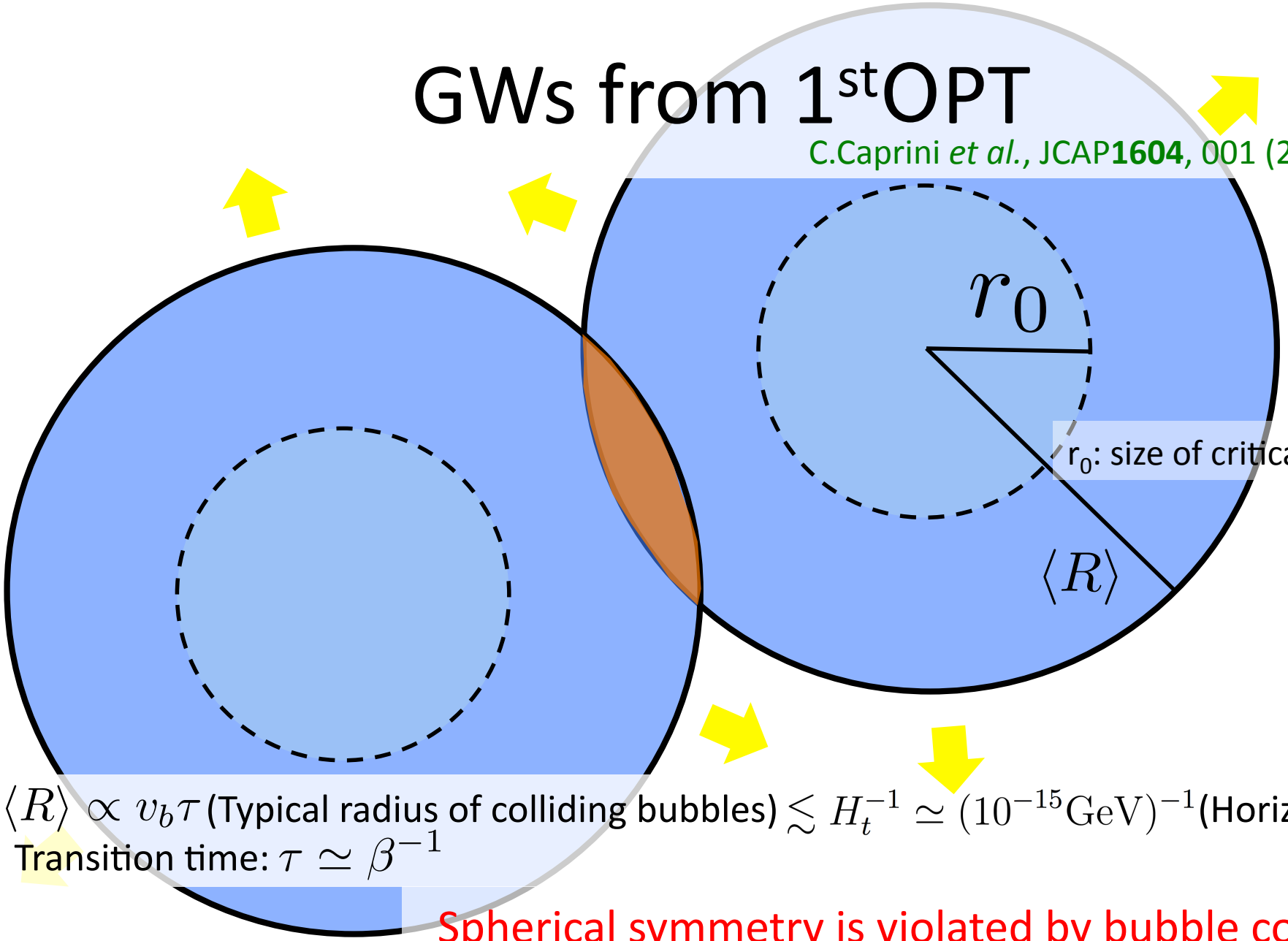

r_0: size of critical bubble

$\langle R \rangle \propto v_b \tau$ (Typical radius of colliding bubbles) $\lesssim H_t^{-1} \simeq (10^{-15}\mathrm{GeV})^{-1}$ (Horizon size),

Transition time: $\tau \simeq \beta^{-1}$

Spherical symmetry is violated by bubble collisions

GWs from 1stOPT

C.Caprini *et al.*, JCAP**1604**, 001 (2016)

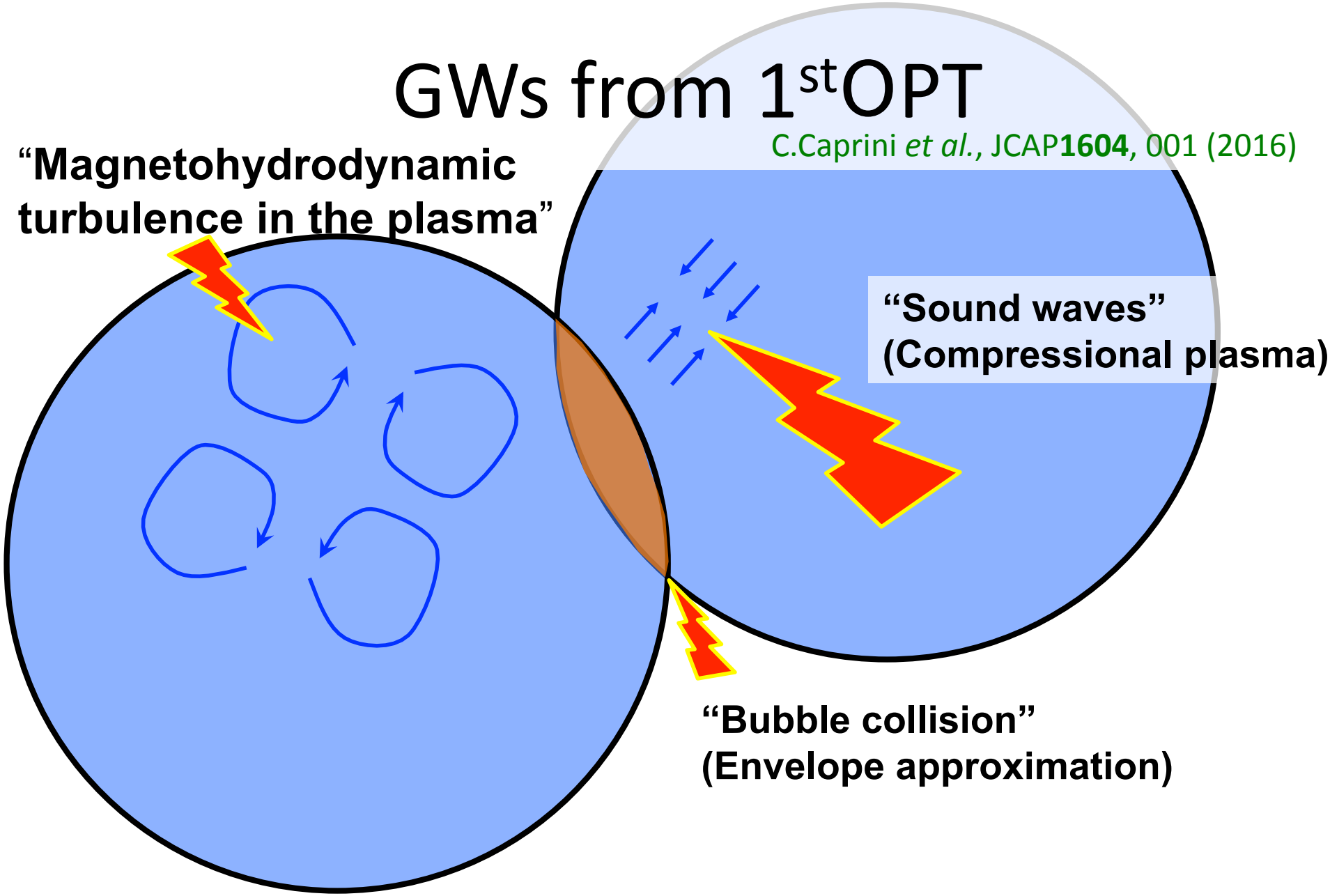

Relic abundance of GWs

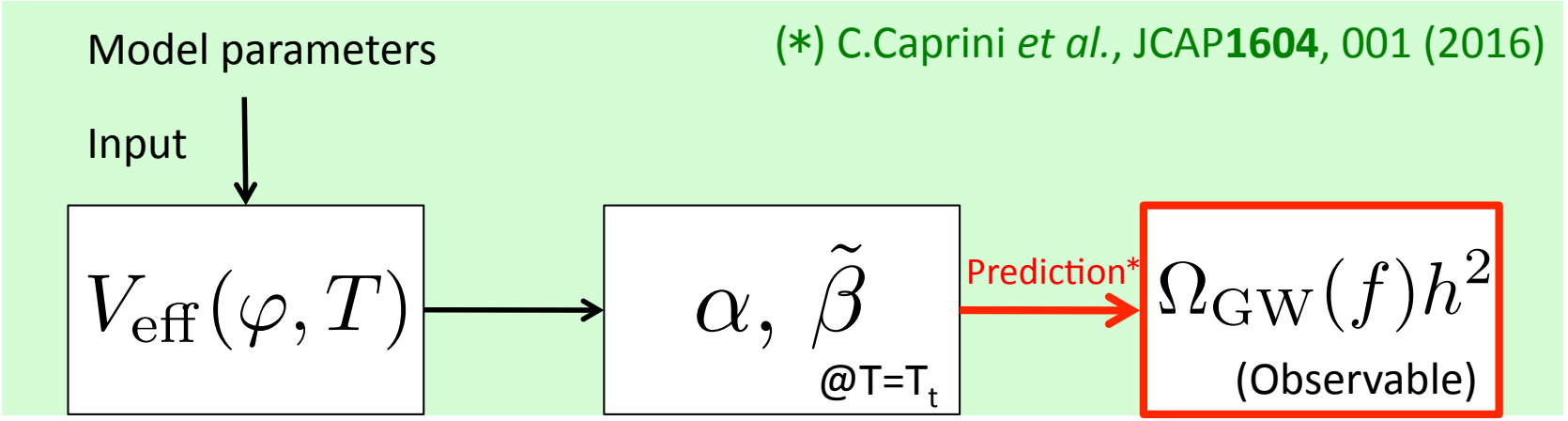

Relic abundance of GWs @ peak frequency

$$\widetilde{\Omega}_{\rm sw}h^2 \simeq 2.65\times10^{-6}\frac{v_b}{\tilde{\beta}}\left(\frac{\kappa(v_b,\alpha)\alpha}{1+\alpha}\right)^2 \quad @\ \tilde{f}_{\rm sw} \simeq 1.9\times10^{-5}\ {\rm Hz}\frac{\tilde{\beta}(T_t/100\ {\rm GeV})}{v_b}$$

$$\widetilde{\Omega}_{\rm env}h^2 \simeq \frac{1.84\times10^{-6}v_b^3}{(0.42+v_b^2)\tilde{\beta}^2}\left(\frac{\kappa(v_b,\alpha)\alpha}{1+\alpha}\right)^2 \quad @\ \tilde{f}_{\rm env} \simeq 1.0\times10^{-5}\ {\rm Hz}\frac{\tilde{\beta}(T_t/100\ {\rm GeV})}{1.8-0.1v_b+v_b^2}$$

$$\widetilde{\Omega}_{\rm turb}h^2 \simeq \frac{9.35\times10^{-8}v_b^2}{0.00354v_b\tilde{\beta}+\tilde{\beta}^2}\left(\frac{\epsilon\kappa(v_b,\alpha)\alpha}{1+\alpha}\right)^{3/2} \quad @\ \tilde{f}_{\rm turb} \simeq 2.7\times10^{-5}\ {\rm Hz}\frac{\tilde{\beta}(T_t/100\ {\rm GeV})}{v_b}$$

Models of 1stOPT

Higgs potential by high temperature approximation

$$V_{\rm eff} = D(T^2 - T_0^2)\varphi^2 - (ET - e)\varphi^3 + \frac{\lambda(T)}{4}\varphi^4 \Rightarrow \frac{\varphi_c}{T_c} = \frac{2E}{\lambda}\left(1 - \frac{e\lambda}{ET}\right)$$

- E : thermal coupling (the non-decoupling effects due to the additional boson loop)
- $-e$: non-thermal coupling (the field mixing of the Higgs boson with additional scalar fields)

Contents

- Motivation: EWBG is detectable at future colliders and GW observations
- Review: GWs from 1st order phase transition
- Models: "O(N) models & "Higgs singlet model"

Models of 1stOPT

Higgs potential by high temperature approximation

$$V_{\rm eff} = D(T^2 - T_0^2)\varphi^2 - (ET - e)\varphi^3 + \frac{\lambda(T)}{4}\varphi^4$$

$$\frac{\varphi_c}{T_c} = \frac{2E}{\lambda}\left(1 - \frac{e\lambda}{ET}\right)$$

- E : thermal coupling (the non-decoupling effects due to the additional boson loop)
- $-e$: non-thermal coupling (the field mixing of the Higgs boson with additional scalar fields)

J.Kehayias and S.Profumo, JCAP**1003**, 003 (2010)

$$115\text{GeV} \le m_h < 348\text{GeV}$$

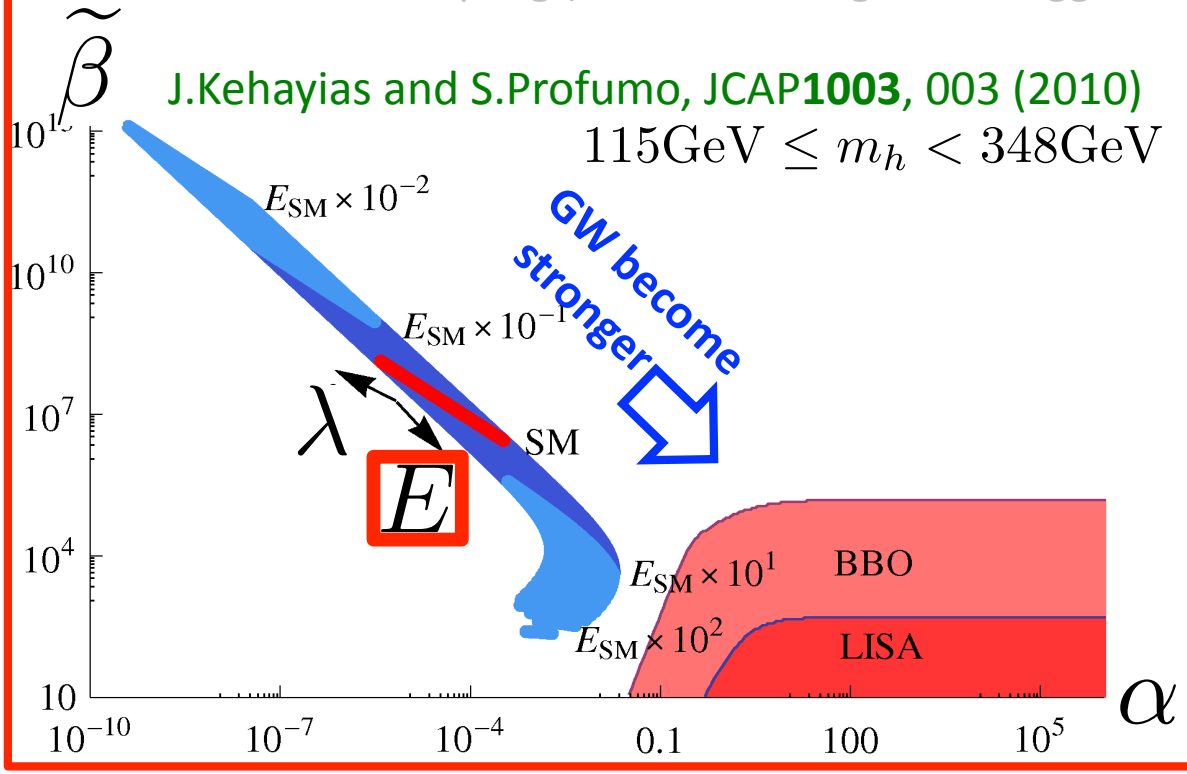

As the simplest model, we have investigated **the O(N) model**.

Models of 1stOPT

Higgs potential by high temperature approximation

$$V_{\rm eff} = D(T^2 - T_0^2)\varphi^2 - (ET - e)\varphi^3 + \frac{\lambda(T)}{4}\varphi^4 \Rightarrow \frac{\varphi_c}{T_c} = \frac{2E}{\lambda}\left(1 - \frac{e\lambda}{ET}\right)$$

- E : thermal coupling (the non-decoupling effects due to the additional boson loop)
- $-e$: non-thermal coupling (the field mixing of the Higgs boson with additional scalar fields)

``O(*N*) model''

N iso-singlet fields with O(*N*) sym. $\vec{S} = (S_1, S_2, \cdots, S_N)^T$

M.Kakizaki, S.Kanemura, T.Matsui, Phys. Rev. D **92**, no. 11, 115007 (2015)

$$V_0(\Phi, \vec{S}) = -\mu^2|\Phi|^2 + \frac{\mu_S^2}{2}|\vec{S}|^2 + \frac{\lambda}{4}|\Phi|^4 + \frac{\lambda_S}{4}|\vec{S}|^4 + \frac{\lambda_{\Phi S}}{2}|\Phi|^2|\vec{S}|^2$$

- O(*N*) is not broken →Common mass of S_i: $m_S^2 = \mu_S^2 + \frac{\lambda_{\Phi S}}{2}v^2$
- Model parameters: (N, m_S, μ_S)
- 1stOPT: $E = \frac{1}{12\pi v^3}\left\{6m_{W^\pm}^3 + 3m_Z^3 + N\, m_S^3\left(1 - \frac{\mu_S^2}{m_S^2}\right)^3\left(1 + \frac{3}{2}\frac{\mu_S^2}{m_S^2}\right)\right\}$

$V_{\rm eff}(\varphi, T)$ → $\Delta\lambda_{hhh}$

$\varphi_c/T_c \nearrow \Rightarrow \Delta\lambda_{hhh} \nearrow$

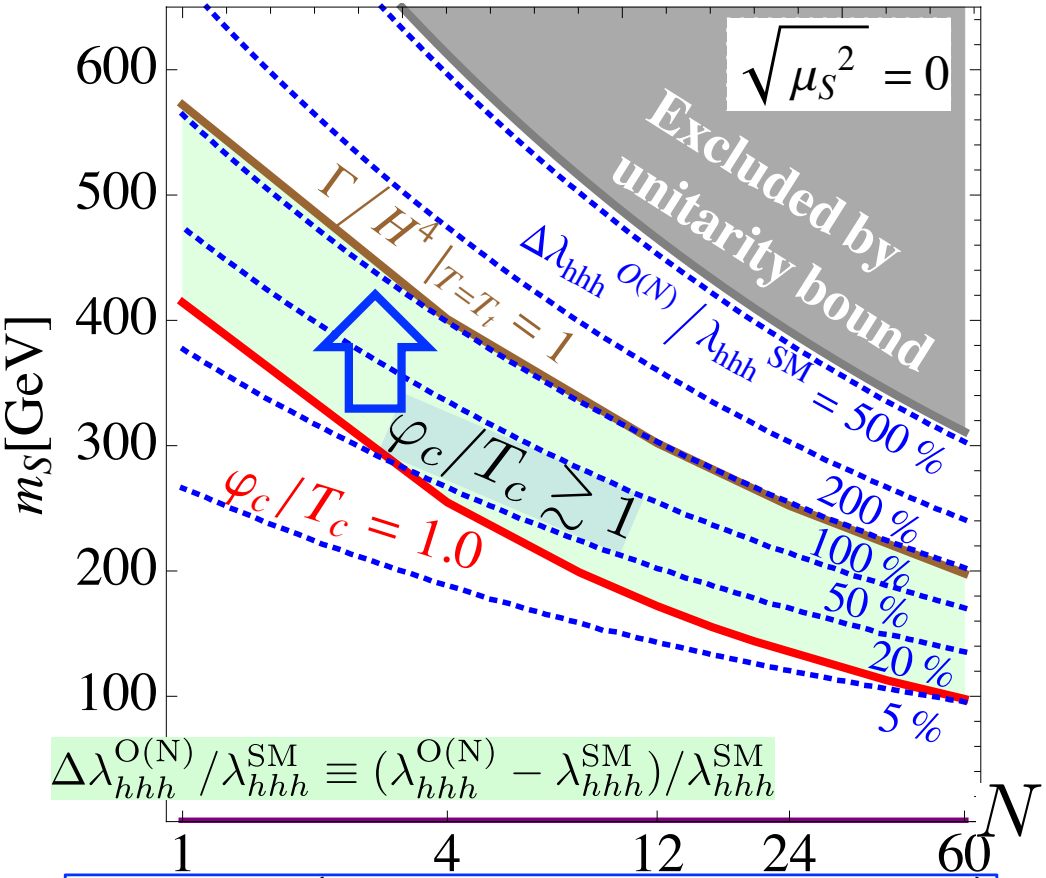

$$\lambda_{hhh}^{\rm O(N)} \equiv \frac{3m_h^2}{v}\left\{1 - \frac{m_t^4}{\pi^2 m_h^2 v^2} + \frac{N m_S^4}{12\pi^2 m_h^2 v^2}\left(1 - \frac{\mu_S^2}{m_S^2}\right)^3\right\}$$

M.Kakizaki, S.Kanemura, T.Matsui, Phys. Rev. D **92**, no. 11, 115007 (2015)

$\varphi_c/T_c \nearrow \Rightarrow \Delta\lambda_{hhh} \nearrow$

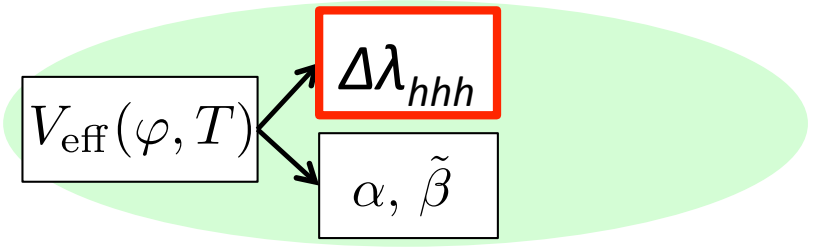

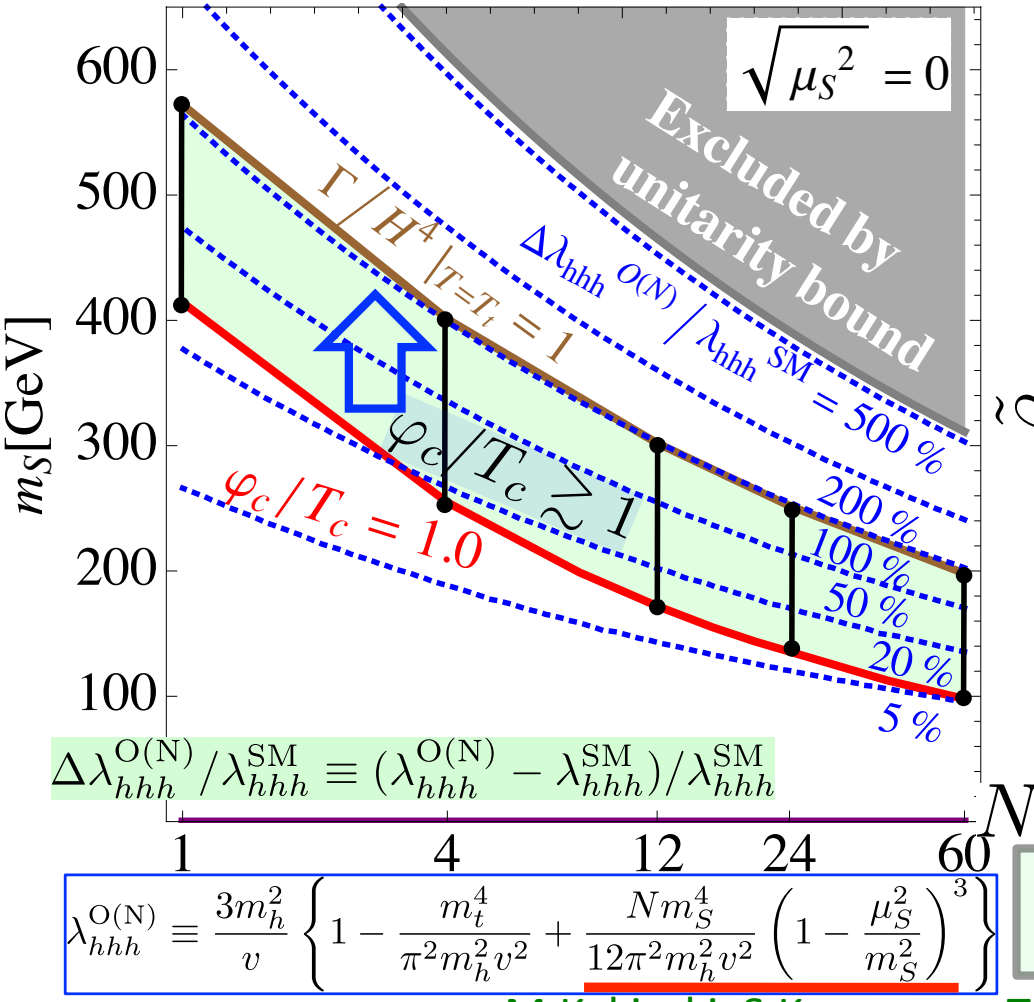

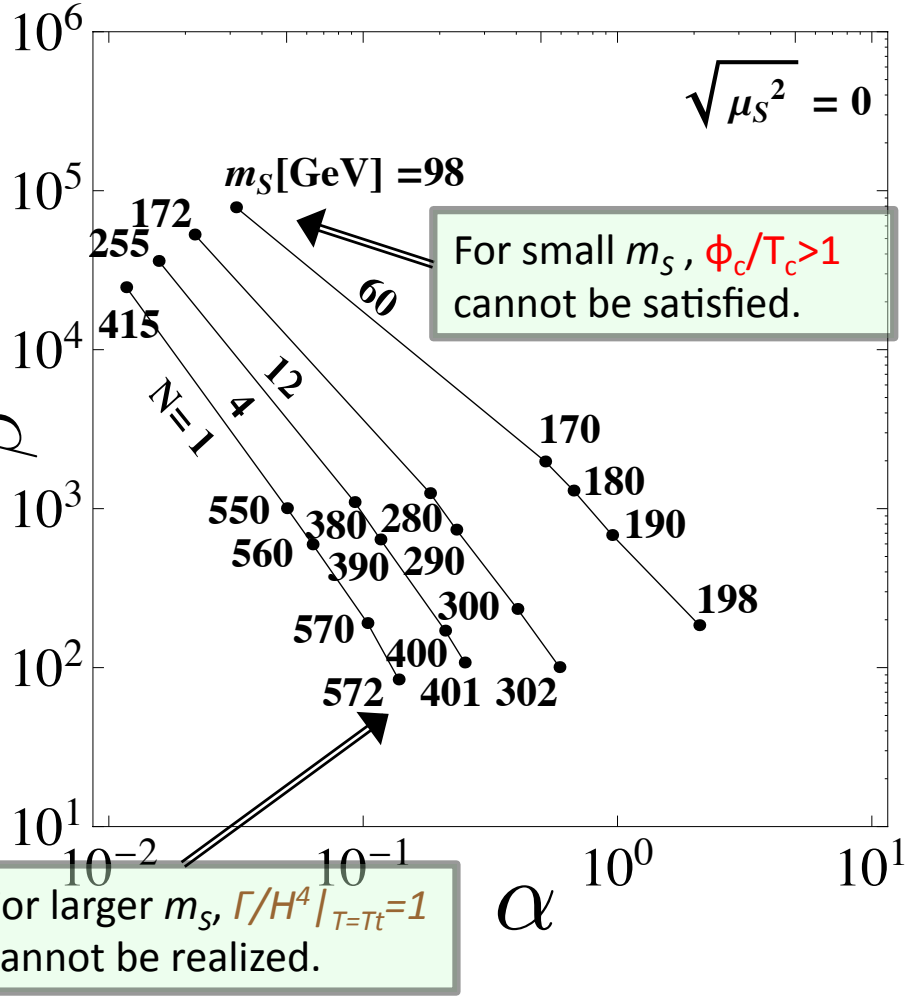

For small m_S, ϕ_c/T_c>1 cannot be satisfied.

For larger m_S, $\Gamma/H^4|_{T=Tt}$=1 cannot be realized.

M.Kakizaki, S.Kanemura, T.Matsui, Phys. Rev. D **92**, no. 11, 115007 (2015)

$V_{\rm eff}(\varphi, T)$ → $\Delta\lambda_{hhh}$, α, $\tilde{\beta}$

$\varphi_c/T_c \nearrow \Rightarrow \Delta\lambda_{hhh} \nearrow$

If the deviation in *hhh* is measured at future colliders, …

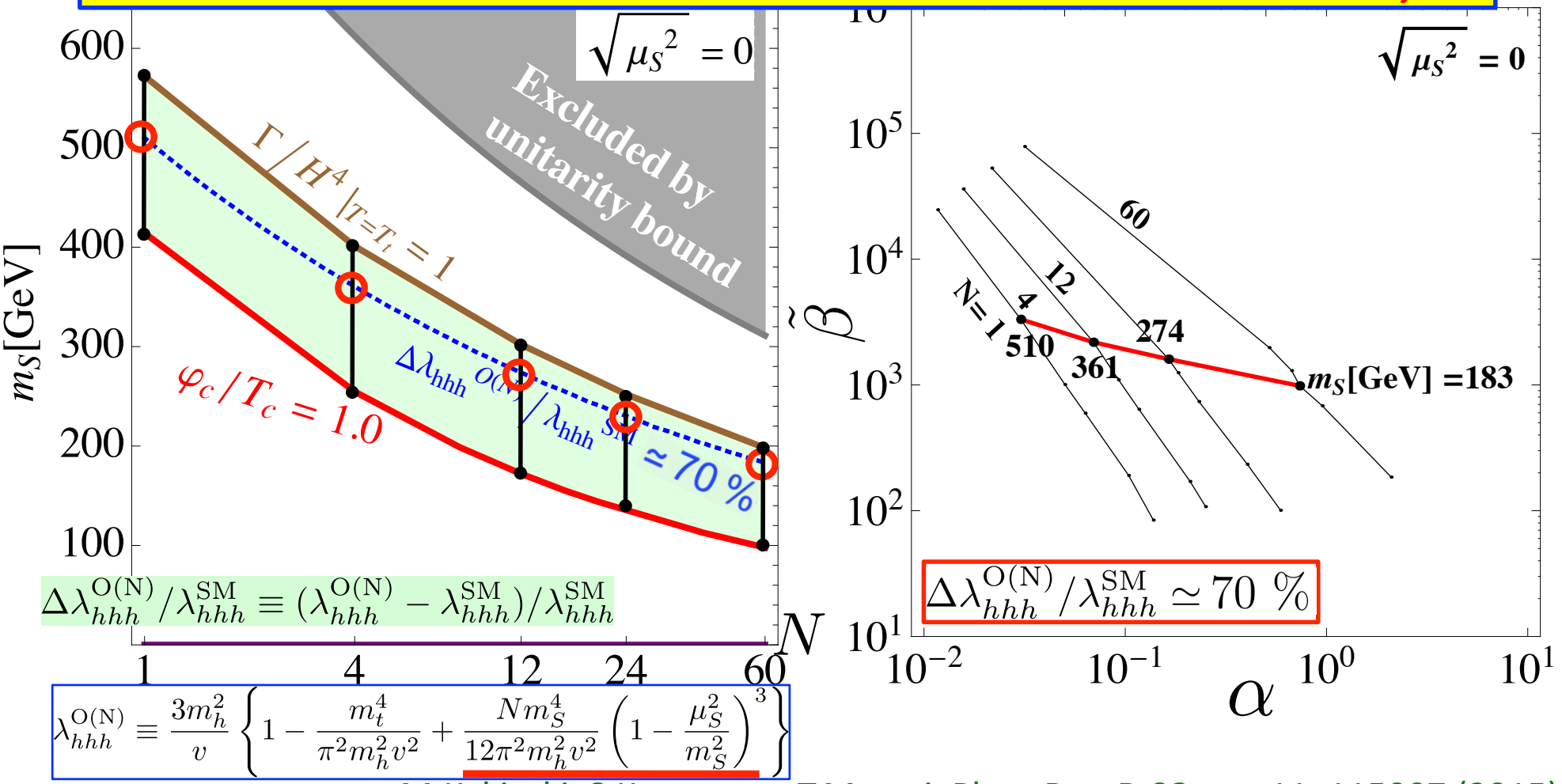

M.Kakizaki, S.Kanemura, T.Matsui, Phys. Rev. D **92**, no. 11, 115007 (2015)

$\varphi_c/T_c \nearrow \Rightarrow \Delta\lambda_{hhh} \nearrow$

$V_{\rm eff}(\varphi, T)$ → $\Delta\lambda_{hhh}$, α, $\tilde{\beta}$

If the deviation in *hhh* is measured at future colliders, …

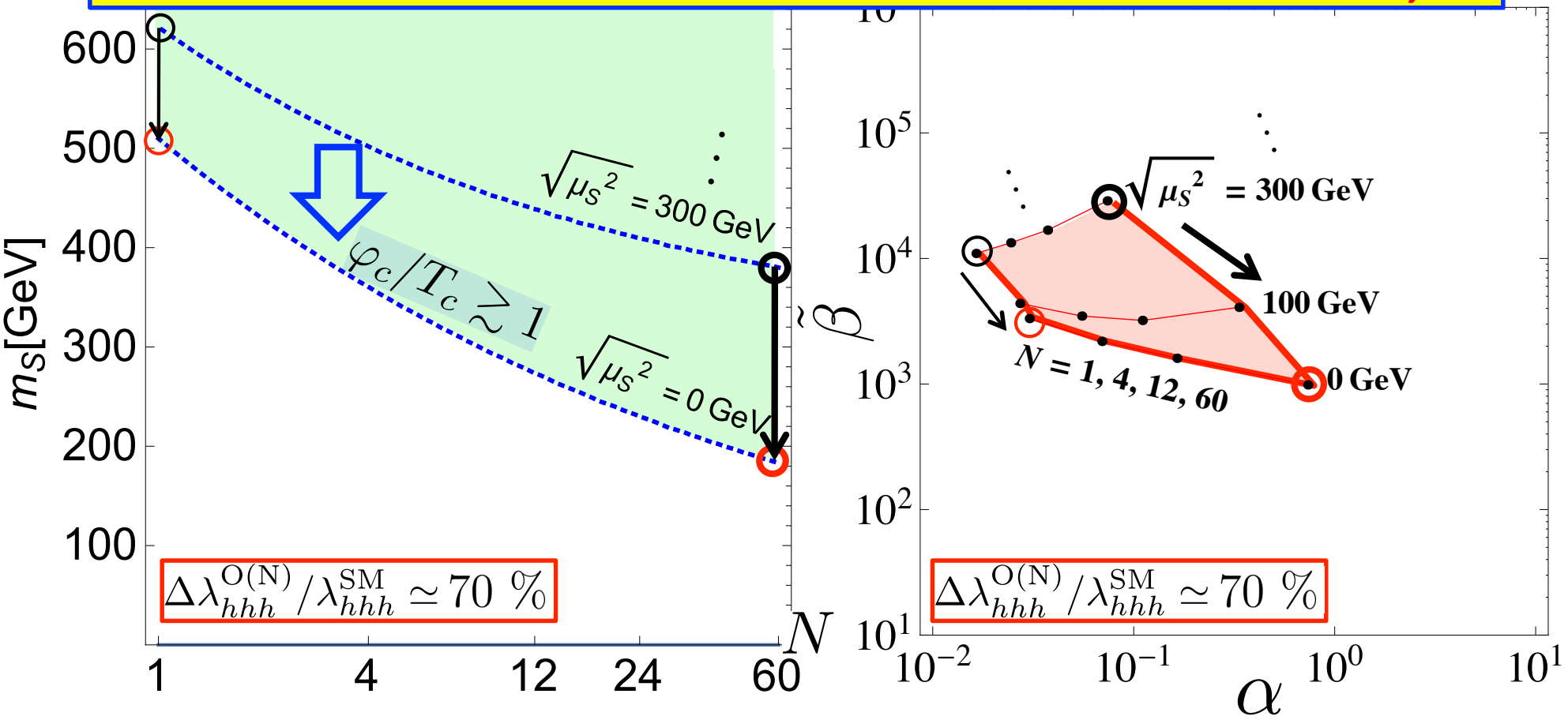

M.Kakizaki, S.Kanemura, T.Matsui, Phys. Rev. D **92**, no. 11, 115007 (2015)

$V_{\rm eff}(\varphi, T)$ → $\Delta\lambda_{hhh}$, α, $\tilde{\beta}$

$\varphi_c/T_c \nearrow \Rightarrow \Delta\lambda_{hhh} \nearrow$

If the deviation in *hhh* is measured at future colliders, …

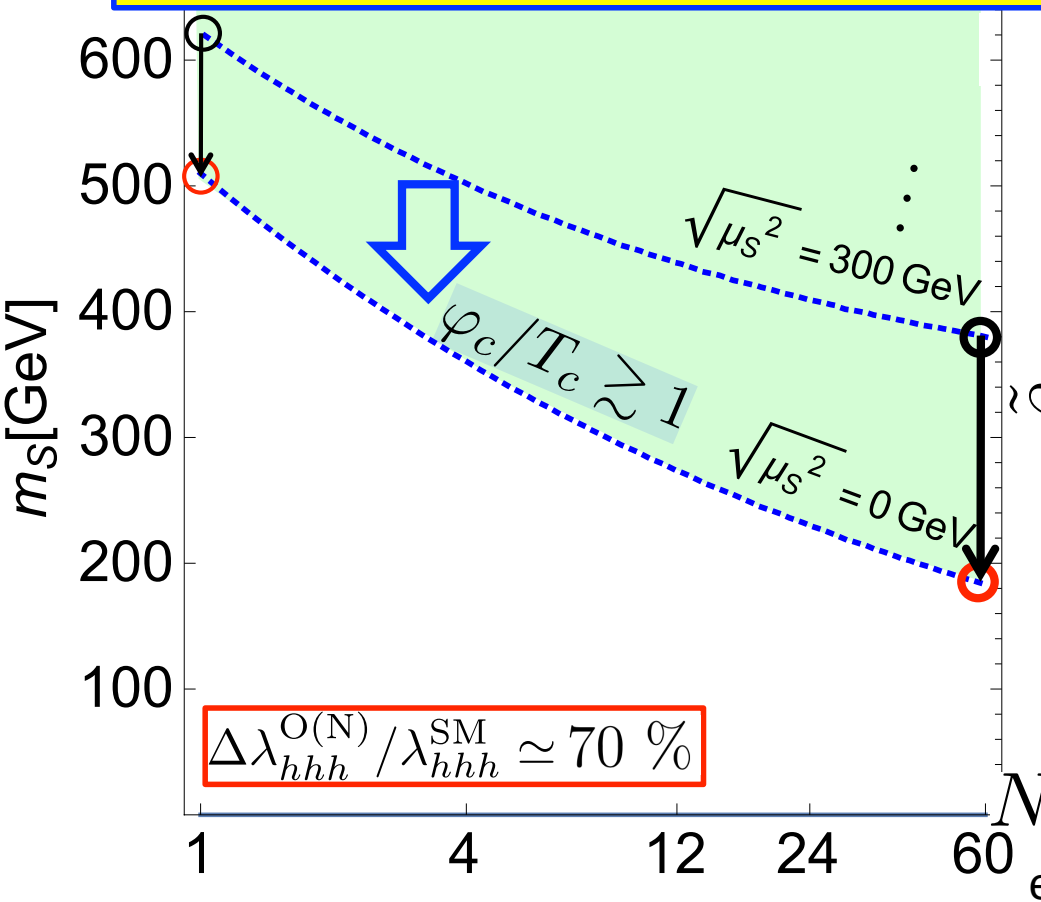

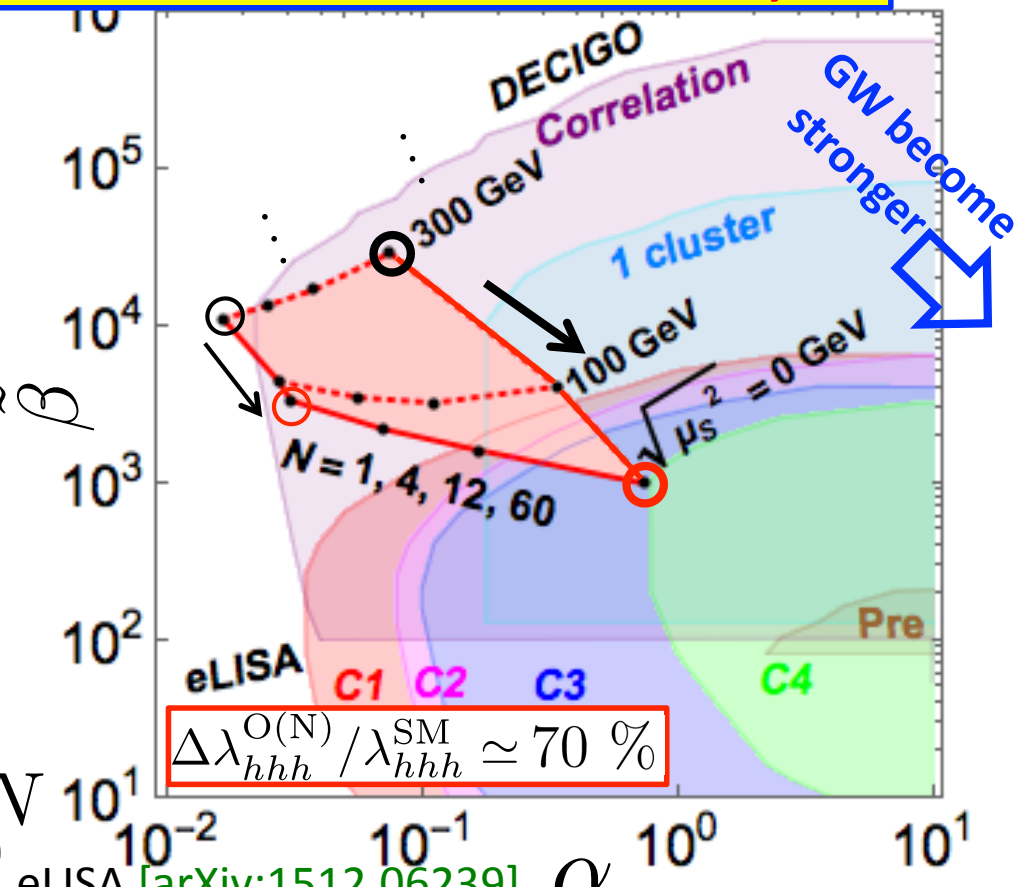

eLISA [arXiv:1512.06239],
DECIGO [Class. Quant. Grav. 28, 094011 (2011)]
M.Kakizaki, S.Kanemura, T.Matsui, Phys. Rev. D **92**, no. 11, 115007 (2015)

$\varphi_c/T_c \nearrow \Rightarrow \Delta\lambda_{hhh} \nearrow$ & $\Omega_{\rm GW}h^2 \nearrow$

$V_{\rm eff}(\varphi, T)$ → $\Delta\lambda_{hhh}$

$V_{\rm eff}(\varphi, T)$ → $\alpha,\ \tilde{\beta}$ → $\Omega_{\rm GW}(f)h^2$

If the deviation in *hhh* is measured at future colliders, …

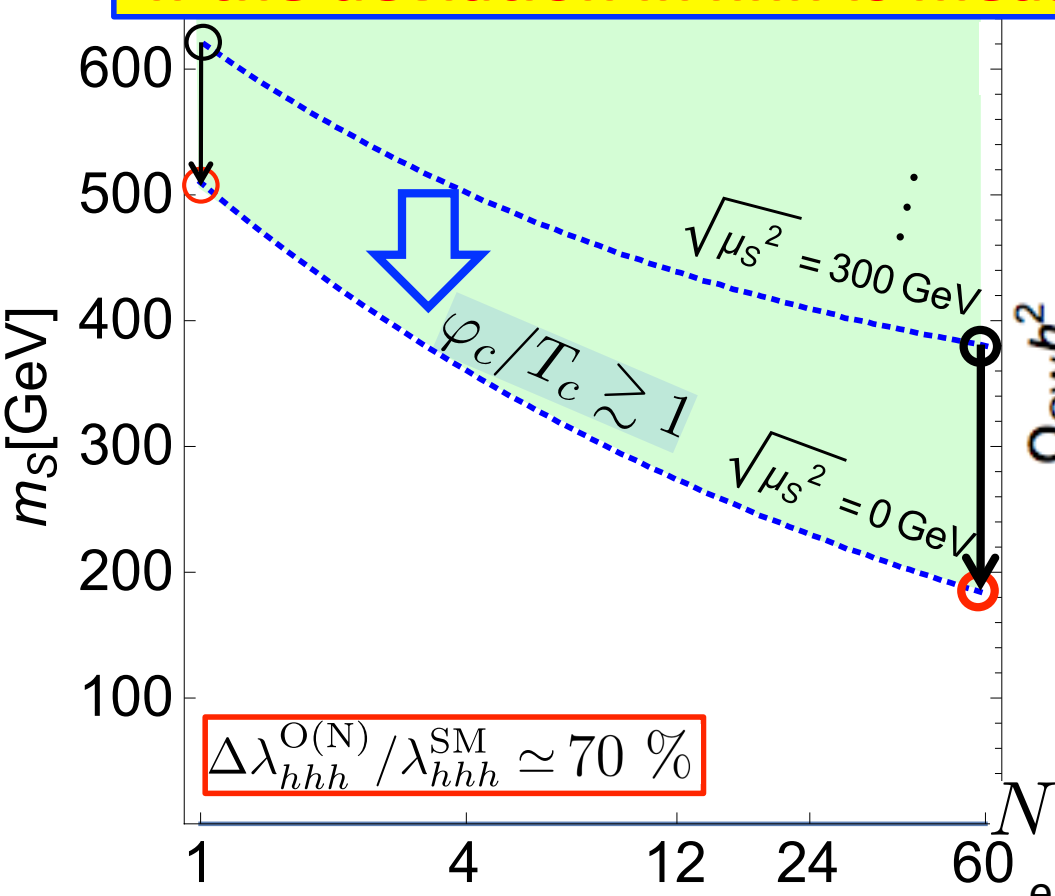

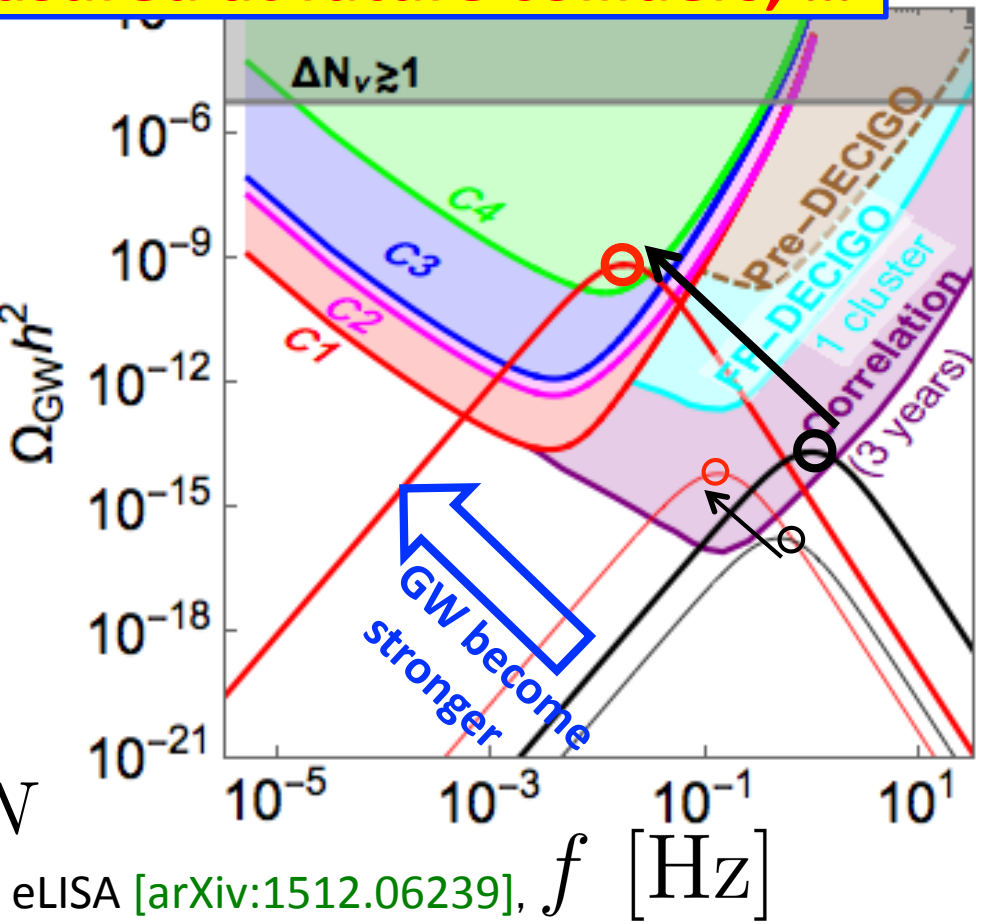

eLISA [arXiv:1512.06239], DECIGO [Class. Quant. Grav. 28, 094011 (2011)]

M.Kakizaki, S.Kanemura, T.Matsui, Phys. Rev. D **92**, no. 11, 115007 (2015)

$\varphi_c/T_c \nearrow \Rightarrow \Delta\lambda_{hhh} \nearrow$ & $\Omega_{\rm GW}h^2 \nearrow$

$V_{\rm eff}(\varphi, T)$ → $\Delta\lambda_{hhh}$, α, $\tilde{\beta}$ → $\Omega_{\rm GW}(f)h^2$

If the deviation in *hhh* is measured at future colliders, …

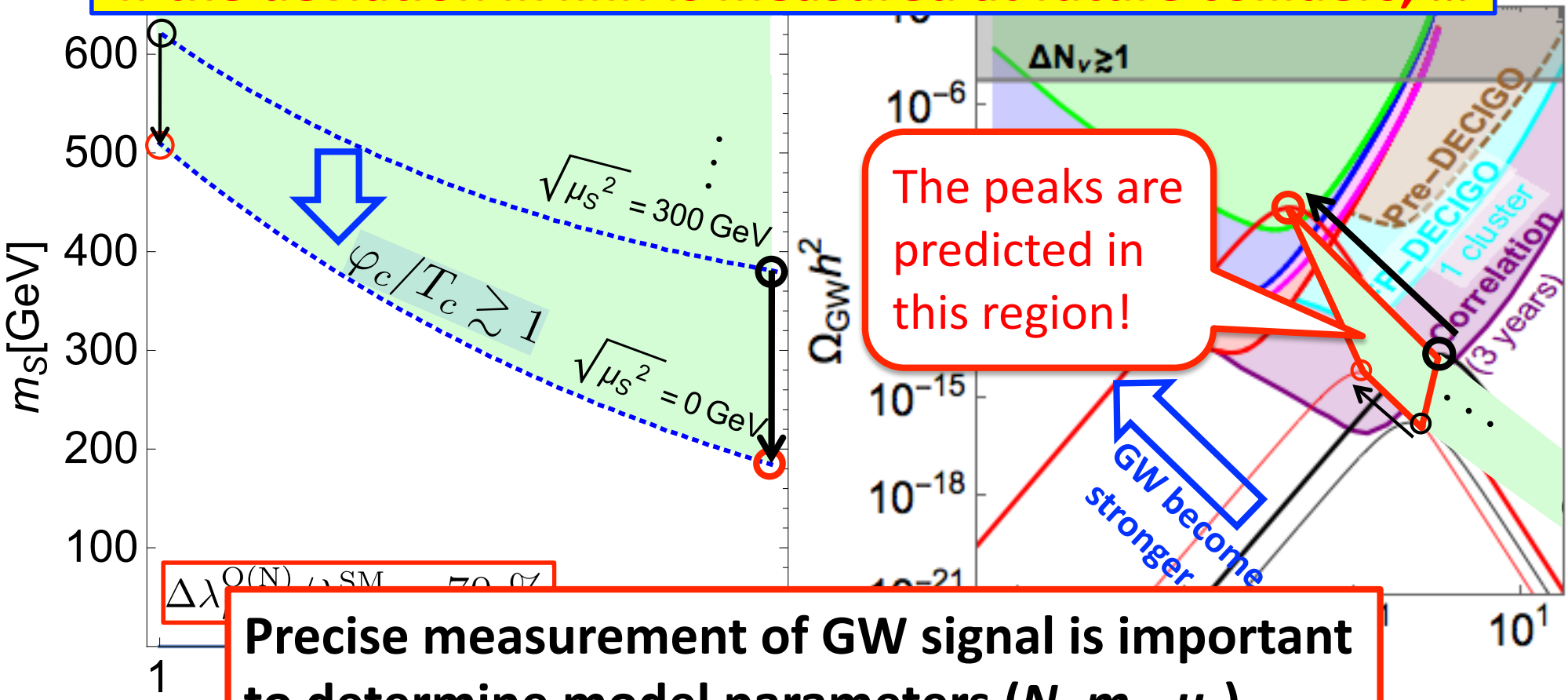

Precise measurement of GW signal is important to determine model parameters (N, m_S, μ_S).

DECIGO [Class. Quant. Grav. 28, 094011 (2011)]

M.Kakizaki, S.Kanemura, T.Matsui, Phys. Rev. D **92**, no. 11, 115007 (2015)

Models of 1stOPT

Higgs potential by high temperature approximation

$$V_{\rm eff} = D(T^2 - T_0^2)\varphi^2 - (ET - e)\varphi^3 + \frac{\lambda(T)}{4}\varphi^4 \quad \Rightarrow \quad \frac{\varphi_c}{T_c} = \frac{2E}{\lambda}\left(1 - \frac{e\lambda}{ET}\right)$$

- E : thermal coupling (the non-decoupling effects due to the additional boson loop)
- $-e$: non-thermal coupling (the field mixing of the Higgs boson with additional scalar fields)

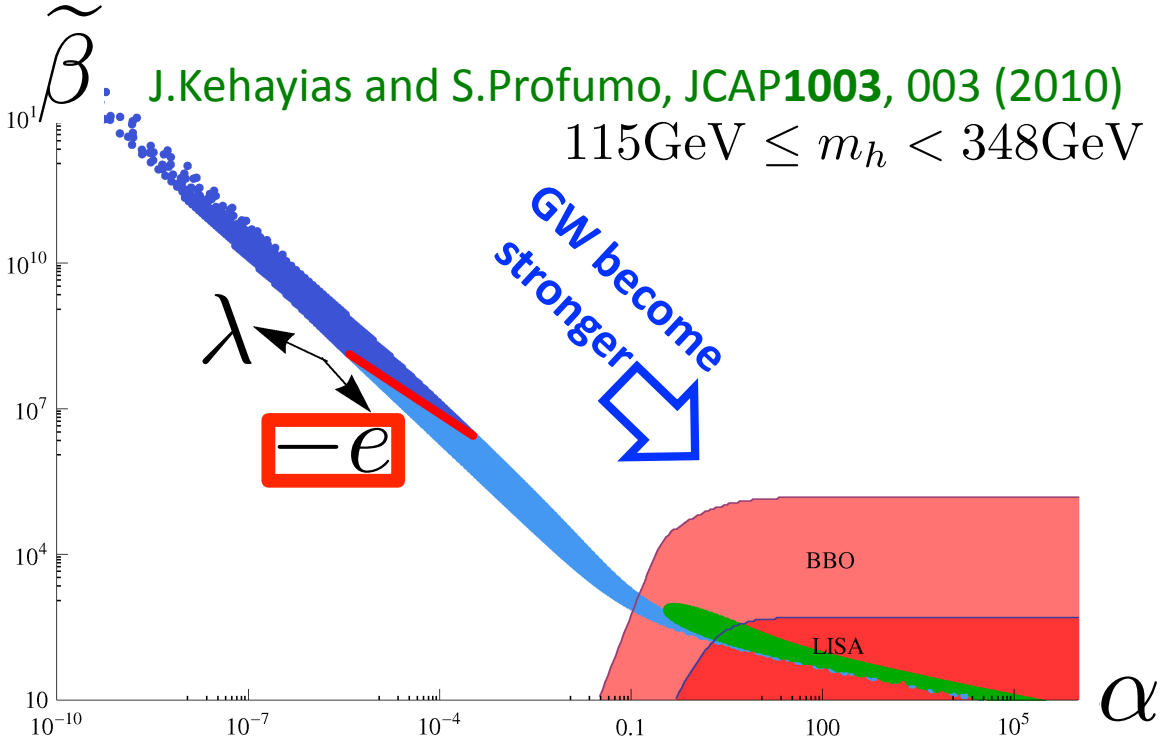

As the simplest model, we have investigated **the Higgs singlet model (HSM)**.

Models of 1stOPT

Higgs potential by high temperature approximation

$$V_{\rm eff} = D(T^2 - T_0^2)\varphi^2 - (ET - e)\varphi^3 + \frac{\lambda(T)}{4}\varphi^4 \Rightarrow \frac{\varphi_c}{T_c} = \frac{2E}{\lambda}\left(1 - \frac{e\lambda}{ET}\right)$$

- E : thermal coupling (the non-decoupling effects due to the additional boson loop)
- $-e$: non-thermal coupling (the field mixing of the Higgs boson with additional scalar fields)

``Higgs singlet model (HSM)''

$$\Phi = \begin{pmatrix} G^+ \\ \frac{1}{\sqrt{2}}(v_\Phi + \phi_1 + iG^0) \end{pmatrix}, \quad S = v_S + \phi_2$$

K.Hashino, M.Kakizaki, S.Kanemura, T.Matsui, P.Ko, arXiv:1609.00297

$$V_0 = -\mu_\Phi^2|\Phi|^2 + \lambda_\Phi|\Phi|^4 + \mu_{\Phi S}|\Phi|^2 S + \frac{\lambda_{\Phi S}}{2}|\Phi|^2 S^2 + \mu_S^3 S + \frac{m_S^2}{2}S^2 + \frac{\mu_S'}{3}S^3 + \frac{\lambda_S}{4}S^4$$

eight parameters $\mu_\Phi^2, m_S^2, \lambda_\Phi, \lambda_S, \lambda_{\Phi S}, \mu_{\Phi S}, \mu_S'$ and μ_S^3

- Tadpole conditions → (v_Φ, v_S)
- Diagonalized mass matrix in (ϕ_1, ϕ_2) → (m_h, m_H) and θ
- 1stOPT is calculated by two-field analysis @finite T.

Constraints

- Higgs couplings: $\kappa \equiv \kappa_V = \kappa_F = \cos\theta$
  - recent LHC data: $\kappa_Z = 1.03^{+0.11}_{-0.11}, \kappa_W = 0.91^{+0.10}_{-0.10}$
    (1σ; combination of ATLAS and CMS) [ATLAS-CONF-2015-044]
  - Expected accuracy: 2%@HL-LHC 14TeV 3000fb^{-1} [1307.7135],
    0.37% (0.51%) for κ_Z (κ_W)@ILC 500GeV 500fb^{-1} [1506.05992]
- Deviation of *hhh* coupling from SM: $\Delta\lambda_{hhh} \equiv \frac{\lambda^{\rm HSM}_{hhh} - \lambda^{\rm SM}_{hhh}}{\lambda^{\rm SM}_{hhh}}$
  - Expected accuracy: 54%@HL-LHC 14TeV 3000fb^{-1} [CMS-PAS-FTR-15-002],
    27%@ILC 500GeV 4000fb^{-1} [1506.05992],
    16% (10%)@ILC 1TeV 2000fb^{-1} (5000fb^{-1}) [1506.05992]
- Benchmark points K. Fuyuto and E. Senaha, PRD 90, 015015 (2014)

v_Φ [GeV]	v_S [GeV]	m_h [GeV]	$\mu_{\Phi S}$ [GeV]	μ'_S [GeV]	μ_S [GeV]	m_H [GeV]	θ [degrees]
246.2	90	125.5	−80	−30	0	[160, 240]	[−15, −35]

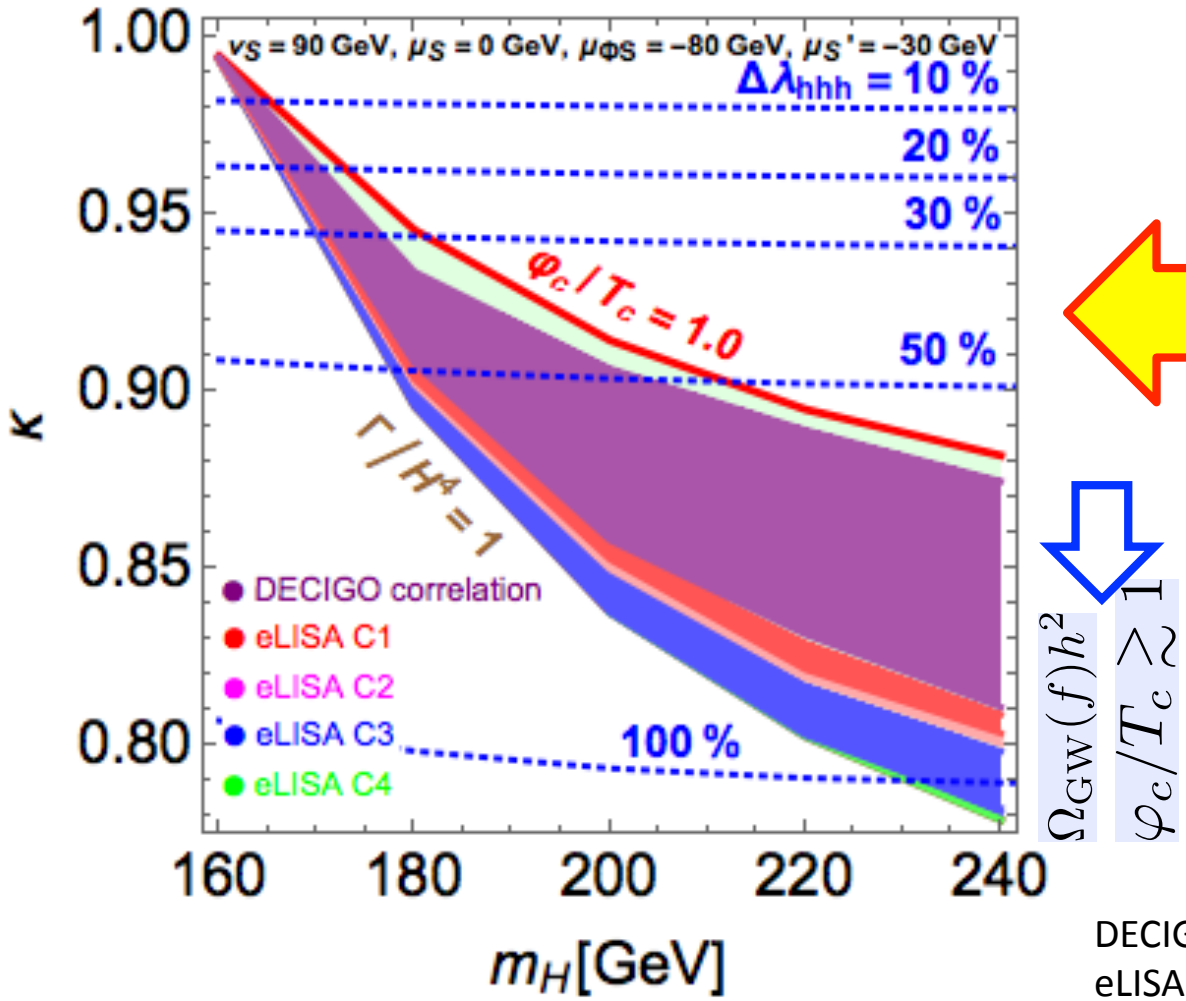

$\Omega_{GW}(f)h^2 \gtrsim 1$

$\varphi_c/T_c \gtrsim 1$

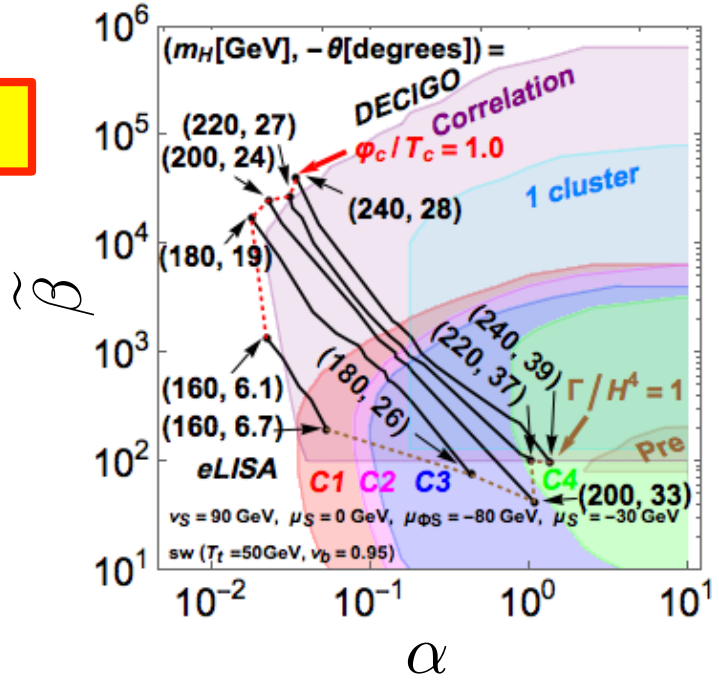

DECIGO [Class. Quant. Grav. 28, 094011 (2011)],
eLISA [arXiv:1512.06239]

K.Hashino, M.Kakizaki, S.Kanemura, T.Matsui, P.Ko, arXiv:1609.00297

The synergy between the precision measurements of the Higgs boson couplings and GWs at future experiments is important!

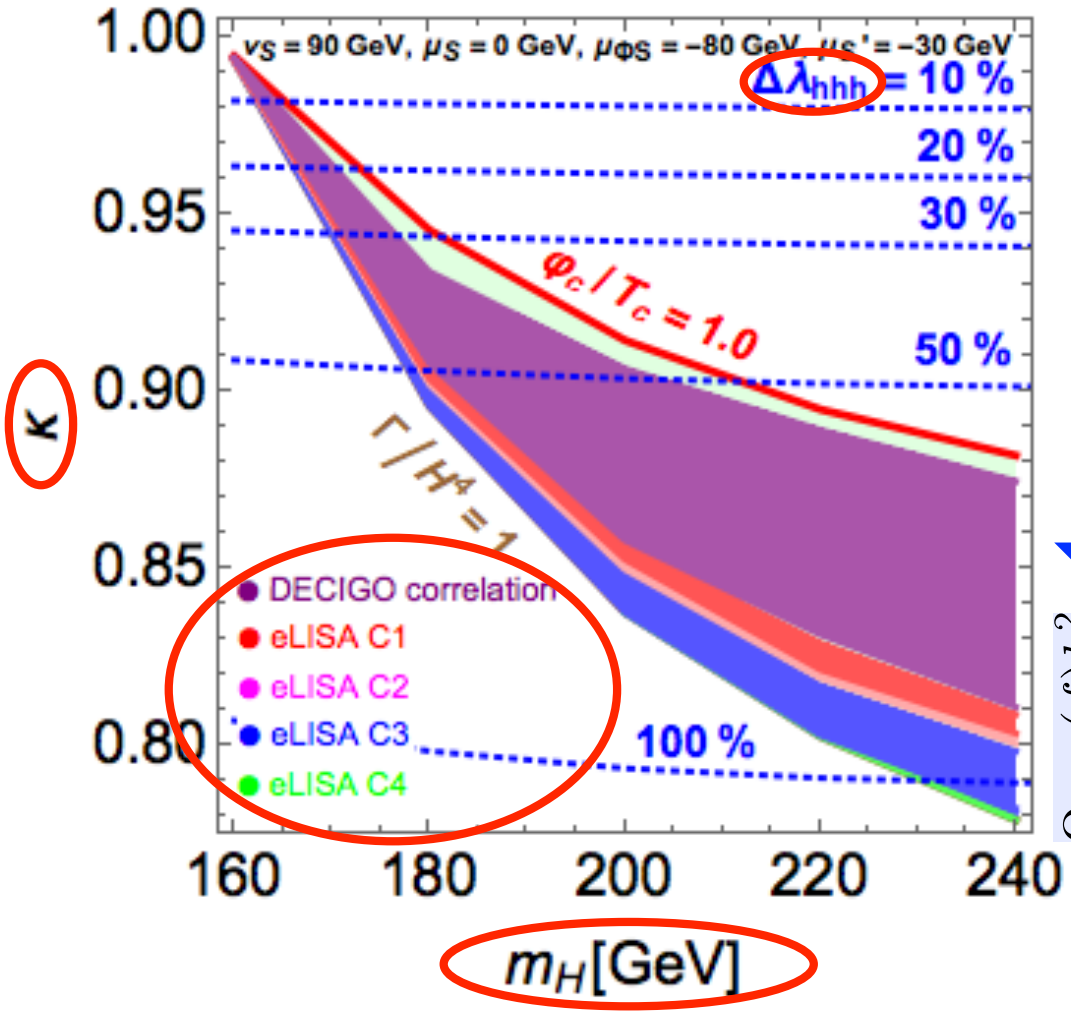

$\Omega_{GW}(f)h^2 \gtrsim 1$

$\varphi_c/T_c \gtrsim 1$

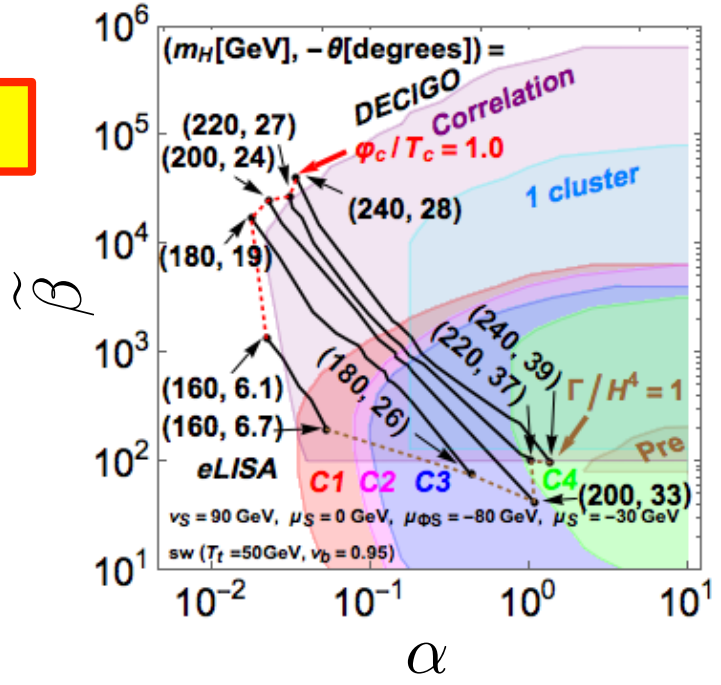

DECIGO [Class. Quant. Grav. 28, 094011 (2011)],
eLISA [arXiv:1512.06239]

K.Hashino, M.Kakizaki, S.Kanemura, T.Matsui, P.Ko, arXiv:1609.00297

Conclusions

- Exploring the structure of the Higgs sector is important to understand physics behind EWSB.
- We have investigated various models of 1stOPT.
- The strongly 1stOPT of EWSB can be tested by the measurements of various Higgs boson couplings @LHC, the *hhh* coupling @ILC and GWs @future space-based interferometers.

Back Up

Triple Higgs boson coupling measurements

- HL-LHC (14TeV, 3000fb^{-1})

$\Delta\lambda_{hhh}/\lambda_{hhh}$~50%(gg→hh)

Snowmass Higgs working group,
arXiv:1310.8361 [hep-ex]

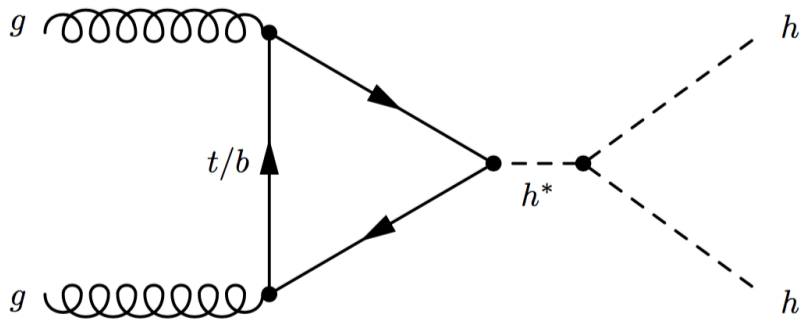

- ILC1000-up (500/1000GeV, 1600+2500fb^{-1})

$\Delta\lambda_{hhh}/\lambda_{hhh}$~10%(ee→vvhh)

K.Fujii *et al.*, arXiv:1506.05992 [hep-ex]

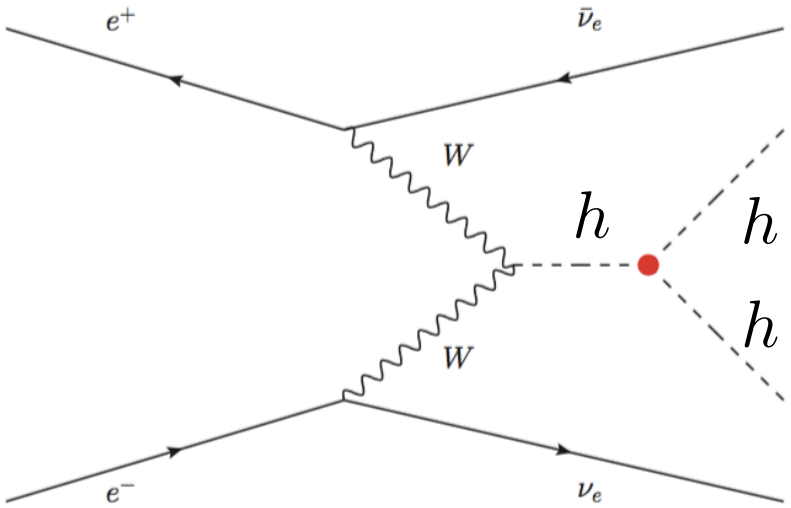

LIGO have detected GWs

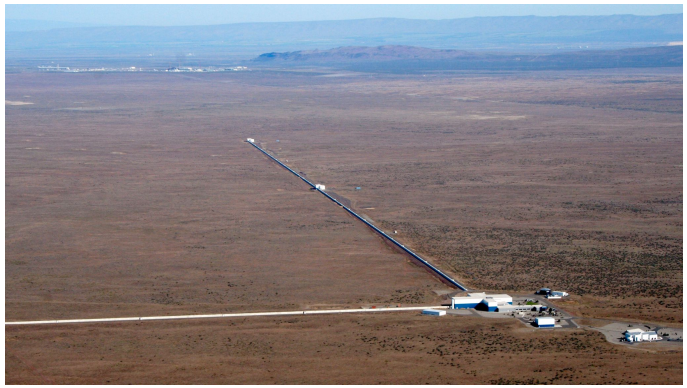

- “GW150914” LIGO Scientific and Virgo Collaborations, Phys. Rev. Lett. **116**, no. 6, 061102 (2016)
  - BH merger (36+29→62 in the unit of solar mass)
  - 410Mpc (1.3 billion years ago)
  - Signal/Noise=24 (>5.1σ), frequency: 35-250 Hz
- "GW151226” LIGO Scientific and Virgo Collaborations, Phys. Rev. Lett. **116**, no. 24, 241103 (2016)
  - BH merger (14+8→21 in the unit of solar mass)
  - 440Mpc (1.4 billion years ago)
  - Signal/Noise=13 (>5σ), frequency: 35-450 Hz,

Prospects for LIGO/Virgo

- LIGO 1st RUN (2015/09/12-2016/01/19)
- LIGO 2nd RUN (from the fall 2016)
  - 15-25% improvement in sensitivity performance over 1st RUN
  - The event rate will be increased by 1.5-2 times

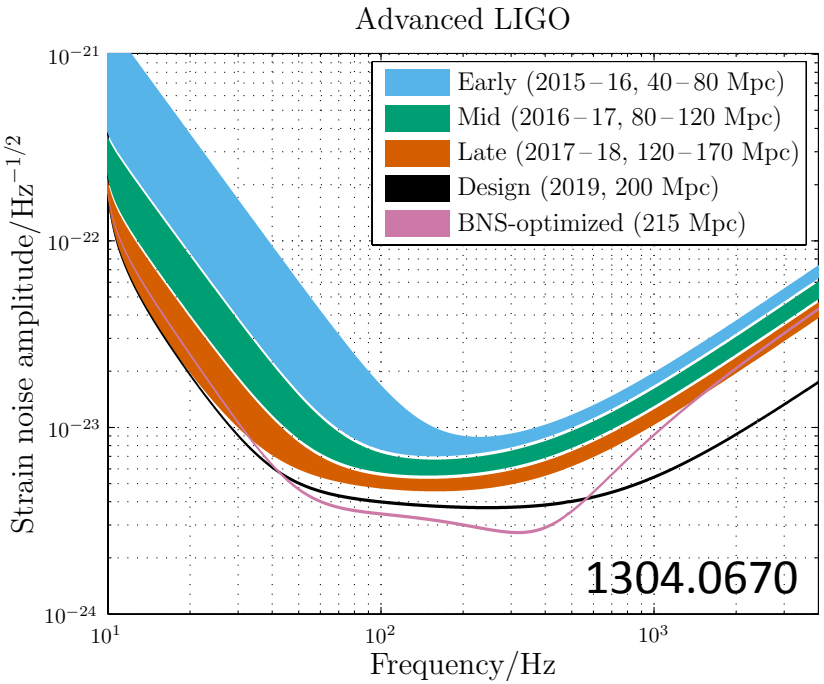

Observing run	Epoch	Duration (months)	aLIGO sensitivity	AdVirgo sensitivity
O1	2015–2016	4	Early	—
O2	2016–2017	6	Mid	Early
O3	2017–2018	9	Late	Mid
O4	2019	12	Design	Late
O5	2020+	–	Design	Design

1602.03847

Pulsar Timing Array

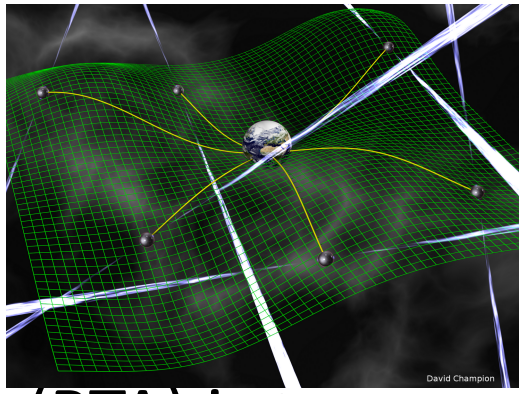

- The main idea behind pulsar timing array (PTA) is to use ultra-stable millisecond pulsars as beacons for detecting GW in the nano-Hz range (10^{-9} – 10^{-7} Hz).
- Pulsars are neutron stars with rapid rotation and strong magnetic field. Period from few seconds to few milliseconds.

Pulsar Timing Array

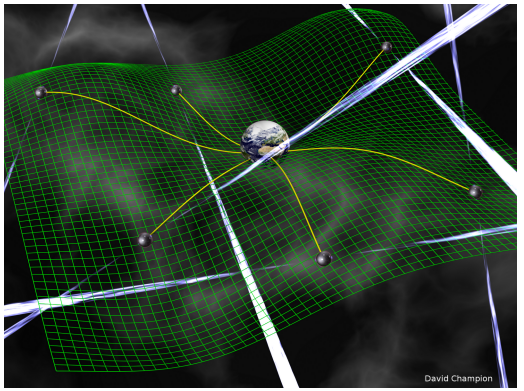

- Current limit: $\Omega_{GW}h^2>\sim10^{-9}$

  EPTA Collaboration [Mon. Not. Roy. Astron. Soc. **453**, no. 3, 2576 (2015) [arXiv:1504.03692]]

  NANOGrav Collaboration [Astrophys. J. **821**, no. 1, 13 (2016) [arXiv:1508.03024]]

- **International Pulsar Timing Array** (IPTA): combined three PTAs [PPTA (Australian), EPTA (European)*, NanoGrav (North American)]. *EPTA consists of 5 radio telescopes

  1st data release Mon. Not. Roy. Astron. Soc. **458**, 1267 (2016) [arXiv:1602.03640]

  Expected limit: $\Omega_{GW}h^2>\sim10^{-12}$ Publ. Astron. Soc. Austral. **30**, 17 (2013) [arXiv:1210.6130]

- **Square Kilometer Array** (SKA)

  : The next great advancement in radio astronomy

  Expected limit: $\Omega_{GW}h^2>\sim10^{-15}$ https://www.skatelescope.org

Properties of the representative eLISA configurations

eLISA cosmology WG report, JCAP**1604**, 001 (2016) [arXiv:1512.06239]

- **Number of laser links :** 4 or 6, corresponding to 2 or 3 interferometer arms

- **Arm length :** 1 / 2 / 5 million km
- **Duration :** 2 / 5 years data taking
- **Noise level** : N2 (LISA pathfinder expected) is 10 times larger than N1 (LISA pathfinder required)

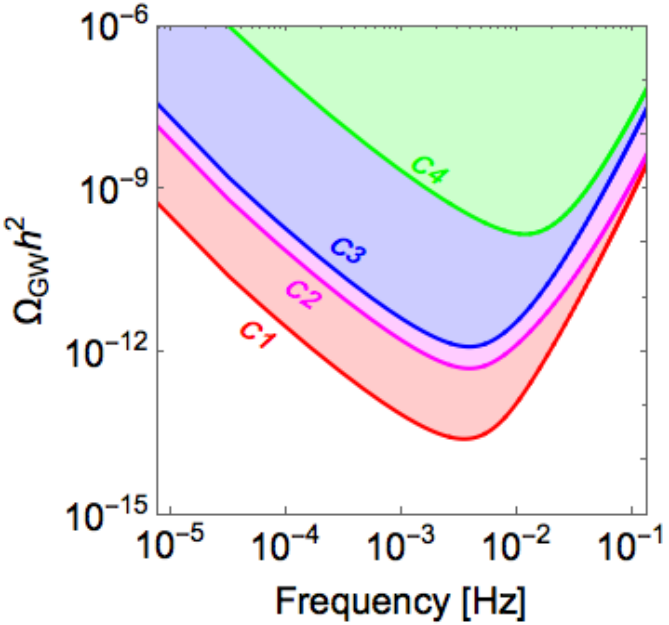

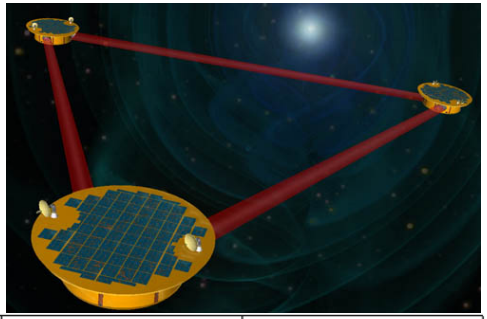

Name	C1	C2	C3	C4
Full name	N2A5M5L6	N2A1M5L6	N2A2M5L4	N1A1M2L4
# links	6	6	4	4
Arm length [km]	5M	1M	2M	1M
Duration [years]	5	5	5	2
Noise level	N2	N2	N2	N1

eLISA design decided

Extra budget (partially because of re-analyses of costs, partially because of NASA+Japan)

- **Number of laser links :** ~~4 or~~ **6**, corresponding to ~~2 or~~ **3** interferometer arms
  → Determined at eLISA symposium (Sept. 2016, U. of Zurich) http://www.physik.uzh.ch/events/lisa2016
- **Arm length :** ~~1 / 2 / 5~~ **2 - 5** million km
- **Duration :** ~~2 / 5~~ **3 - 10** years data taking
- **Noise level** : **N2** (LISA pathfinder expected) is 10 times larger than ~~N1 (LISA pathfinder required)~~
  → Determined by receiving the pathfinder result [PRL**116**, 231101 (2016)]

ESA approval : 2017, eLISA launch : **2028**

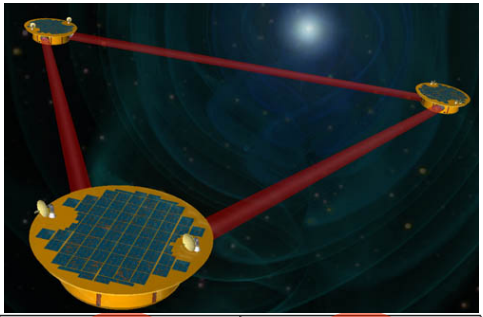

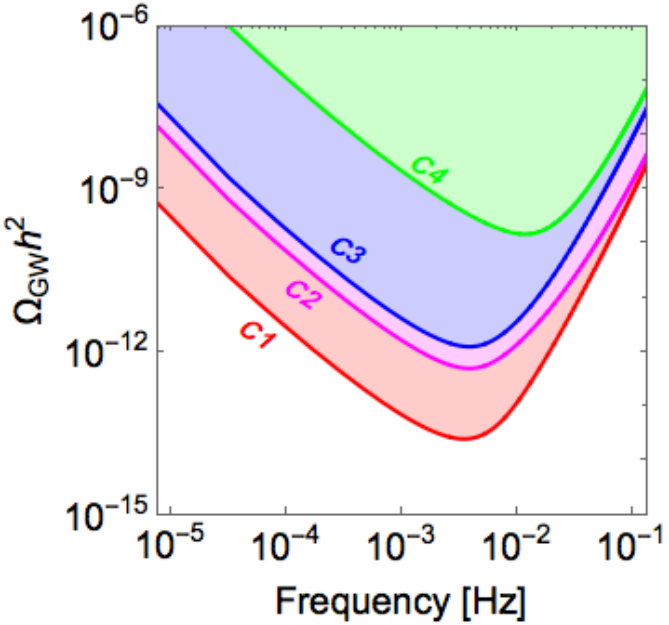

Name	C1	C2	~~C3~~	~~C4~~
Full name	N2A5M5L6	N2A1M5L6	N2A2M5L4	N1A1M2L4
# links	6	6	4	4
Arm length [km]	5M	1M	2M	1M
Duration [years]	5	5	5	2
Noise level	N2	N2	N2	N1

C1 corresponds to the old LISA configuration

$\varphi_c/T_c \nearrow \Rightarrow \Delta\lambda_{hhh} \nearrow$

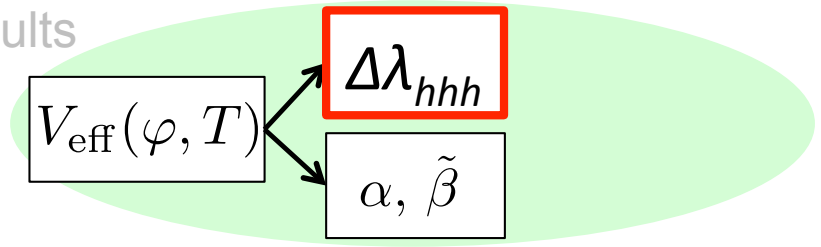

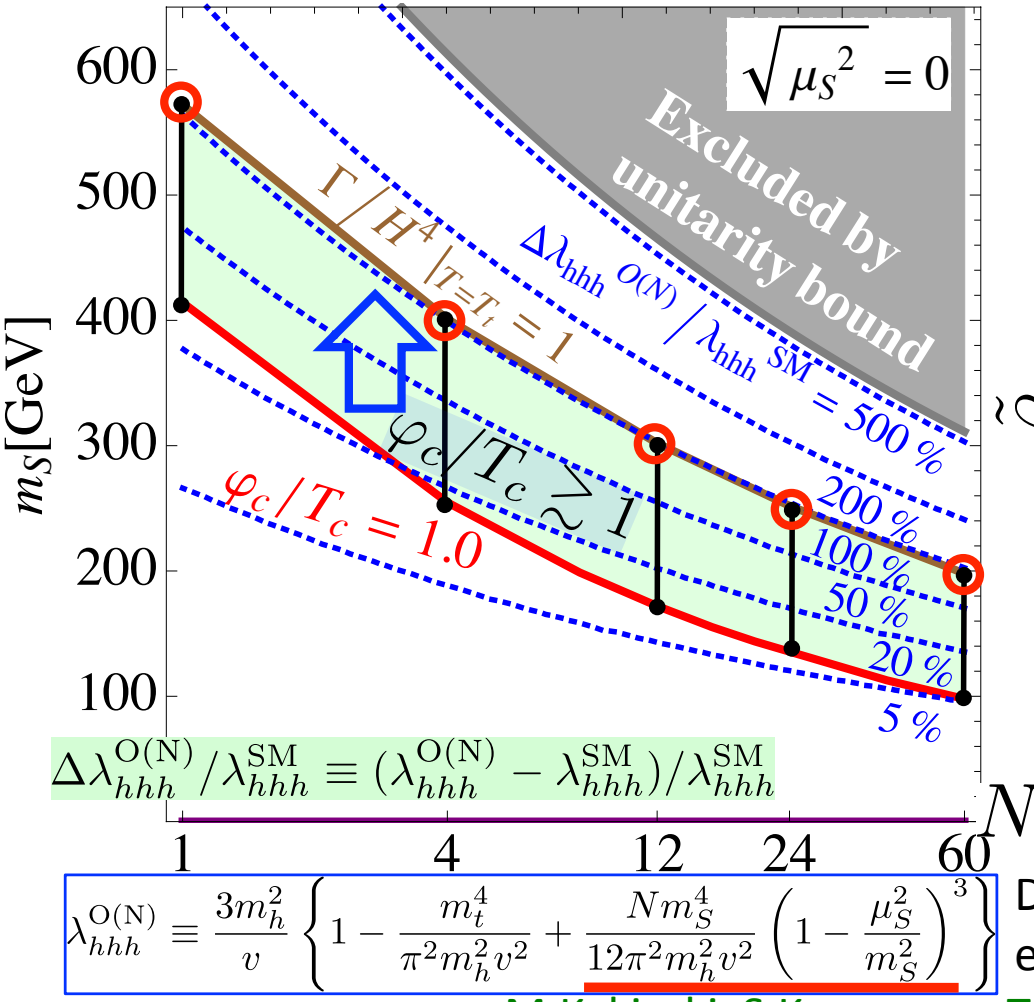

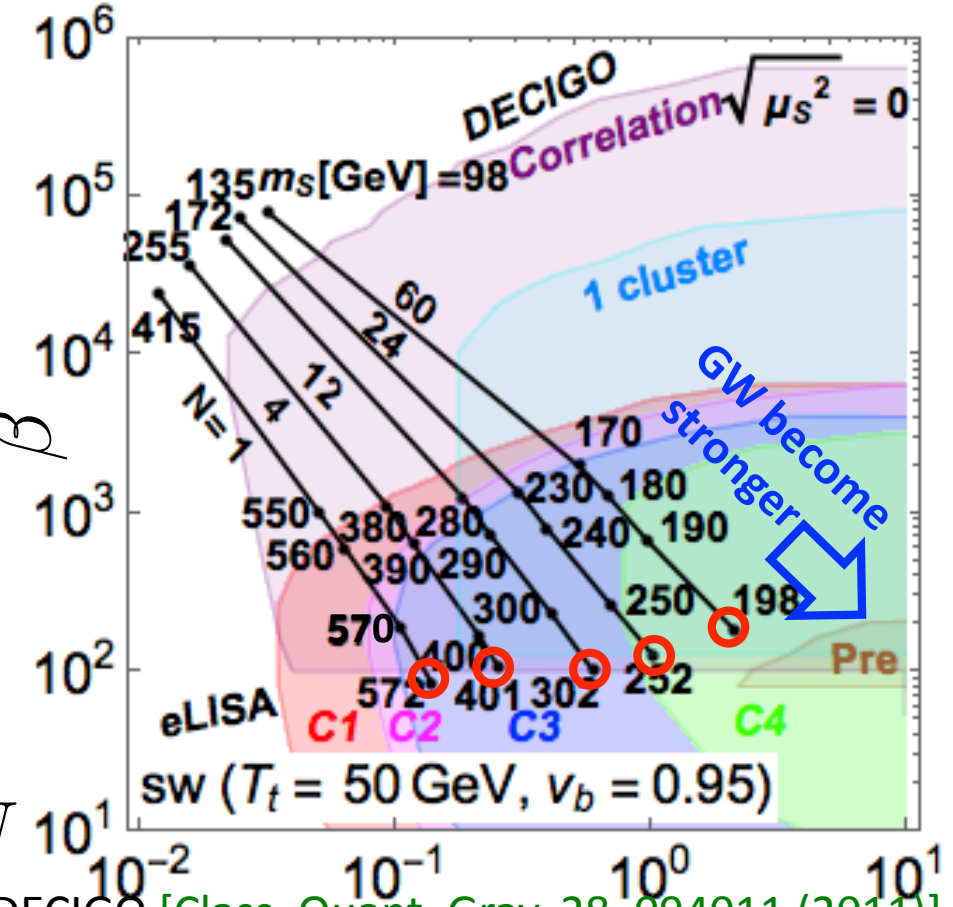

$$\lambda_{hhh}^{\rm O(N)} \equiv \frac{3m_h^2}{v}\left\{1 - \frac{m_t^4}{\pi^2 m_h^2 v^2} + \frac{N m_S^4}{12\pi^2 m_h^2 v^2}\left(1 - \frac{\mu_S^2}{m_S^2}\right)^3\right\}$$

DECIGO [Class. Quant. Grav. 28, 094011 (2011)],
eLISA [arXiv:1512.06239]

M.Kakizaki, S.Kanemura, T.Matsui, Phys. Rev. D **92**, no. 11, 115007 (2015)

$\varphi_c/T_c \nearrow \Rightarrow \Delta\lambda_{hhh} \nearrow$ & $\Omega_{GW}h^2 \nearrow$

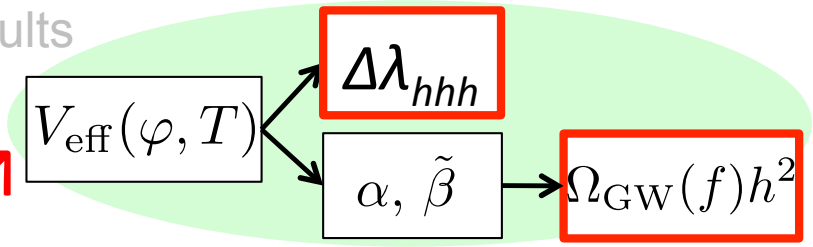

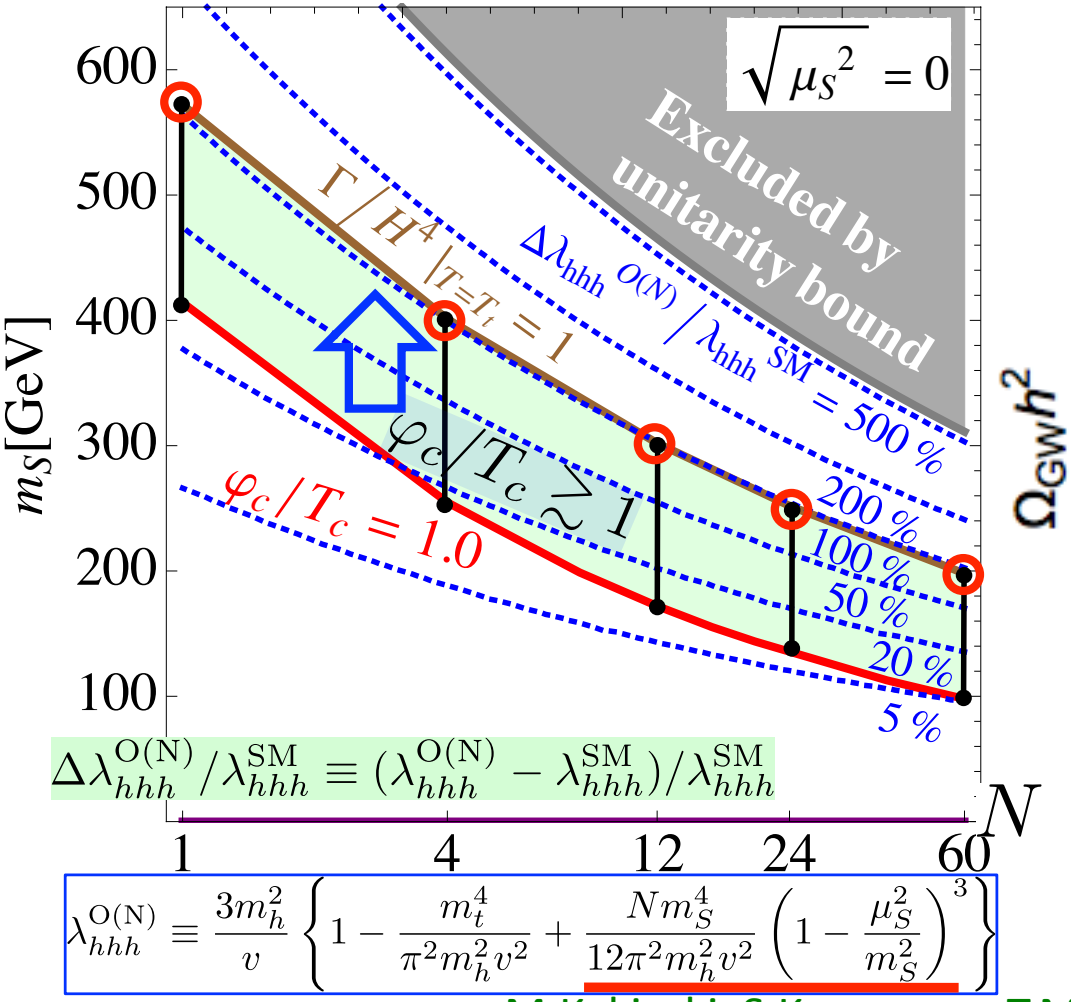

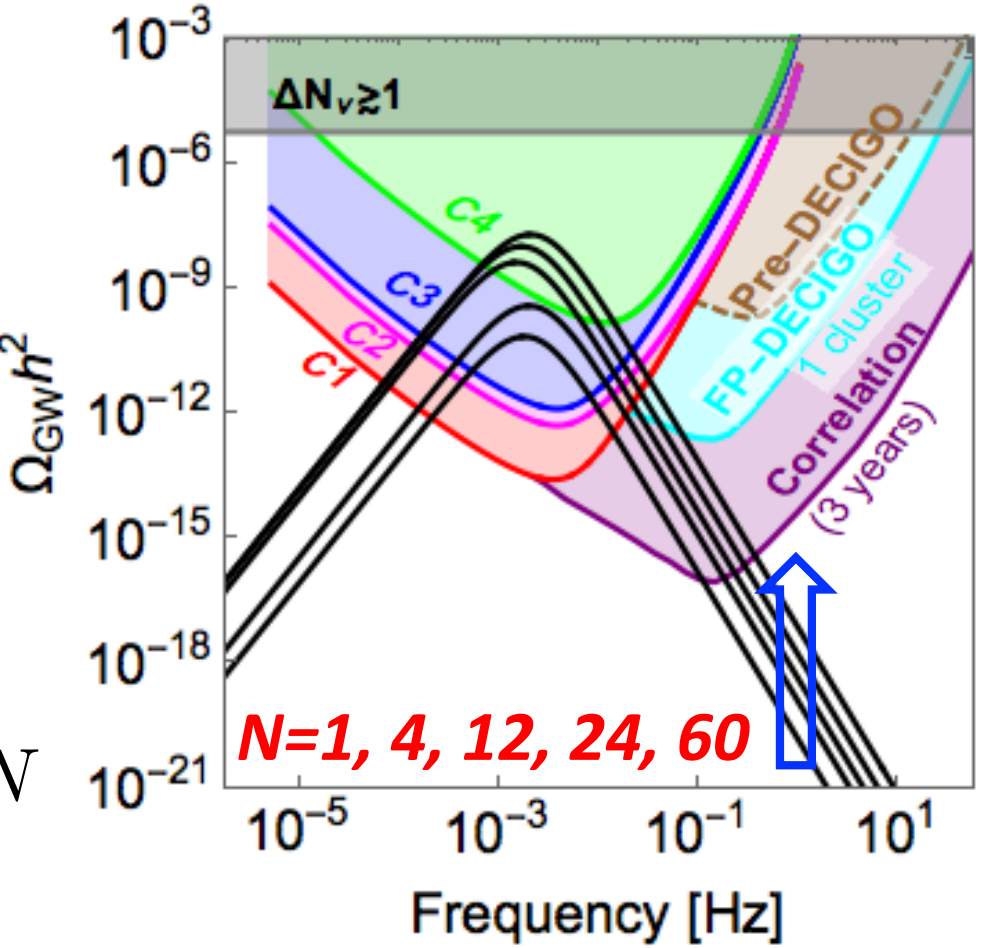

M.Kakizaki, S.Kanemura, T.Matsui, Phys. Rev. D **92**, no. 11, 115007 (2015)

The other example: 1stOPT by the non-decoupling effects

Model B

$$\vec{S} = (S_1, S_2, \cdots, S_N)^T$$

``O(*N*) models with Classical Scale Invariance"

- Mass parameters are forbidden at tree level.
- EWSB is directly caused by radiative corrections.

$$V_{\rm eff}(\varphi) = \sum_i \frac{n_i}{64\pi^2} M_i^4(\varphi) \left(\ln \frac{M_i^2(\varphi)}{Q^2} - \frac{3}{2} \right)$$

Coleman, Weinberg '73; Gildener, Weinberg '76

Characteristic predictions

- Higgs mass: $m_h^2 = (6m_{W^\pm}^4 + 3m_Z^4 - 12m_t^4 + Nm_S^4)/(8\pi^2 v^2)$
- *hhh* coupling: $\Delta\lambda_{hhh}^{\rm O(N)SI} / \lambda_{hhh}^{\rm SM_{tree}} \simeq 66.7\%$

(N, m_S) are strongly constrained.

Deviation from the SM is universally independent of (N, m_S).

Endo, Sumino, 2015; Fuyuto, Senaha, 2015; Hashino, Kanemura, Orikasa, 2015

- 1stOPT: $E = \frac{1}{12\pi v^3} \{6m_{W^\pm}^3 + 3m_Z^3 + Nm_S^3\}$ $\quad \frac{\varphi_c}{T_c} = \frac{2E}{\lambda}(1 - \frac{e\lambda}{ET})$

Predicted parameter region

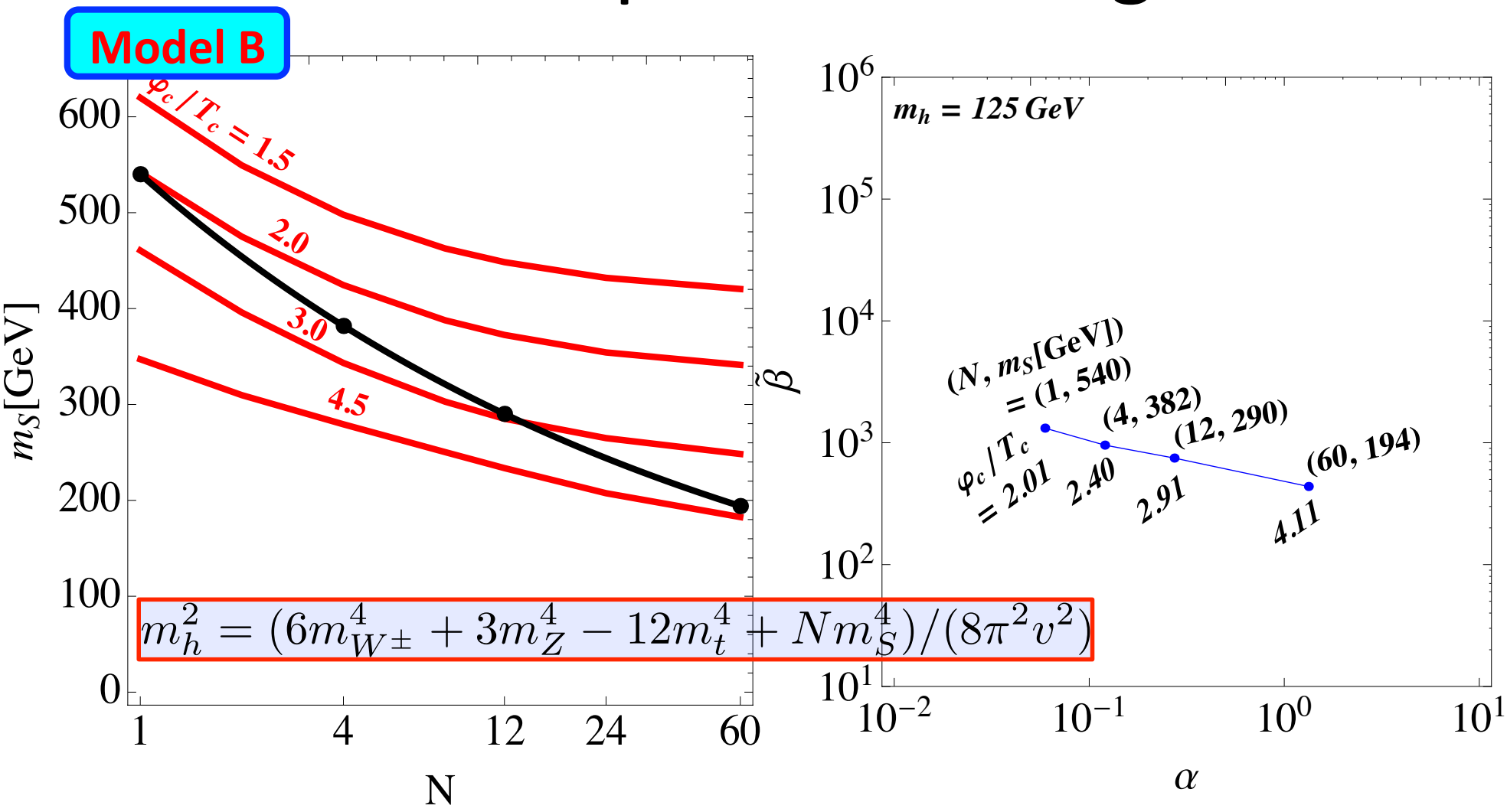

Predicted parameter region

Model A

M.Kakizaki, S.Kanemura, T.Matsui, Phys. Rev. D **92**, no. 11, 115007 (2015)

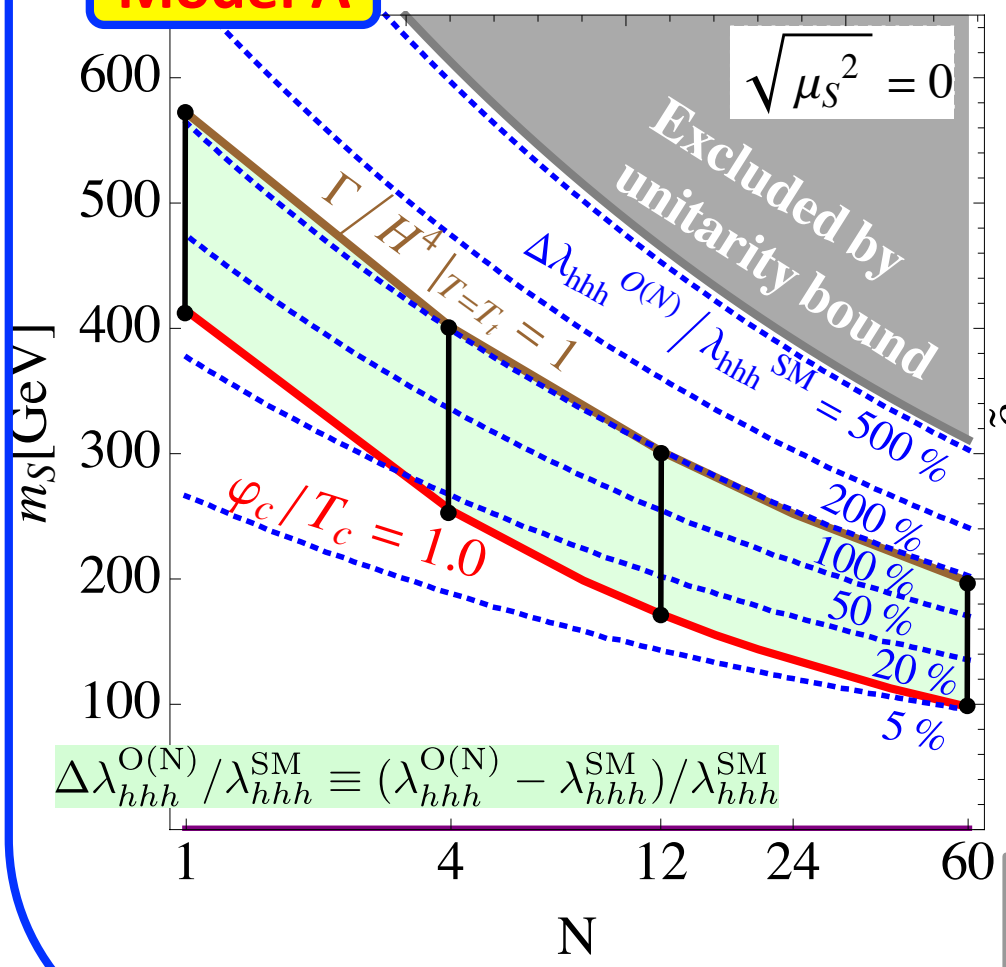

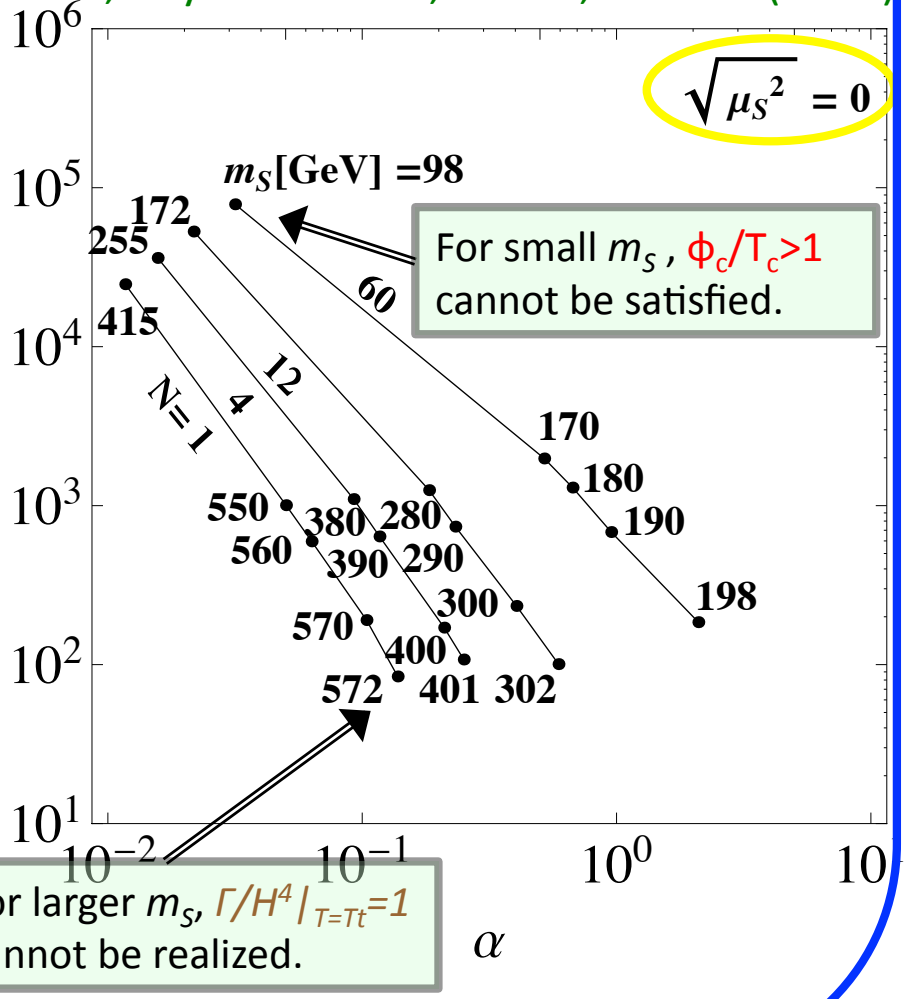

For small m_S , $\phi_c/T_c>1$ cannot be satisfied.

For larger m_S, $\Gamma/H^4|_{T=Tt}=1$ cannot be realized.

Predicted parameter region

Model A

M.Kakizaki, S.Kanemura, T.Matsui, Phys. Rev. D **92**, no. 11, 115007 (2015)

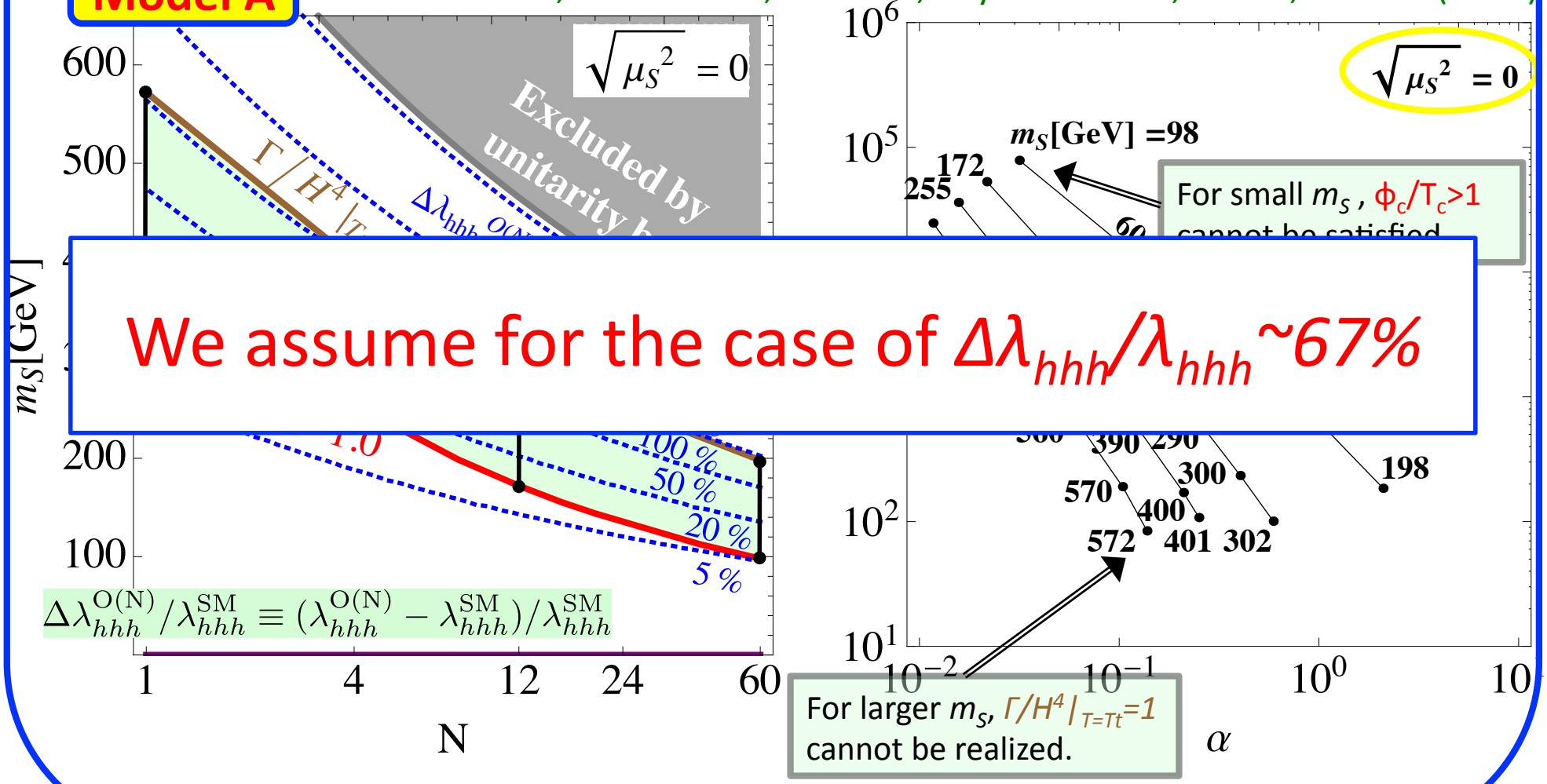

We assume for the case of $\Delta\lambda_{hhh}/\lambda_{hhh}$~67%

Predicted parameter region

Model A

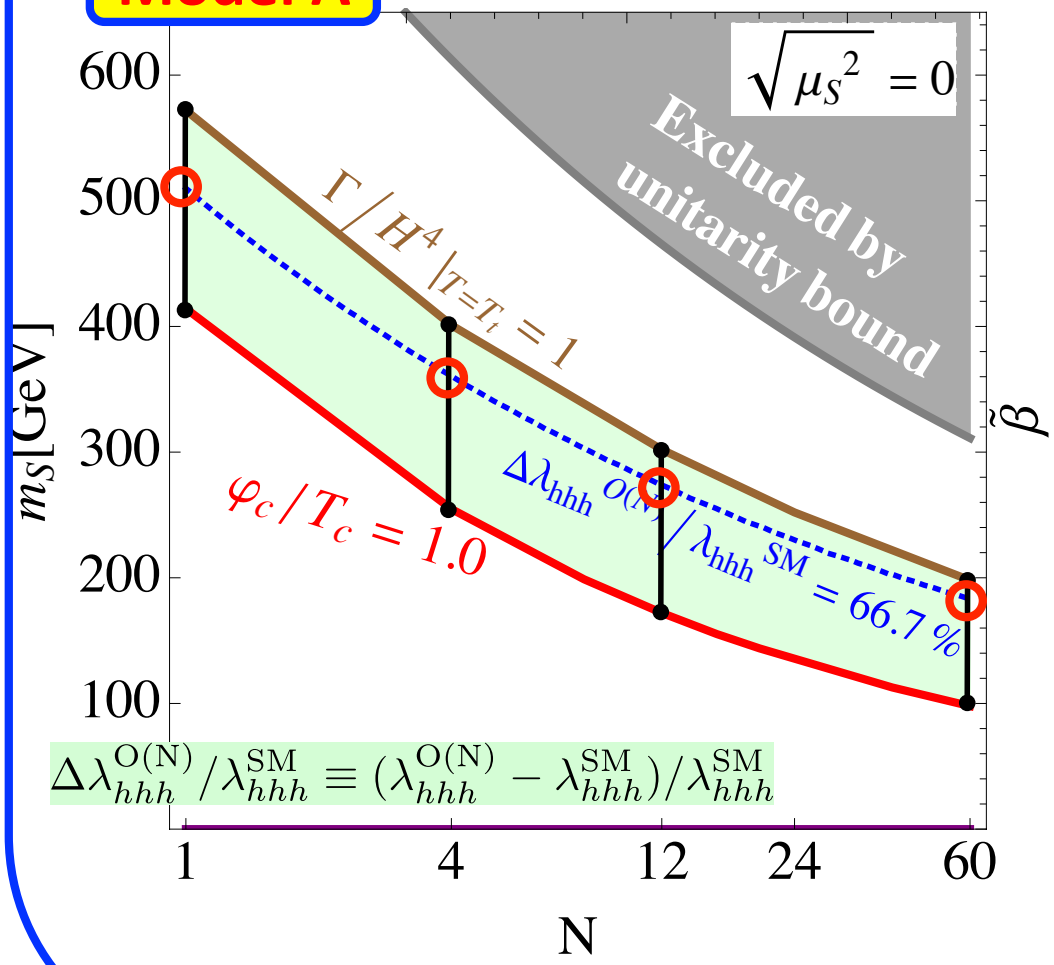

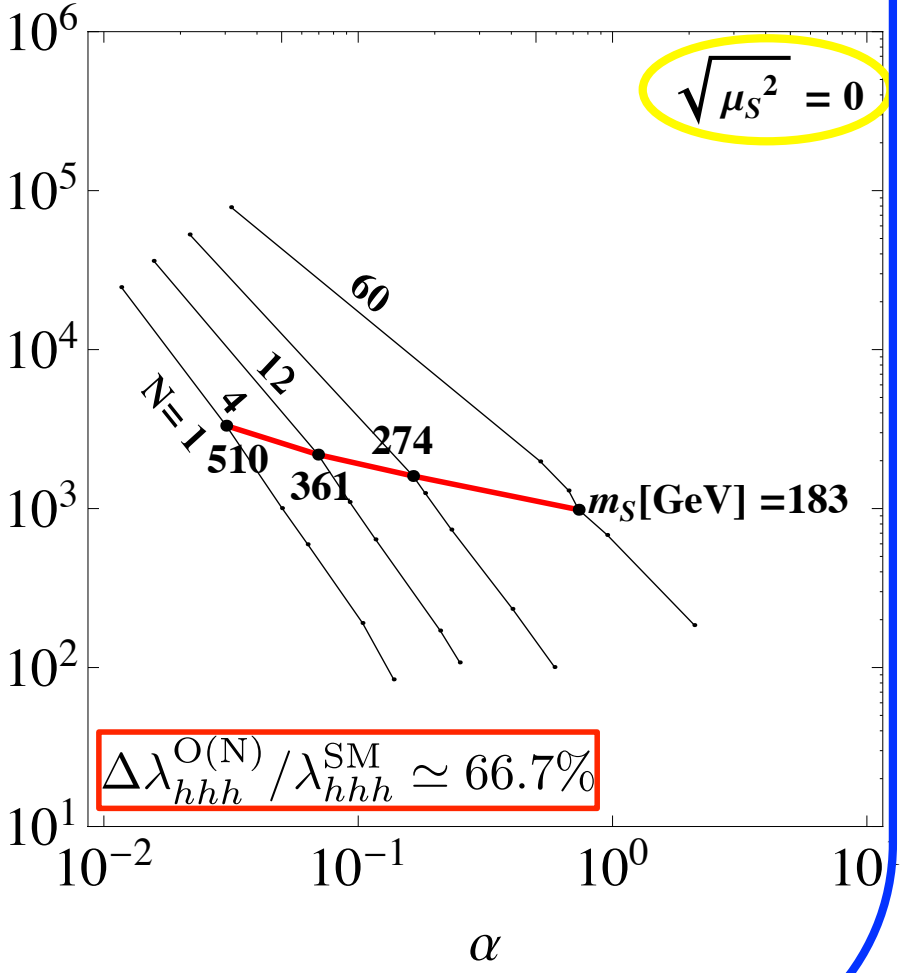

Predicted parameter region

Model A

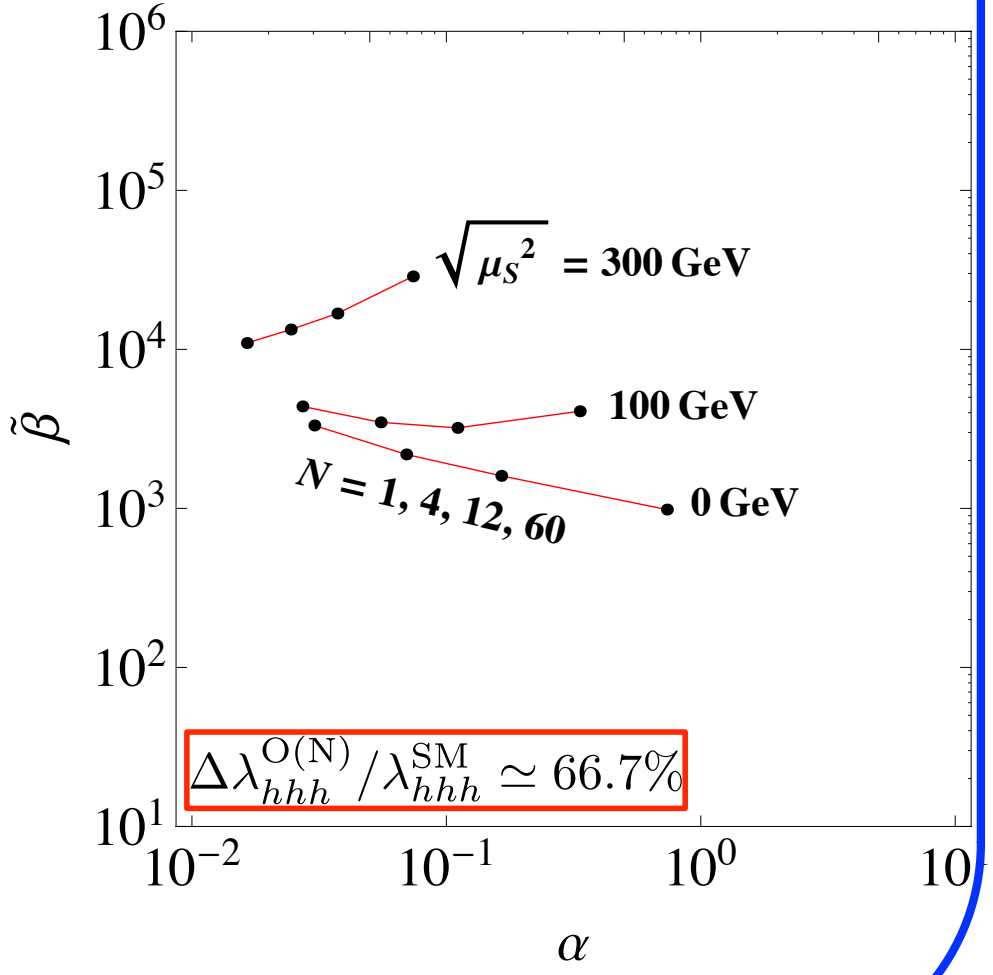

Predicted parameter region

Model A

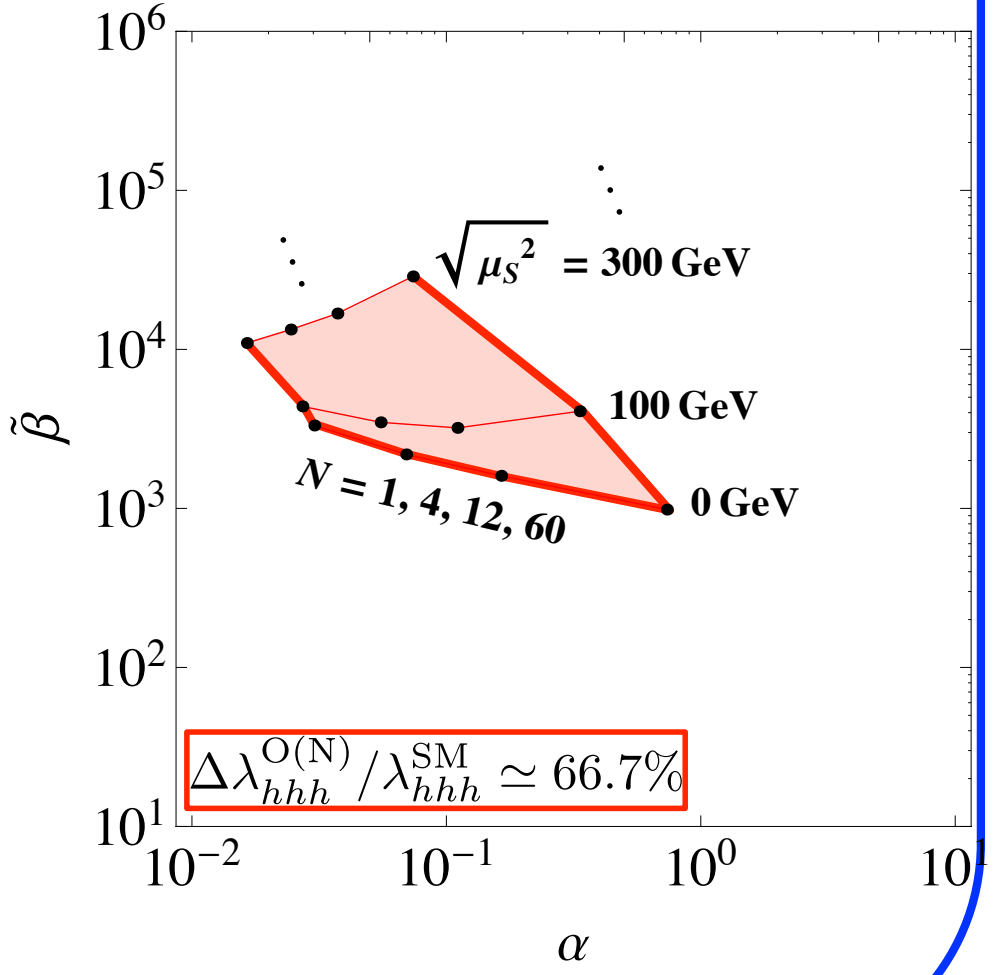

Even if $\Delta\lambda_{hhh}/\lambda_{hhh}$~67% is measured at ILC

K.Hashino, M.Kakizaki, S.Kanemura, T.Matsui, Phys. Rev. D **94**, no. 1, 015005 (2016)

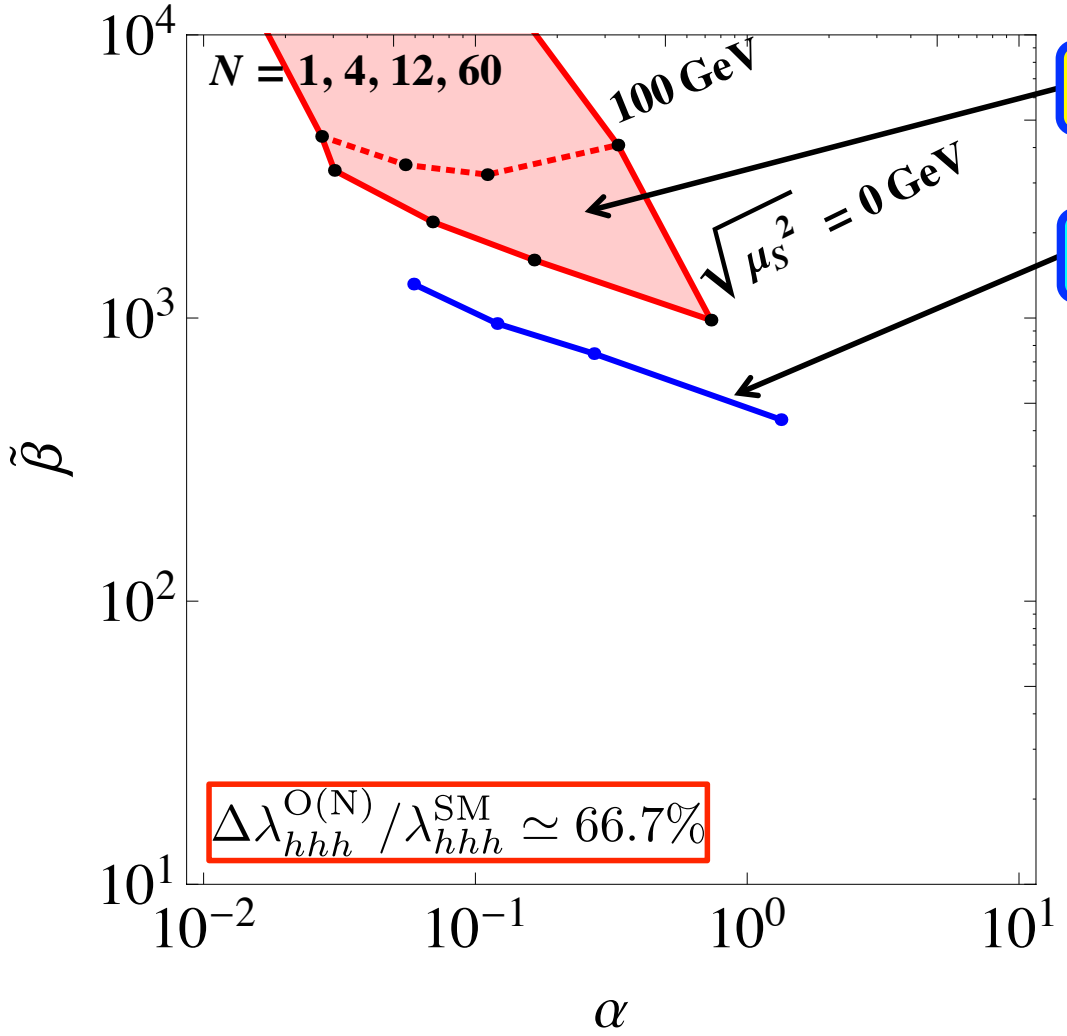

Model A

(O(*N*) models without CSI)

Model B

(CSI O(*N*) models)

Even if $\Delta\lambda_{hhh}/\lambda_{hhh}$~67% is measured at ILC

K.Hashino, M.Kakizaki, S.Kanemura, T.Matsui, Phys. Rev. D **94**, no. 1, 015005 (2016)

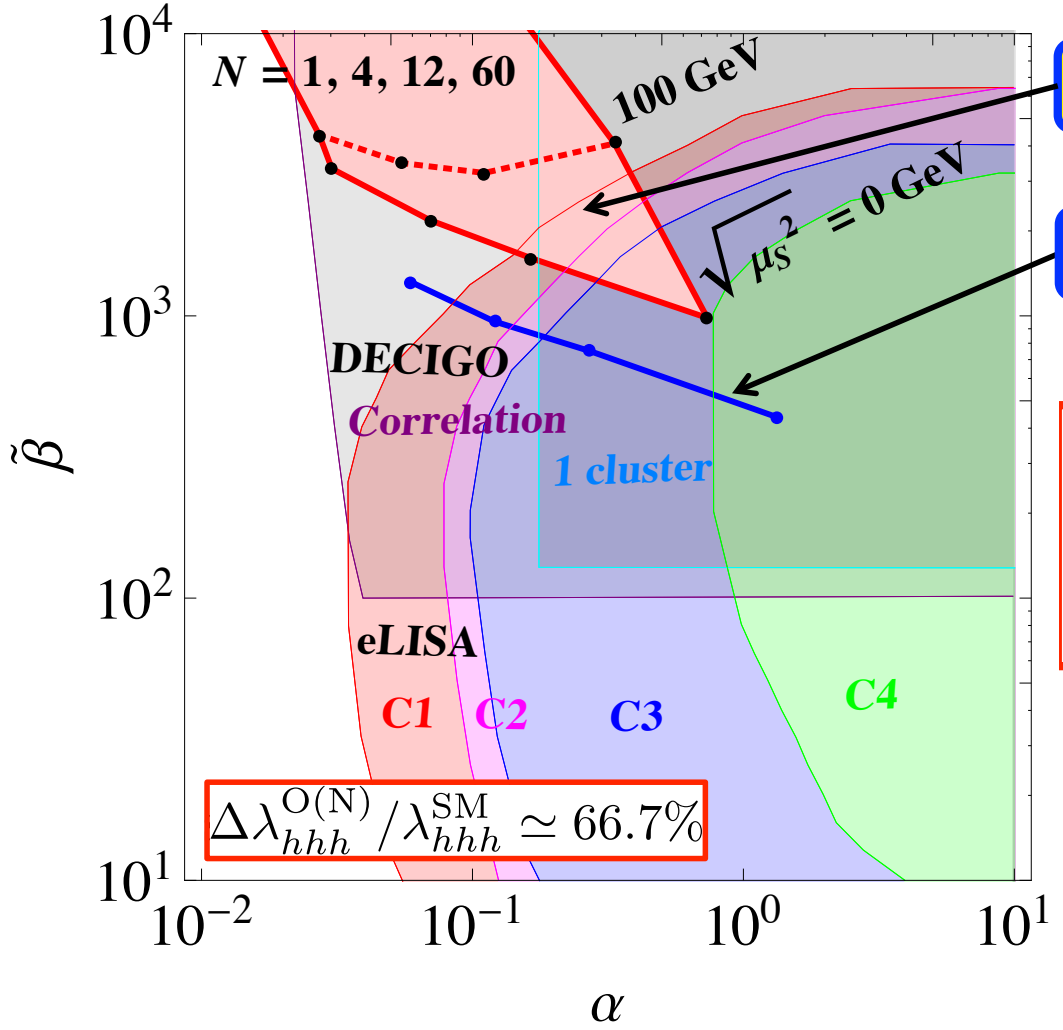

Model A

(O(N) models without CSI)

Model B

(CSI O(N) models)

Models with and without CSI can be distinguished at future GW interferometers.

Sensitivities

- DECIGO [S.Kawamura, et al., Class. Quant. Grav. 28, 094011 (2011)]
- eLISA [C.Caprini *et al.*, arXiv:1512.06239 [astro-ph.CO]]

Multi-field analysis of EWPT

K. Funakubo, S. Tao and F. Toyoda, Prog. Theor. Phys. 114, 369 (2005) (NMSSM)
K. Fuyuto and E. Senaha, Phys. Rev. D 90, no. 1, 015015 (2014) (HSM)

- EWPT:

$$(\varphi_\Phi, \varphi_S)_{\rm SYM} \to (\varphi_\Phi, \varphi_S)_{\rm EW} \quad @T=T_c,\ \varphi_c \equiv \varphi_\Phi(T_c)$$

- Diverse patterns of the EWPT:

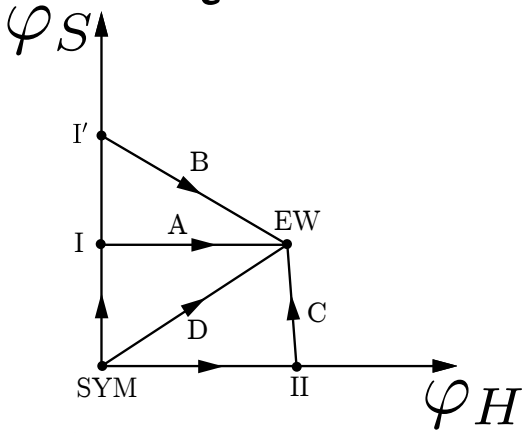

- EW phase needs to be the global min.:

$$V_{{\rm eff},T=0}(\text{EW phase}) < V_{{\rm eff},T=0}(\text{other phases})$$

- Public tool “CosmoTransition” (Python code) is used.

Theoretical constraints

- Perturbative unitarity: $|a_0(W_L^+W_L^- \to W_L^+W_L^-)| \leq 1$

$$m_h^2 \cos^2\theta + m_H^2 \sin^2\theta \leq \frac{4\pi\sqrt{2}}{3G_F} \approx (700\mathrm{GeV})^2$$

- Vacuum stability:

$$\lambda_\Phi(\mu) > 0, \qquad \lambda_S(\mu) > 0, \qquad 4\lambda_\Phi(\mu)\lambda_S(\mu) > \lambda_{\Phi S}^2(\mu)$$

- Landau pole:

$$|\lambda_{\Phi,S,\Phi S}(\Lambda_{\mathrm{LP}})| = 4\pi$$

- Oblique parameters (*S*, *T*, *U*):

$$\cos\theta \gtrsim 0.92 \quad \text{when } m_H \gtrsim 400\mathrm{GeV}\ (m_h \approx 125\mathrm{GeV})$$

S. Baek, P. Ko, W. I. Park and E. Senaha, JHEP 1211, 116 (2012)

K.Hashino, M.Kakizaki, S.Kanemura, T.Matsui, P.Ko, arXiv:1609.00297

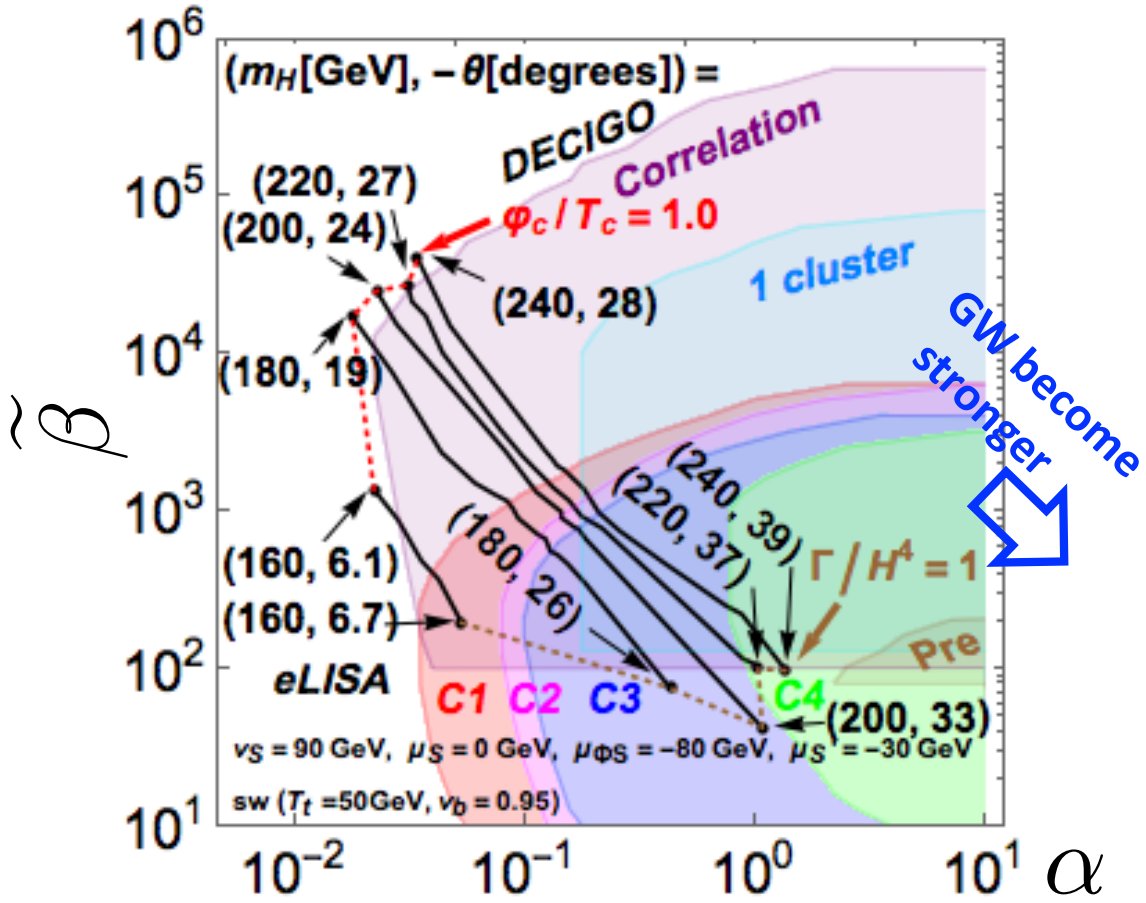

DECIGO [Class. Quant. Grav. 28, 094011 (2011)], eLISA [arXiv:1512.06239]

eLISA or DECIGO is capable of detecting GWs
in the most of the HSM parameter region with 1st OPT.

Singlet extension of the SM (non-thermal)

A.Ashoorioon, T.Konstandin, JCAP**0809**, 022 (2008)

- Potential $S = s + x$

$$V_0(\Phi, S) = V_{\rm SM}(\Phi) + b_1 S + \frac{b_2}{2} S^2 + \frac{b_3}{3} S^3 + \frac{b_4}{4} S^4 + \frac{a_1}{2} |\Phi|^2 S + \frac{a_2}{2} |\Phi|^2 S^2$$

- An example of the paths (assumption)

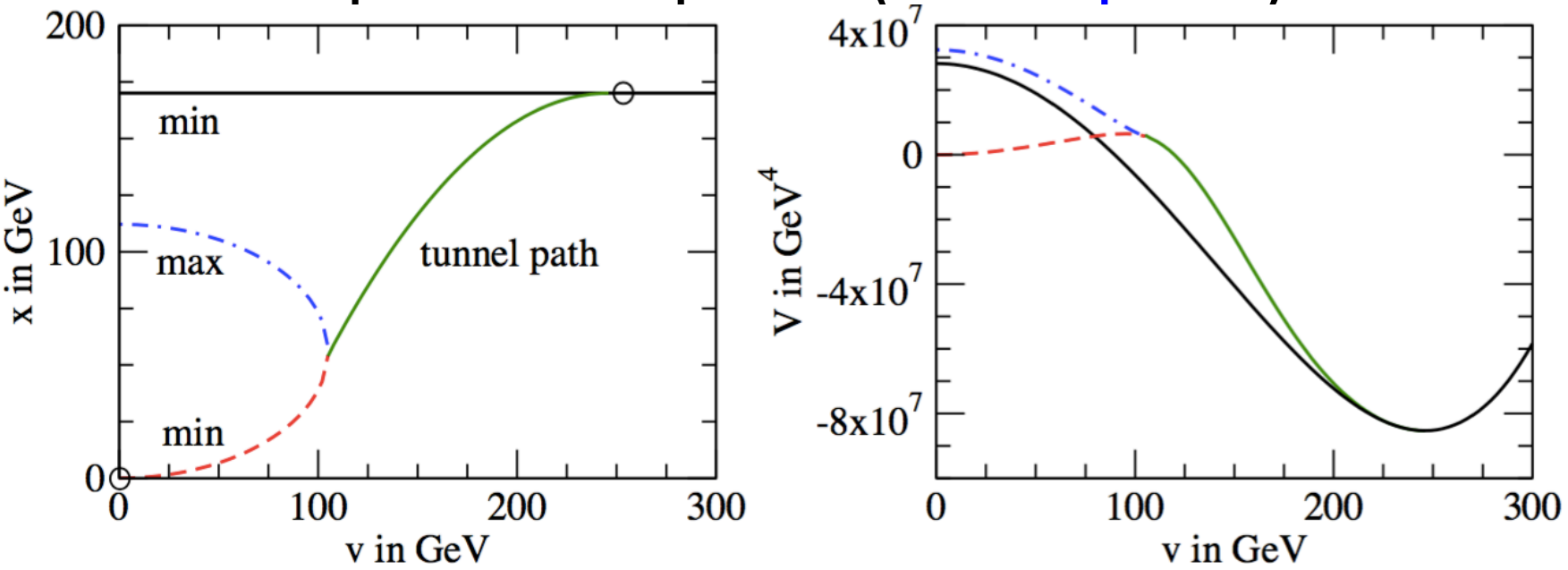

Singlet extension of the SM (non-thermal)

A.Ashoorioon, T.Konstandin, JCAP**0809**, 022 (2008)

$\bar{\mu}_s$/ GeV	α	β/H	v/T	T / GeV
190	0.14	121	3.1	75
186	0.18	88	3.4	69
183	0.25	53	3.7	63
181	0.33	25	4.0	57
180	0.42	8	4.2	54
179	symmetric phase stable			

Results(↑,→)

$$\bar{\mu}_h^2 = \left.\frac{\partial^2 V}{\partial v^2}\right|_{v=\bar{v},\,x=\bar{x}}, \quad \bar{\mu}_s^2 = \left.\frac{\partial^2 V}{\partial x^2}\right|_{v=\bar{v},\,x=\bar{x}}, \quad \bar{\mu}_{hs}^2 = \left.\frac{\partial^2 V}{\partial v \partial x}\right|_{v=\bar{v},\,x=\bar{x}}$$

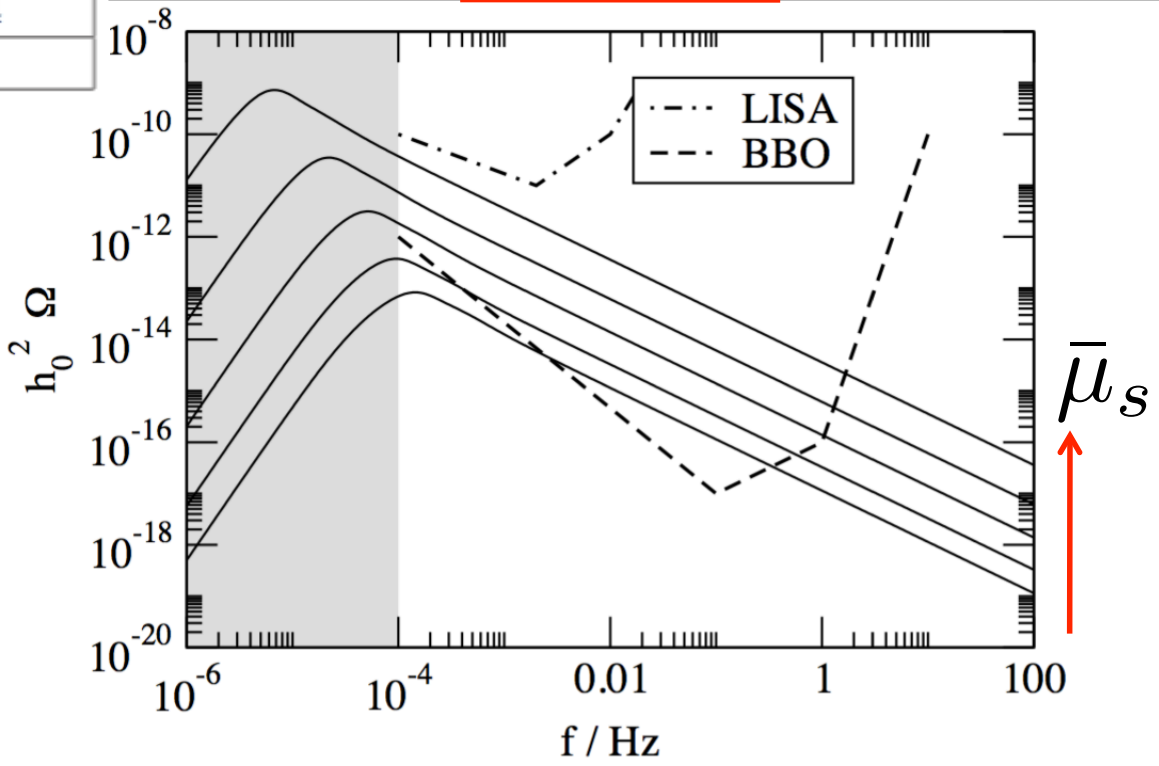

GWs from 1stOPT

Model parameters

Input

$V_{\rm eff}(\varphi, T)$ → $S_3(T)$

Definition of phase transition temperature T_t

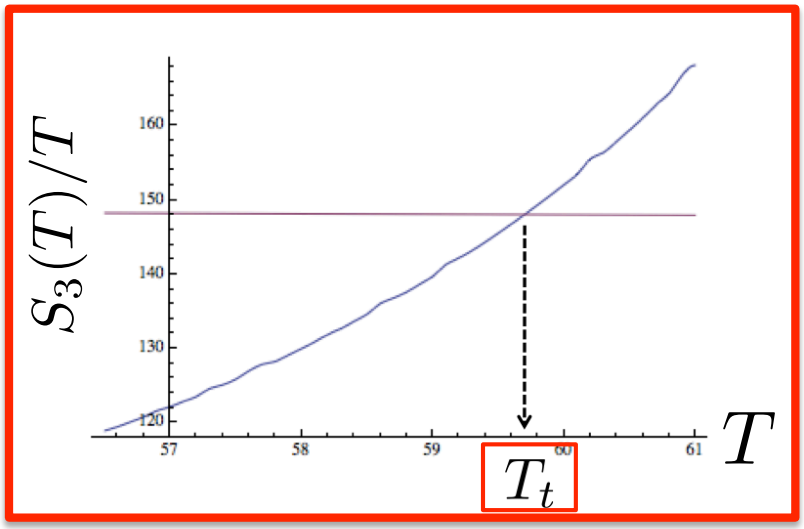

$$\left.\frac{\Gamma}{H^4}\right|_{T=T_t} \simeq 1 \quad \leftrightarrows \quad \left.\frac{S_3(T)}{T}\right|_{T=T_t} \simeq 140-150$$

$$\Gamma(T) \simeq T^4 e^{-\frac{S_3(T)}{T}}$$

$$S_3(T) = \int dr^3 \left\{ \frac{1}{2}\left(\vec{\nabla}\varphi\right)^2 + V_{\rm eff}(\varphi, T) \right\}$$

Behavior of S_3/T↑

GWs from 1stOPT

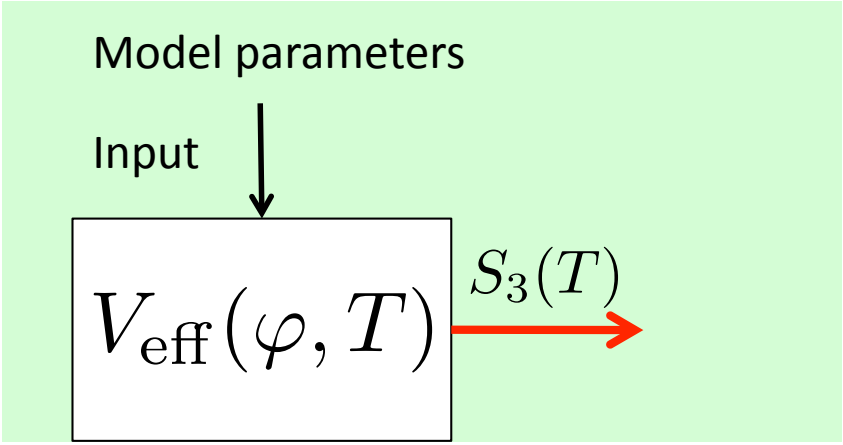

Definition of phase transition temperature T_t

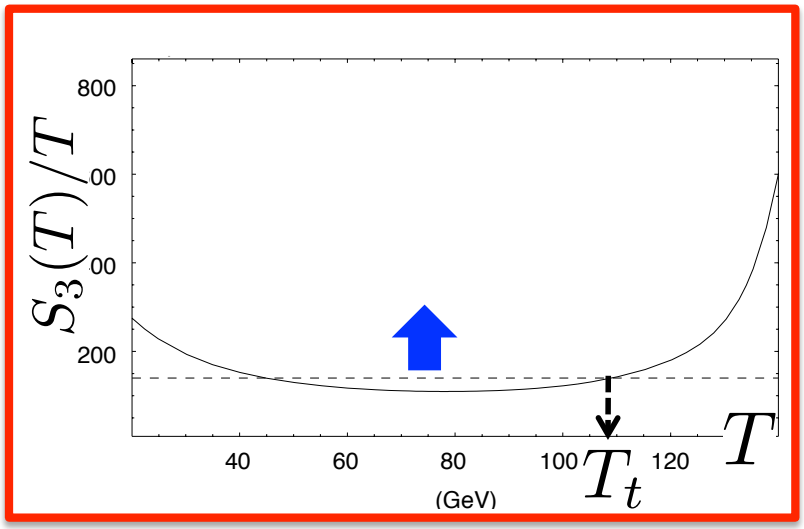

$$\left.\frac{\Gamma}{H^4}\right|_{T=T_t} \simeq 1 \quad \leftrightarrows \quad \left.\frac{S_3(T)}{T}\right|_{T=T_t} \simeq 140-150$$

Model parameters are constrained.

R.Apreda et al., NPB**631**, 342 (2002)

Behavior of S_3/T↑

Estimation of the relic abundance

M.Kamionkowski, PRD**49**, 2837 (1994)

- Wave eq. from Einstein eq. in weak field approximation

$$-\Box\left(h_{\mu\nu}-\frac{1}{2}\eta_{\mu\nu}h^{\alpha}{}_{\alpha}\right)=16\pi G T_{\mu\nu}$$

- Stochastic backgrounds of GWs

$$\rho_{\rm GW}=\frac{1}{32\pi G}<\dot{h}_{\alpha\beta}\dot{h}^{\alpha\beta}>\sim 8\pi G\rho_{\rm kin}^2/\beta^2$$

$$T_0^0=\rho_{\rm kin}+\cdots \qquad \frac{d}{dt}\simeq\beta$$

$$\rho_{\rm tot}(=\underbrace{\rho_{\rm vac}}_{(=\epsilon)}+\rho_{\rm rad})=\frac{3H^2}{8\pi G} \qquad \alpha=\frac{\rho_{\rm vac}}{\rho_{\rm rad}} \qquad \kappa=\frac{\rho_{\rm vac}}{\rho_{\rm vac}}$$

Efficiency factor

$$\Omega_{\rm GW}=\frac{\rho_{GW}}{\rho_{\rm tot}}\simeq\underbrace{\left(\frac{H}{\beta}\right)^2}_{=\widetilde{\beta}^{-2}\sim(H\langle R\rangle)^2}\left(\frac{\kappa\alpha}{1+\alpha}\right)^2$$

Origins of GWs from EWPT

C.Caprini *et al.*, arXiv:1512.06239 [astro-ph.CO] (review)

2.1 Contributions to the Gravitational Wave Spectrum

To varying degrees, three processes are involved in the production of GWs at a first-order PT:

- Collisions of bubble walls and (where relevant) shocks in the plasma. This can be treated by a technique now generally referred to as the 'envelope approximation' [10–15]. As described below, this approximation can be used to compute the contribution to the GW spectrum from the scalar field, ϕ, itself.
- Sound waves in the plasma after the bubbles have collided but before expansion has dissipated the kinetic energy in the plasma [16–19].
- Magnetohydrodynamic (MHD) turbulence in the plasma forming after the bubbles have collided [20–25].

We improve our analysis in accordance with the recent simulation result.

Recent work of other souse of GW "sound wave"

M.Hindmarsh, *et al*., PRL **112**, 041301 (2014); arXiv:1504.03291 [astro-ph.CO].

Numerical simulations of acoustically generated gravitational waves at a first order phase transition

Mark Hindmarsh,[1,2,*] Stephan J. Huber,[1,†] Kari Rummukainen,[2,‡] and David J. Weir[3,§]

[1] *Department of Physics and Astronomy, University of Sussex, Falmer, Brighton BN1 9QH, U.K.*
[2] *Department of Physics and Helsinki Institute of Physics, PL 64, FI-00014 University of Helsinki, Finland*
[3] *Institute of Mathematics and Natural Sciences, University of Stavanger, 4036 Stavanger, Norway*

(Dated: April 14, 2015)

We present details of numerical simulations of the gravitational radiation produced by a first order thermal phase transition in the early universe. We confirm that the dominant source of gravitational waves is sound waves generated by the expanding bubbles of the low-temperature phase. We demonstrate that the sound waves have a power spectrum with power-law form between the scales set by the average bubble separation (which sets the length scale of the fluid flow L_f) and the bubble wall width. The sound waves generate gravitational waves whose power spectrum also has a power-law form, at a rate proportional to L_f and the square of the fluid kinetic energy density. We identify a dimensionless parameter $\tilde{\Omega}_{GW}$ characterising the efficiency of this "acoustic" gravitational wave production whose value is $8\pi\tilde{\Omega}_{GW} \simeq 0.8 \pm 0.1$ across all our simulations. We compare the acoustic gravitational waves with the standard prediction from the envelope approximation. Not only is the power spectrum steeper (apart from an initial transient) but the gravitational wave energy density is generically two orders of magnitude or more larger.

Origins of GWs from EWPT

C.Caprini *et al.*, arXiv:1512.06239 [astro-ph.CO] (review)

- Vacuum bubble velocity v_b
- Efficiency factor $\kappa(v_b, \alpha)$

$$\widetilde{\Omega}_{\rm sw}h^2 \simeq 2.65\times10^{-6}\frac{v_b}{\tilde{\beta}}\left(\frac{\kappa(v_b,\alpha)\alpha}{1+\alpha}\right)^2 \quad @\ \tilde{f}_{\rm sw} \simeq 1.9\times10^{-5}{\rm Hz}\frac{\tilde{\beta}}{v_b}$$

$$\widetilde{\Omega}_{\rm env}h^2 \simeq \frac{1.84\times10^{-6}v_b^3}{(0.42+v_b^2)\tilde{\beta}^2}\left(\frac{\kappa(v_b,\alpha)\alpha}{1+\alpha}\right)^2 \quad @\ \tilde{f}_{\rm env} \simeq 1.0\times10^{-5}{\rm Hz}\frac{\tilde{\beta}}{1.8-0.1v_b+v_b^2}$$

$$\widetilde{\Omega}_{\rm turb}h^2 \simeq \frac{9.35\times10^{-8}v_b^2}{0.00354v_b\tilde{\beta}+\tilde{\beta}^2}\left(\frac{\epsilon\kappa(v_b,\alpha)\alpha}{1+\alpha}\right)^{3/2} \quad @\ \tilde{f}_{\rm turn} \simeq 2.7\times10^{-5}{\rm Hz}\frac{\tilde{\beta}}{v_b}$$

Origins of GWs from EWPT

C.Caprini *et al.*, arXiv:1512.06239 [astro-ph.CO] (review)

- Vacuum bubble velocity v_b

- Efficiency factor $\kappa(v_b, \alpha)$

$$\kappa(v_b, \alpha) \simeq O(0.01 - 0.1)$$

J.R.Espinosa, *et al*, JCAP **1006**, 028 (2010)

$$\widetilde{\Omega}_{\rm sw} h^2 \simeq 2.65 \times 10^{-6} \frac{v_b}{\tilde{\beta}} \left(\frac{\kappa(v_b, \alpha)\alpha}{1+\alpha} \right)^2 \quad @ \quad \tilde{f}_{\rm sw} \simeq 1.9 \times 10^{-5} {\rm Hz} \frac{\tilde{\beta}}{v_b}$$

$$\widetilde{\Omega}_{\rm env} h^2 \simeq \frac{1.84 \times 10^{-6} v_b^3}{(0.42 + v_b^2)\tilde{\beta}^2} \left(\frac{\kappa(v_b, \alpha)\alpha}{1+\alpha} \right)^2 \quad @ \quad \tilde{f}_{\rm env} \simeq 1.0 \times 10^{-5} {\rm Hz} \frac{\tilde{\beta}}{1.8 - 0.1 v_b + v_b^2}$$

$$\widetilde{\Omega}_{\rm turb} h^2 \simeq \frac{9.35 \times 10^{-8} v_b^2}{0.00354 v_b \tilde{\beta} + \tilde{\beta}^2} \left(\frac{\kappa(v_b, \alpha)\alpha}{1+\alpha} \right)^{3/2} \quad @ \quad \tilde{f}_{\rm turn} \simeq 2.7 \times 10^{-5} {\rm Hz} \frac{\tilde{\beta}}{v_b}$$

Origins of GWs from EWPT

C.Caprini *et al.*, arXiv:1512.06239 [astro-ph.CO] (review)

- Vacuum bubble velocity v_b
- Efficiency factor $\kappa(v_b, \alpha)$

$$\kappa(v_b, \alpha) \simeq O(0.01 - 0.1)$$

J.R.Espinosa, *et al*, JCAP **1006**, 028 (2010)

- The fraction of bulk motion from the bubble walls

The result from resent simulation

$$\epsilon \simeq 0.05 - 0.10$$

Hindmarsh, Huber, Rummukainen, Weir, PRD **92**, no. 12, 123009 (2015)

$$\widetilde{\Omega}_{\rm sw} h^2 \simeq 2.65 \times 10^{-6} \frac{v_b}{\tilde{\beta}} \left(\frac{\kappa(v_b, \alpha)\alpha}{1+\alpha} \right)^2 \quad @ \ \tilde{f}_{\rm sw} \simeq 1.9 \times 10^{-5} {\rm Hz} \frac{\tilde{\beta}}{v_b}$$

$$\widetilde{\Omega}_{\rm env} h^2 \simeq \frac{1.84 \times 10^{-6} v_b^3}{(0.42 + v_b^2)\tilde{\beta}^2} \left(\frac{\kappa(v_b, \alpha)\alpha}{1+\alpha} \right)^2 \quad @ \ \tilde{f}_{\rm env} \simeq 1.0 \times 10^{-5} {\rm Hz} \frac{\tilde{\beta}}{1.8 - 0.1 v_b + v_b^2}$$

$$\widetilde{\Omega}_{\rm turb} h^2 \simeq \frac{9.35 \times 10^{-8} v_b^2}{0.00354 v_b \tilde{\beta} + \tilde{\beta}^2} \left(\frac{\epsilon \kappa(v_b, \alpha)\alpha}{1+\alpha} \right)^{3/2} \quad @ \ \tilde{f}_{\rm turn} \simeq 2.7 \times 10^{-5} {\rm Hz} \frac{\tilde{\beta}}{v_b}$$

$(\alpha, \beta\text{tilde}) \leftrightarrow (f, \Omega_{GW}h^2)_{new}$

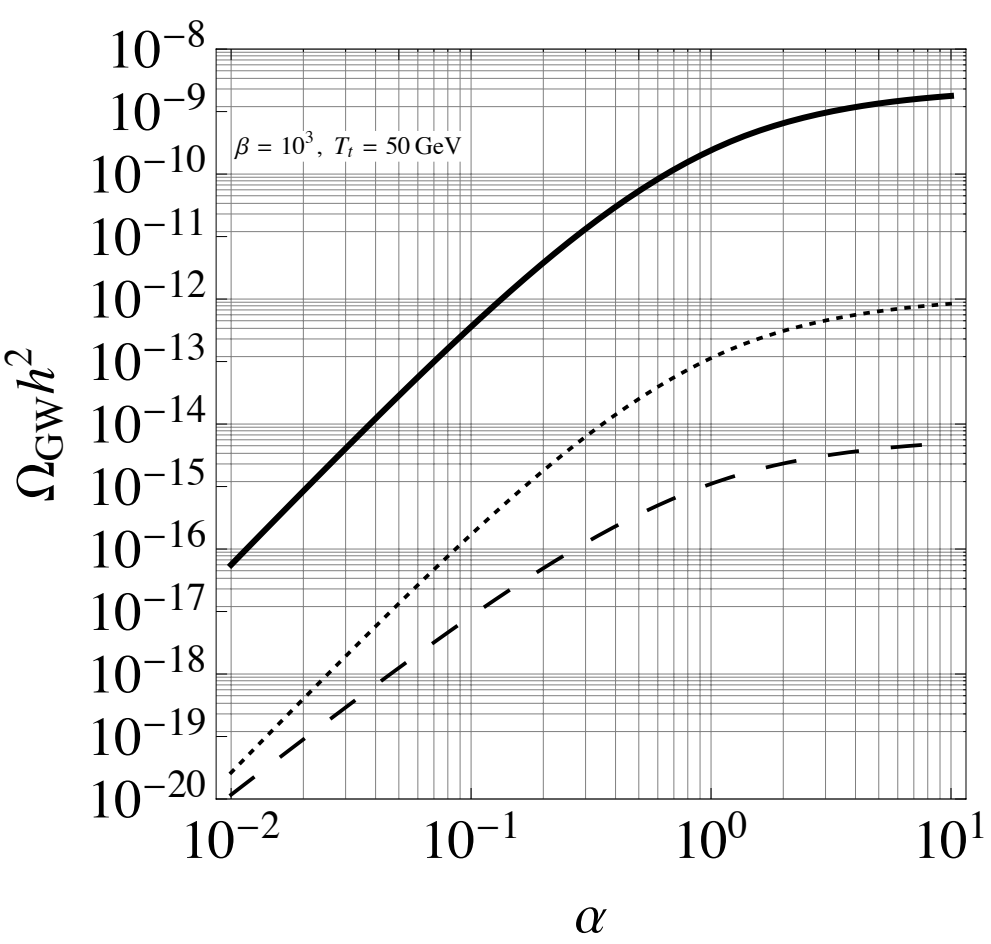

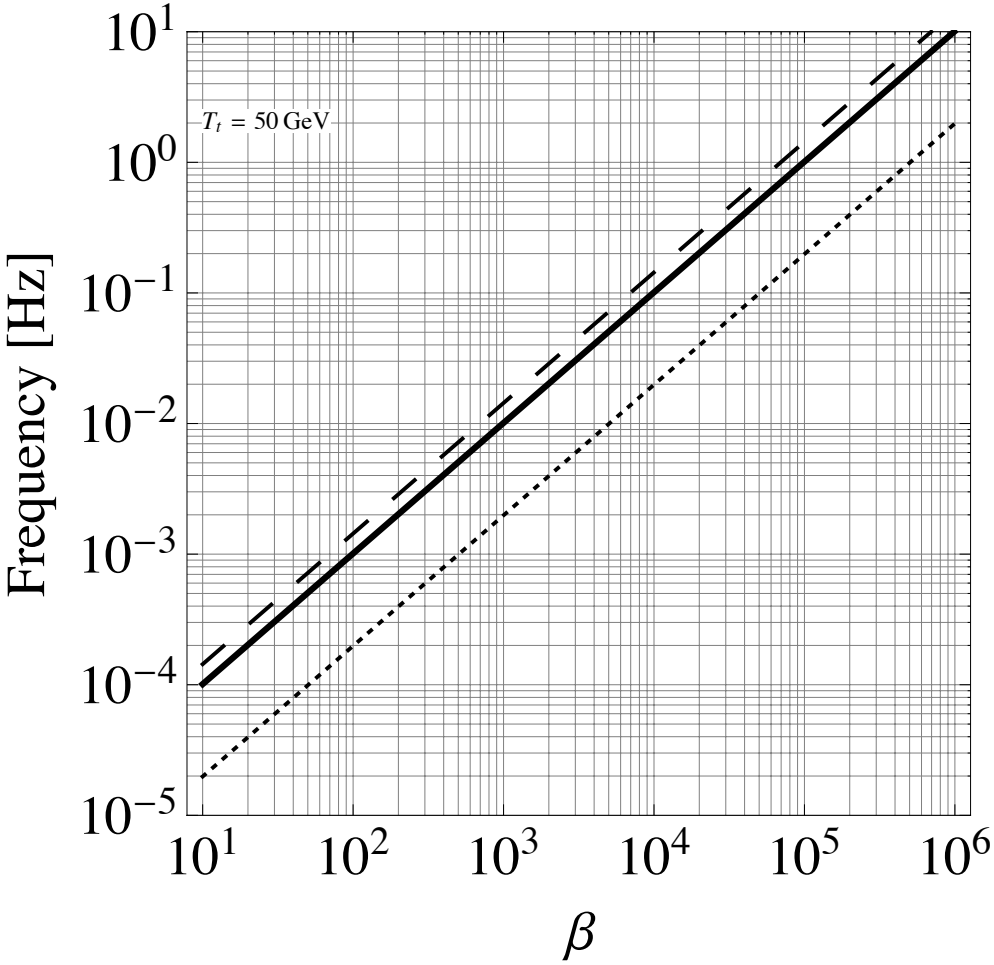

(α, βtilde)_exp. by New spectra (T_t=50GeV)

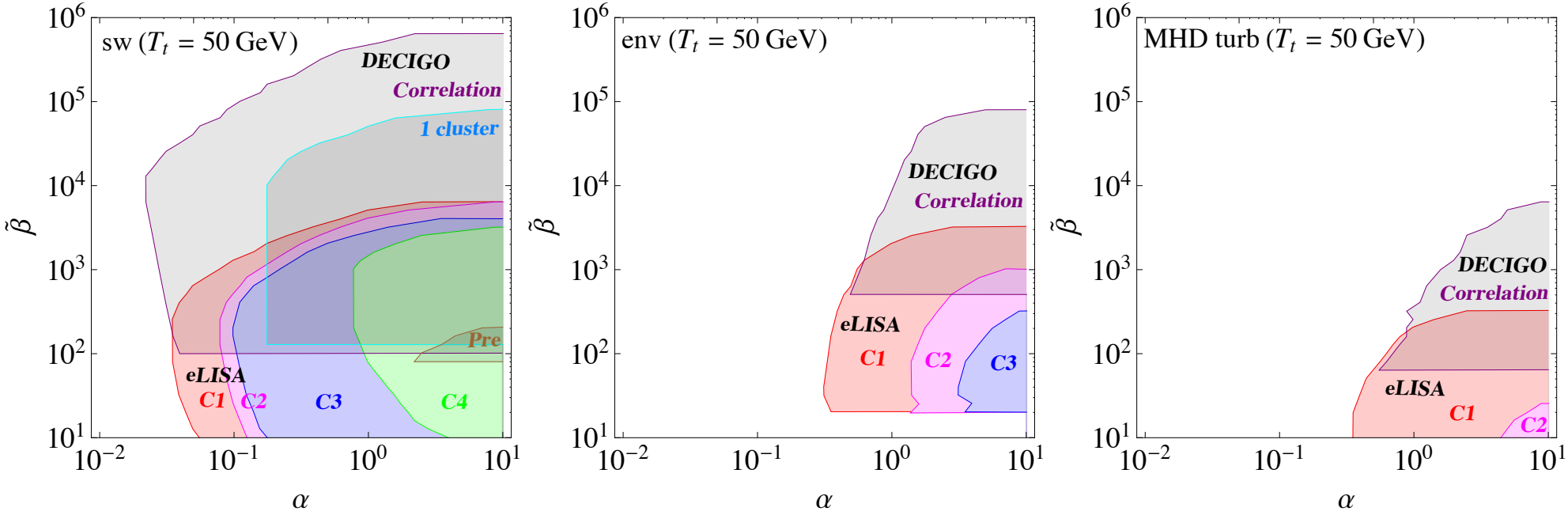

(α, βtilde)_exp. by New spectra (T_t=100GeV)

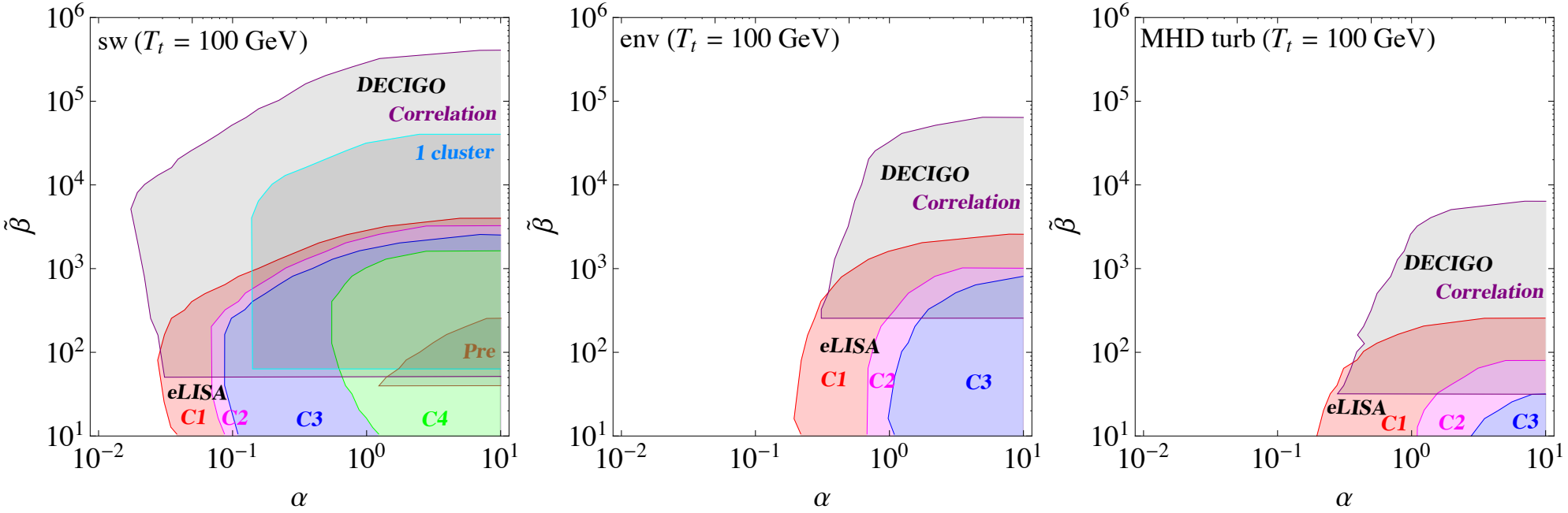

Efficiency factor $\kappa(v_b, \alpha)$

J.R.Espinosa, *et al*, JCAP **1006**, 028 (2010)

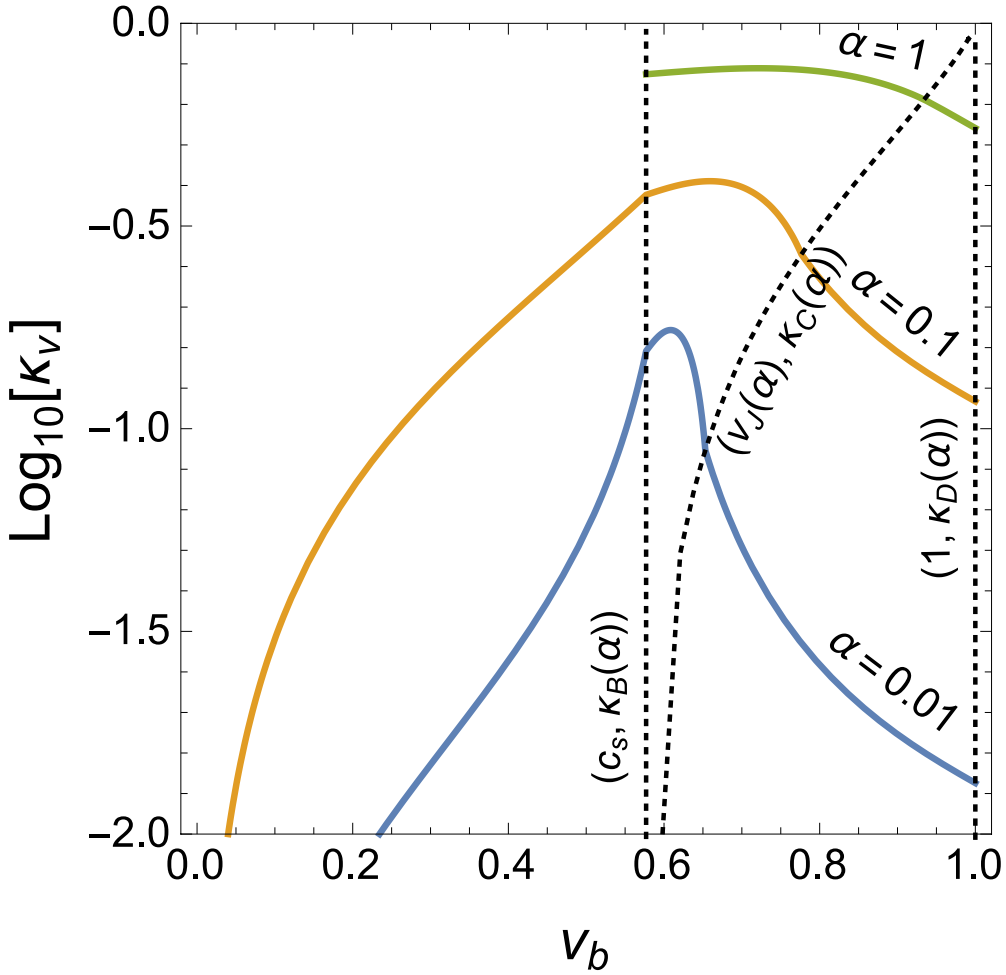

A Numerical fits to the efficiency coefficients

J.R.Espinosa, *et al.*

In this section we provide fits to the numerical results of section 4. These fits facilitate the functions $\kappa(\xi_w, \alpha_N)$ and $\alpha_+(\xi_w, \alpha_N)$ without solving the flow equations and with a precision better that 15% in the region $10^{-3} < \alpha_N < 10$.

In order to fit the function $\kappa(\xi_w, \alpha_N)$, we split the parameter space into three regions and provide approximations for the four boundary cases and three families of functions that interpolate in-between: For small wall velocities one obtains ($\xi_w \ll c_s$)

$$\kappa_A \simeq \xi_w^{6/5} \frac{6.9\alpha_N}{1.36 - 0.037\sqrt{\alpha_N} + \alpha_N} \,. \tag{A.1}$$

For the transition from subsonic to supersonic deflagrations ($\xi_w = c_s$)

$$\kappa_B \simeq \frac{\alpha_N^{2/5}}{0.017 + (0.997 + \alpha_N)^{2/5}} \,. \tag{A.2}$$

ξ_J is same as our $v_b(\alpha)$

For Jouguet detonations ($\xi_w = \xi_J$), as stated in eq. (4.2)

$$\kappa_C \simeq \frac{\sqrt{\alpha_N}}{0.135 + \sqrt{0.98 + \alpha_N}} \quad \text{and} \quad \xi_J = \frac{\sqrt{\frac{2}{3}\alpha_N + \alpha_N^2} + \sqrt{1/3}}{1 + \alpha_N} \,. \tag{A.3}$$

And finally for very large wall velocity, ($\xi_w \to 1$) as stated in eq. (4.4)

$$\kappa_D \simeq \frac{\alpha_N}{0.73 + 0.083\sqrt{\alpha_N} + \alpha_N} \,. \tag{A.4}$$

For subsonic deflagrations a good fit to the numerical results is provided by

$$\kappa(\xi_w \lesssim c_s) \simeq \frac{c_s^{11/5} \kappa_A \kappa_B}{(c_s^{11/5} - \xi_w^{11/5})\kappa_B + \xi_w c_s^{6/5} \kappa_A} \,, \tag{A.5}$$

and for detonations by

$$\kappa(\xi_w \gtrsim \xi_J) \simeq \frac{(\xi_J - 1)^3 \xi_J^{5/2} \xi_w^{-5/2} \kappa_C \kappa_D}{[(\xi_J - 1)^3 - (\xi_w - 1)^3]\xi_J^{5/2} \kappa_C + (\xi_w - 1)^3 \kappa_D} \,. \tag{A.6}$$

The numerical result for the hybrid (supersonic deflagration) region is well described by a cubic polynomial. As boundary conditions, one best uses the two values of κ and the first derivative of κ at $\xi_w = c_s$. Notice that the derivative of κ in ξ_w is not continuous at the point ξ_J. The derivative at $\xi_w = c_s$ is approximately given by

$$\delta\kappa \simeq -0.9 \log \frac{\sqrt{\alpha_N}}{1 + \sqrt{\alpha_N}} \,. \tag{A.7}$$

This differs from the derivative one would obtain from the fit in the region $\xi_w < c_s$, but mostly for values $\alpha \gtrsim 1$, where no solutions exist for $\xi_w < c_s$. The expression for supersonic deflagrations then reads

$$\kappa(c_s < \xi_w < \xi_J) \simeq \kappa_B + (\xi_w - c_s)\delta\kappa + \frac{(\xi_w - c_s)^3}{(\xi_J - c_s)^3}[\kappa_C - \kappa_B - (\xi_J - c_s)\delta\kappa] \,. \tag{A.8}$$

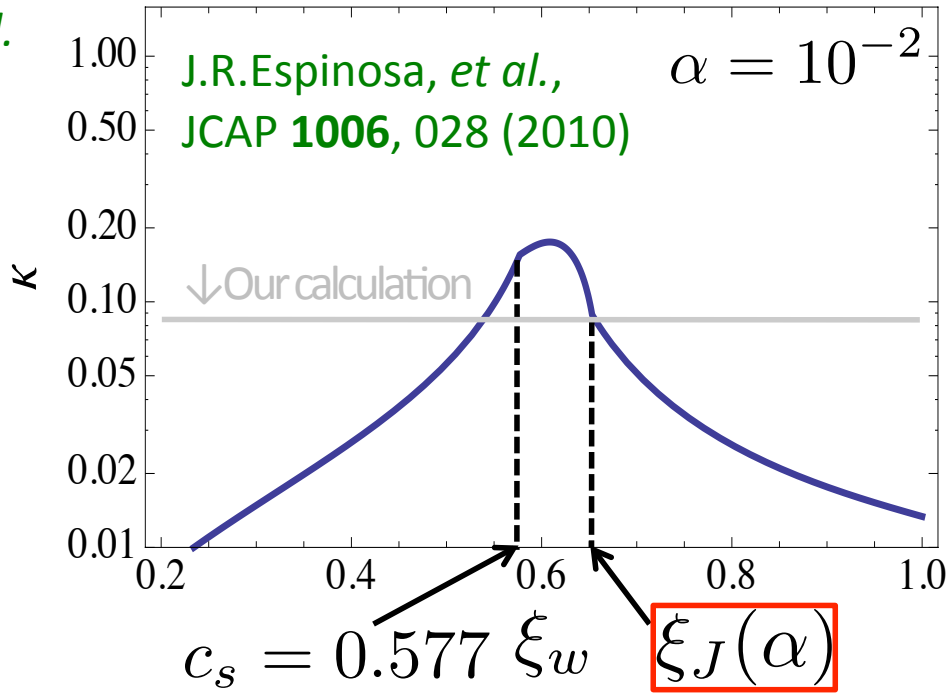

$$\tilde{\Omega}_{\rm coll} h^2 \simeq \frac{1.8 \times 10^{-6} (\kappa(\alpha, \xi_w))^2 \xi_w^3}{0.42 + \xi_w^2} \times \left(\frac{\alpha}{1+\alpha}\right)^2 \tilde{\beta}^{-2}$$

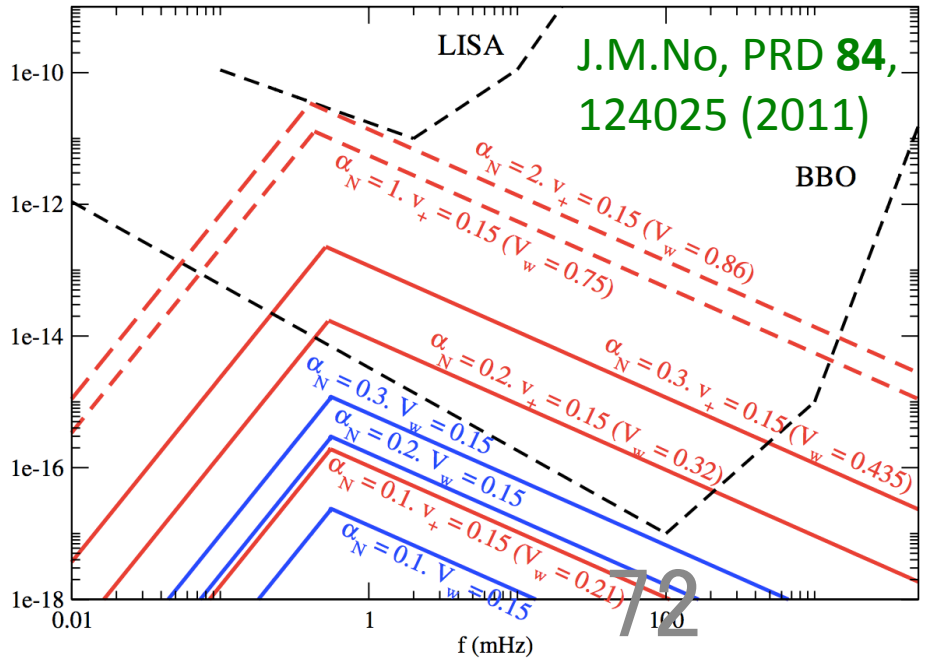

Contour plot of α on (ξ_w, v_+) plane

α is given by effective potential.

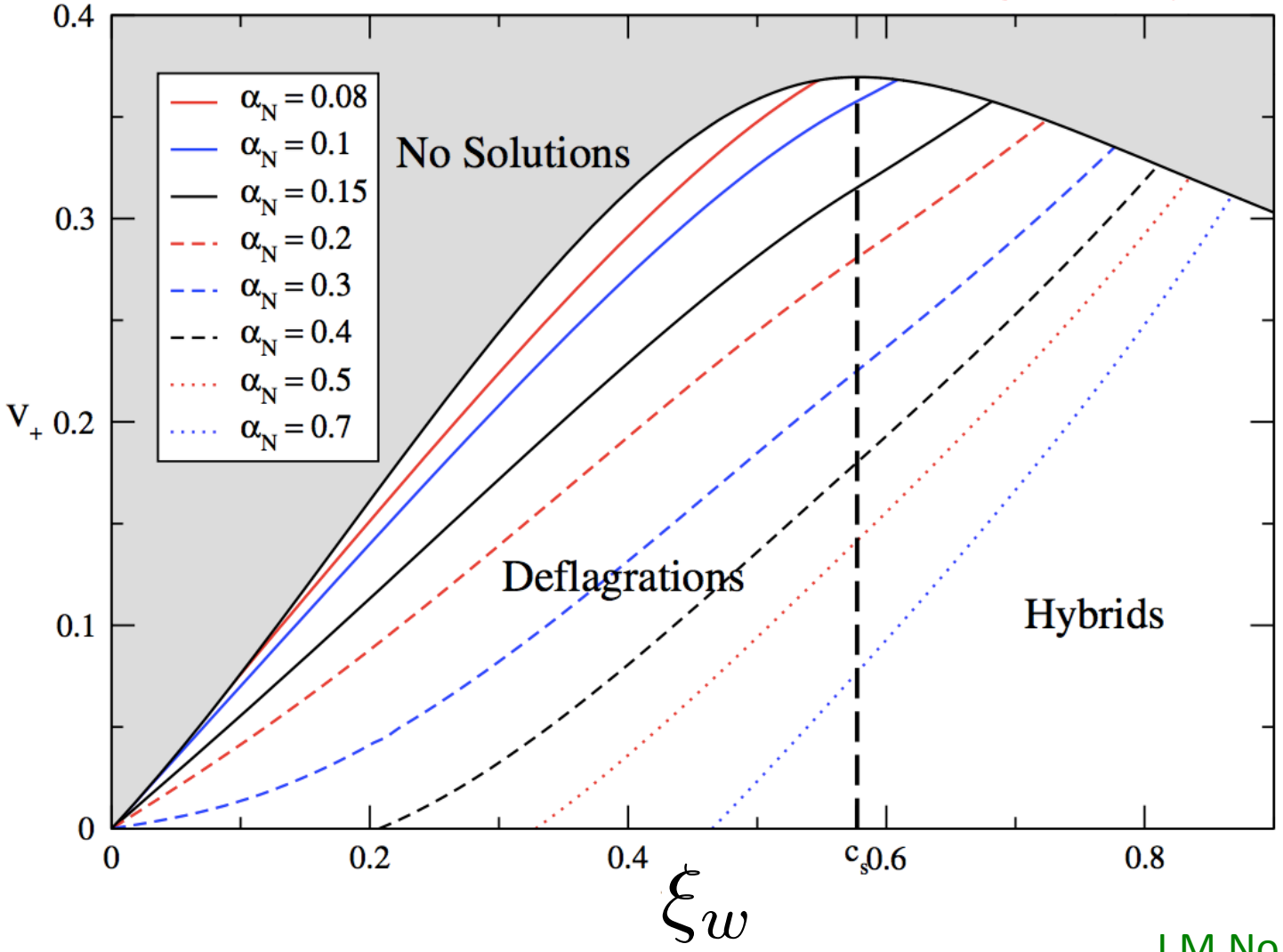

Diffusion upper bound of EWBG

EWBG requires small ξ_w
⇆GW requires large

J.M.No, PRD84, 124025 (2011)

Contour plot of v_+ on (ξ_w, α) plane

α is given by effective potential.

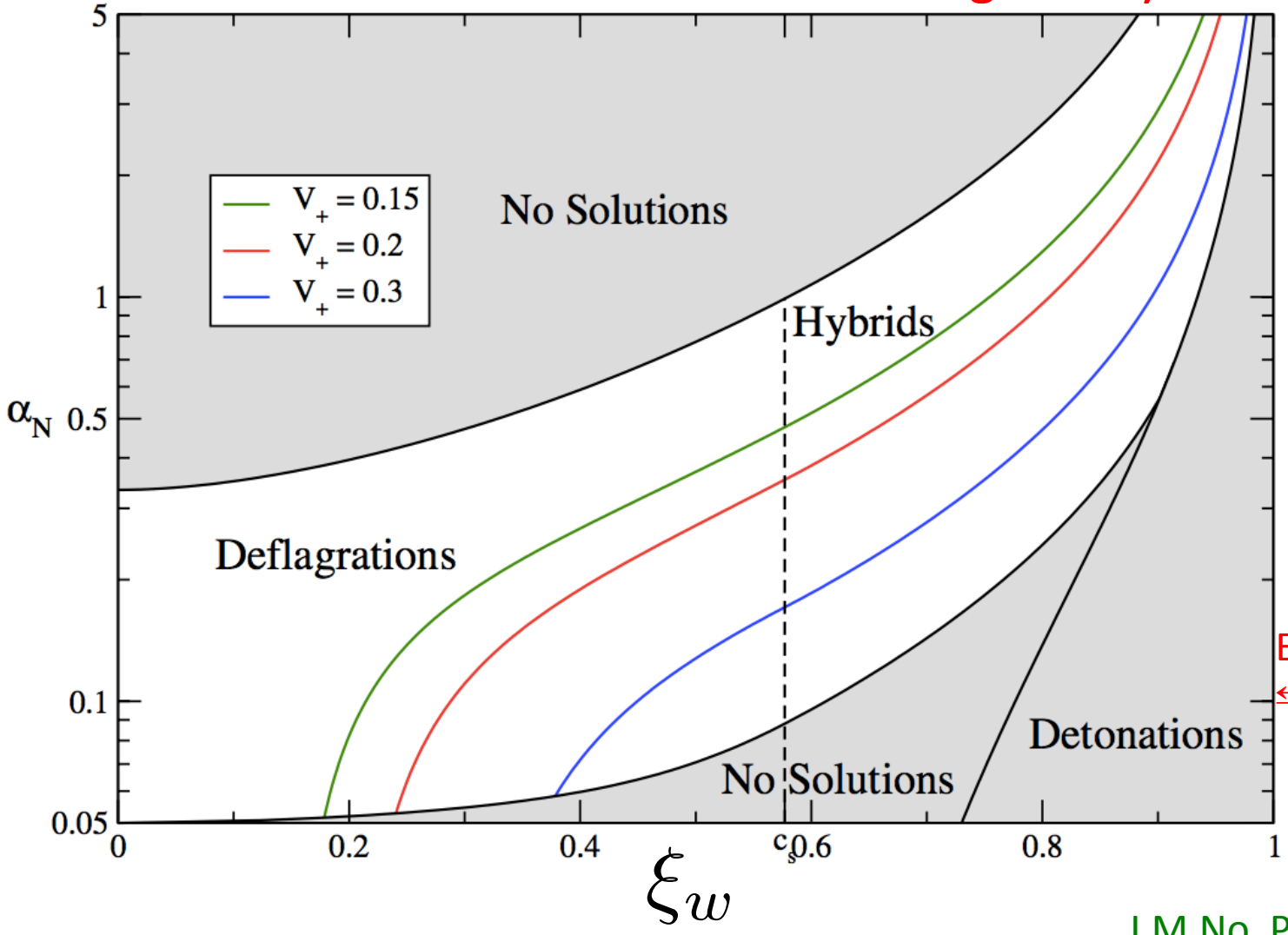

EWBG requires small ξ_w
⇆GW requires large

J.M.No, PRD84, 124025 (2011)

Foreground noise from white dwarf binaries

R.Schneider, S.Marassi, V.Ferrari, Class. Quant. Grav. **27**, 194007 (2010)

Stochastic backgrounds of gravitational waves from extragalactic sources

R Schneider[1], S Marassi[2], V Ferrari[2]

[1] INAF, Osservatorio Astrofisico di Arcetri, Largo Enrico Fermi 5, 50125, Firenze, Italy

[2] Dipartimento di Fisica G.Marconi, Sapienza Universit'a di Roma and Sezione INFN ROMA1, piazzale Aldo Moro 2, I-00185 Roma, Italy

E-mail: raffa@arcetri.astro.it

Abstract.

Astrophysical sources emit gravitational waves in a large variety of processes occurred since the beginning of star and galaxy formation. These waves permeate our high redshift Universe, and form a background which is the result of the superposition of different components, each associated to a specific astrophysical process. Each component has different spectral properties and features that it is important to investigate in view of a possible, future detection. In this contribution, we will review recent theoretical predictions for backgrounds produced by extragalactic sources and discuss their detectability with current and future gravitational wave observatories.